

TC

824

C2

A2

no. 88

75

74

LIBRARY
UNIVERSITY OF CALIFORNIA
DAVIS

STATE OF CALIFORNIA
DEPARTMENT OF WATER RESOURCES
DIVISION OF DESIGN AND CONSTRUCTION

BULLETIN NO. 88

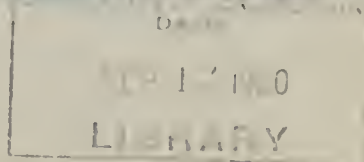
PROCEDURES FOR ESTIMATING
MAXIMUM POSSIBLE
PRECIPITATION

EDMUND G. BROWN
Governor



MAY, 1960

HARVEY O. BANKS
Director of Water Resources

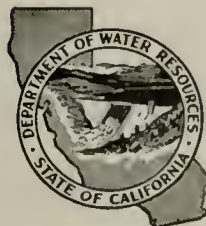


STATE OF CALIFORNIA
DEPARTMENT OF WATER RESOURCES
DIVISION OF DESIGN AND CONSTRUCTION

BULLETIN NO. 88

PROCEDURES FOR ESTIMATING MAXIMUM POSSIBLE PRECIPITATION

EDMUND G. BROWN
Governor



HARVEY O. BANKS
Director of Water Resources

MAY, 1960

LIBRARY
UNIVERSITY OF CALIFORNIA
DAVIS

STATE OF CALIFORNIA
DEPARTMENT OF WATER RESOURCES
DIVISION OF DESIGN AND CONSTRUCTION

BULLETIN NO. 88

PROCEDURES FOR ESTIMATING MAXIMUM POSSIBLE PRECIPITATION

EDMUND G. BROWN
Governor



HARVEY O. BANKS
Director of Water Resources

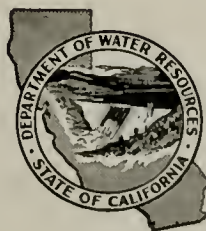
MAY, 1960

STATE OF CALIFORNIA
DEPARTMENT OF WATER RESOURCES
DIVISION OF DESIGN AND CONSTRUCTION

BULLETIN NO. 88

PROCEDURES FOR ESTIMATING MAXIMUM POSSIBLE PRECIPITATION

EDMUND G. BROWN
Governor



HARVEY O. BANKS
Director of Water Resources

MAY, 1960

PROCEDURES FOR ESTIMATING
MAXIMUM POSSIBLE PRECIPITATION

by

Dr. Joseph B. Knox[†]
Meteorological Consultant

[†] Affiliated with the Lawrence Radiation Laboratory,
University of California, Livermore, California.

JOSEPH B. KNOX
37 La Gonda Court
Danville, California

May 10, 1960

Mr. Harvey C. Banks, Director
California State
Department of Water Resources
P. O. Box 388
Sacramento 2, California

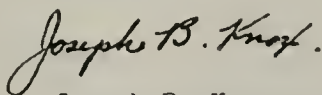
Dear Mr. Banks:

Submitted herewith is a report on procedures for estimating maximum possible precipitation for large watersheds in California.

The study and report were developed at the request of the Department of Water Resources to assist the Department in its determination of necessary reservoir and spillway capacities in mountainous watersheds. Specifically, the investigation applies the extreme values of known meteorological parameters to an atmospheric model in order to estimate the maximum accumulated precipitation and its distribution for the Feather River Basin.

To obtain fairly detailed geographic distributions of the maximum possible (accumulated) precipitation, an electronic computing program was developed. The practical advantage of such a program is that the model and the methods are readily applicable to other mountainous watersheds in the State.

Sincerely,



Joseph B. Knox
Meteorological Consultant

TABLE OF CONTENTS

	Page
Letter of Transmittal	i
Organization	v
Acknowledgements	vi
List of Symbols	vii
1.1 Introduction	1
2.1 Model for Orographic Rainfall	2
2.2 The u, w Computation	3
2.3 The Trajectories of Precipitation Products	6
2.4 The Rate of Orographic Precipitation	9
2.5 The Vorticity Budget Check on the u, w Solution	9
3.1 The Model for Rainfall from Large-scale Synoptic Disturbances	11
4.1 A Model of the Time Distribution of the Precipitation Rate	13
5.1 The Case Study of December 1955 – the Feather River Basin	15
6.1 The “Near-Maximum” Storm	17
7.1 The Estimated Maximum Possible Storm	18
8.1 Concluding Remarks	20
References	23

TABLES

3.1 The Hourly Rate of Synoptic-Scale Precipitation	12
4.1 Values of η Corresponding to Critical Periods for Maximum Precipitation in the Interval t_1	14
5.1 Maximum Values of Meteorological Parameters – December 1955 Storm	16
7.1 Average 72-Hour Precipitation, Feather River Basin	20

APPENDIXES

Appendix A. The Computation of the Topography of the Sacramento Valley Inversion	25
Appendix B. The Computational Stability of the Finite Difference Approximation in Sec. 2.2	27

FIGURES

Figure

- 1 Schematic Cross-section of Terrain, Showing Valley Inversion
- 2a Location Map – Feather River Basin
- 2b Location Map – Profile Strips A, B, and C
- 2c Detailed Location of Profiles Used in Computer Calculations
- 3a Average Elevation of Profile A
- 3b Average Elevation of Profile B
- 3c Average Elevation of Profile C
- 4 Schematic Diagram of Trajectories of Precipitation Products
- 5 Schematic Diagram of a Raindrop Trajectory – Illustrating the Computing Scheme
- 6 Plot of Raindrop Trajectories No. 36 and No. 55 on Profile A
- 7a Distribution of Hourly Rate of Orographic Precipitation on Profile A, Dec. 1955 Storm (4 m/s)
- 7b Distribution of Hourly Rate of Orographic Precipitation on Profile A, Dec. 1955 Storm (6 m/s)
- 7c Distribution of Hourly Rate of Orographic Precipitation on Profile A, Dec. 1955 Storm (8 m/s)
- 8 A Vorticity Budget of the Layer – 1000 to 1500 Meters (Dec. 1955 Storm)
- 9 The Adiabatic Double Couette Flow Model
- 10 Graphical Solution for Adverse Periodicity
- 11a The Calculated 72-hour Isohyetal Map, December 1955 Storm (8 m/s), Feather River Basin
- 11b The Calculated 72-hour Isohyetal Map, December 1955 Storm (6 m/s), Feather River Basin
- 11c The Calculated 72-hour Isohyetal Map, December 1955 Storm (4 m/s), Feather River Basin
- 12 The 72-hour Isohyetal Map of Observed Precipitation, December 1955 Storm, Feather River Basin
- 13 The 72-hour Isohyetal Map, “Near Maximum” Storm, Feather River Basin
- 14 The 72-hour Isohyetal Map, Estimated Maximum Possible Storm, Feather River Basin

ORGANIZATION

HARVEY O. BANKS DIRECTOR, DEPARTMENT OF WATER RESOURCES
RALPH M. BRODY DEPUTY DIRECTOR, DEPARTMENT OF WATER RESOURCES
JAMES F. WRIGHT DEPUTY DIRECTOR, DEPARTMENT OF WATER RESOURCES
WALTER G. SCHULZ CHIEF, DIVISION OF DESIGN & CONSTRUCTION
CARL A. WERNER CHIEF, OPERATIONS BRANCH

* * * * *

This Report Was Prepared By:

DR. JOSEPH B. KNOX METEOROLOGICAL CONSULTANT

* * * * *

With Principal Assistance From:

JOSEPH I. BURNS SUPERVISING HYDRAULIC ENGINEER
WILLIAM A. ARVOLA METEOROLOGIST II
WAYNE J. KAMMERER ASSISTANT HYDRAULIC ENGINEER
WILLIAM B. MIERKE ASSISTANT HYDRAULIC ENGINEER

* * * * *

PAUL L. BARNES CHIEF, DIVISION OF ADMINISTRATION
PORTER TOWNER CHIEF COUNSEL
ISABEL C. NESSLER COORDINATOR OF REPORTS

ACKNOWLEDGEMENTS

Several members of the Department of Water Resources have been of great assistance to the research project:

Mr. William Arvola, Mr. Wayne Kammerer, and Mr. William Mierke for their respective services in meteorology, computation, and programming. The author is also grateful for the interest of Mr. Carl A. Werner in this study, and for the contributions, interest, and frequent discussions on the part of Mr. Joseph I. Burns.

LIST OF SYMBOLS

The symbols frequently used in the study are listed below with their definitions:

D	– the diameter of a raindrop.
E_q	– the export of the vorticity q .
i	– the indexing of the vertical in the computational plane.
j	– the indexing of the discretized vertical coordinate.
m	– the indexing of the straight line segment fitted to the average terrain.
n	– the vertical number (0, 1, 2,) within a given m -region.
p	– the pressure.
P_1	– the rate of precipitation
P_f	– the hourly rate of precipitation from the synoptic-scale disturbances.
P_{max}	– the maximum hourly rate of precipitation.
P_{min}	– the minimum hourly rate of precipitation.
P_o	– the hourly orographic rate of precipitation.
$\bar{P}(x_1)$	– the mean rate of precipitation at the location x_1 during a prescribed period.
q	– the vorticity of the two-dimensional motion in the vertical plane.
r_s	– the saturation mixing ratio.
$S(x)$	– the simplified terrain slope.
t	– time.
t_i	– an interval of time.
T	– the period of the time function used to describe the rate of precipitation.
u	– the component of the horizontal wind normal to the mountain barrier.
u_s	– the value of u at the simplified terrain level.
w	– the vertical velocity.
W_D	– the terminal fall velocity (in still air) of raindrops of size D .
W_o, W_1, \dots	– the terminal fall velocity of raindrops of a particular size, and passing through special grid points in the computational net.
W'_o, W'_1, \dots	– the fall velocity of raindrops relative to the earth.
x	– the space coordinate normal to the barrier.
x_1	– the x -coordinate of the computational verticals.
x_m	– the x -coordinate of discontinuities in the terrain slope.
z	– the vertical coordinate.

LIST OF SYMBOLS (Continued)

- z_a – the z -coordinate of the simplified terrain.
- $z_D(i-1,i)$ – the elevation at the $i-1$ vertical of the raindrop trajectory terminating at x_1 .
- θ_s – the saturation potential temperature.
- ξ – the mesh constant in the x -direction, for m equal a constant.
- ρ – the density of dry air.
- ω – the individual rate of change of pressure on a moving air parcel.

PROCEDURES FOR ESTIMATING MAXIMUM POSSIBLE PRECIPITATION

by

Joseph B. Knox

1.1 INTRODUCTION

By way of introduction, the objectives of this investigation on the estimation of maximum possible precipitation are outlined as follows:

1. To devise a physical model for estimating maximum possible precipitation over large watersheds. (In the model devised, the orographic precipitation, the precipitation from large-scale fields of vertical motion associated with synoptic-scale disturbances, and the spillover can be quantitatively evaluated.)
2. To describe, in some detail, the geographical distribution of maximum possible precipitation over a watershed.
3. To develop proper computing methods so that electronic computers may be used to attain these objectives.
4. To apply the model to the meteorological case study of the December 1955 storm in the Feather River Basin as a verification of the model's capability to specify accumulated precipitation and its geographic distribution.
5. To maximize the parameters of the model, thereby producing an estimate of the maximum possible precipitation.

Precipitation-producing mechanisms that lead to excessive winter rainfall in California are (a) orographic lifting, (b) lifting due to large-scale fields of vertical motion (including frontal lifting), and (c) vertical instability. Great deluges, such as the December 1955 storm in California, occur through the simultaneous operation of the first two factors for a watershed whose horizontal area is of the order of thousands of square miles.

In the proposed model, the hourly rate of precipitation is a function of a number of meteorological variables – (a) the intensity of the wind normal to the mountain range, (b) the available moisture, (c) the intensity of traveling disturbances, (d) the raindrop size assumed in the model, and (e) the height of the low-level inversion overlying the Central Valley of California. Once models of orographic and frontal precipitation are constructed, the parameters representing the five above physical features are physically or statistically adjusted to extreme values; in this way, a quantitative estimate of the maximum hourly precipitation is calculated.

From the maximum hourly rate of precipitation for both orographic and frontal sources, we will construct a simple model of the time distribution of the precipitation rate in which the accumulated precipitation depends not only on the five prior mentioned parameters but also on the storm periodicity (or the periodicity with which disturbances approach the watershed). To maximize the accumulated precipitation, the most adverse storm periodicity is selected. With an electronic computer (IBM 650), we can readily perform the following computations: (a) the detailed geographical distribution of maximum possible precipitation, and (b) the variation of the maximum possible precipitation with the assumed raindrop size. The methods to be described later permit the compu-

tation of the distribution of spillover into the leeward basin. In this study, spillover is defined as that portion of the rain (orographically produced) that falls over onto the lee side of the basin or onto a high, flat plateau from the windward side.

To estimate the hourly orographic rate of precipitation, we shall use a two-dimensional orographic precipitation model, suggested by Professor J. Bjerknes in the 1940's, and adapted for use in the Sacramento Valley and the Feather River Basin.

The estimated maximum rate of precipitation due to large-scale synoptic processes shall be calculated using a vertical velocity distribution from a dynamical model of the atmosphere. During the last decade dynamical models of the atmosphere have been devised and their uses explored. This brief experience, supported by diagnostic vertical motion studies, indicates that calculations of extreme rates of rainfall by these methods will be fruitful.

2.1 MODEL FOR OROGRAPHIC RAINFALL

The first step in devising a simple orographic rainfall model is the selection of a profile describing the terrain and the topography of the inversion surface over which the moist maritime air ascends. A schematic profile normal to the Sierra Nevada is shown in Figure 1. A sloping temperature inversion is depicted over the Sacramento Valley. Beneath this inversion, cold air moves from south to north (or south-southeast to north-northwest) during the approach of a cyclone from the southwest. Since this shallow layer of air does not impinge on western Sierra slopes, it does not contribute to the precipitation in basins like the Feather River. Rather, this shallow layer of cold air is forced to ascend orographically at the north end of the Sacramento Valley, between Mt. Shasta and Crater Peak, as discussed by J. Bjerknes (1946). However, the air mass that is forced to ascend the western Sierra slopes is the warm moist air of maritime origin, moving from a west-southwesterly (or southwesterly) direction. The flow in this warm air mass may be modelled by a uni-directional flow normal to the Sierra. The sloping inversion over the Sacramento Valley in the model represents a narrow zone separating the low-level flow parallel to the Sierra from the warm upper flow normal to the mountains. The inversion slope may be computed from meteorological data, using the procedure outlined in Appendix A. Since the December 1955 storm represents an important test case for this study, it should be mentioned that the three-dimensional analysis of the wind field during this storm, described in a recent paper by Myers (1959), confirms the structure of the orographic precipitation model proposed by Bjerknes (1946). We shall now consider the computation of the maximum orographic rate of precipitation from a two-dimensional model.

A two-dimensional model of orographic precipitation is constructed following the method of Bjerknes (1940); however, in addition, the proposed model contains the following features: (a) a computationally stable computing scheme, (b) a computation of spillover, and (c) a vorticity budget "check" on the proposed steady-state solution.

To devise the model we proceed as follows. Far upwind of the mountain barrier in essentially undisturbed flow, the wind normal to the barrier (designated by u) is known as a function of height. This wind data serves as information on the inflow boundary for computation of an approximate steady-state solution of the flow of saturated adiabatic air over the valley inversion and the mountain barrier. In a manner similar to Bjerknes (1940), we select the following distribution of vertical velocity,

$$w(x, z) = w(x, z_0) \left(\frac{z - z_0}{1000}\right)^{1/2} \quad (1)$$

in which the vertical velocity, w , decreases by a factor of two every 1000 meters. Combined with the equation of continuity for steady-state two-dimensional motion (in which the horizontal variation of the density is neglected),

$$\frac{\partial u}{\partial x} = -\frac{1}{\rho} \frac{\partial}{\partial z} (\rho w), \quad (2)$$

It is possible to compute numerically the $w(x, z)$ and $u(x, z)$ distribution for the region of interest.

2.2 THE u, w COMPUTATION

To compute the distribution of the horizontal wind, u , and the vertical velocity, w , in a vertical plane normal to the mountain barrier, we proceed as follows:

1. Consider the Feather River Basin, shown in Figure 2a. A major part of this basin can be covered by three profile strips, each 16 miles in width. The locations of these profile strips are shown in Figures 2b and 2c. Lines 16 miles in length are drawn normal to the axes of the strips at one-mile intervals along the strips (see Figure 2c). The average terrain elevations along these lines are obtained, and then are plotted to form the average terrain profiles (see Figures 3a, 3b, and 3c).
2. The average terrain profiles produced in this manner are still quite complex for computational purposes; for simplification, straight-line segments are fitted to the average profiles. In this fitting process, the main windward slope is preserved, while minor features are smoothed. The interior mountain valleys are assumed to be filled with cold air capped by a horizontal inversion. Figures 3a, b, c show the average terrain heights, the simplified profile, and the Sacramento Valley inversion for Profiles A, B, and C.
3. To compute the distribution of u and w from Equations (1) and (2) in the vertical plane along a simplified profile, this two-dimensional space is discretized so that

$$x_{m,n} = n\xi_{m+1} + x_m, \quad (3)$$

and

$$z_j = j\Delta z, \quad (4)$$

where x_m is the x -coordinate (in miles) of the discontinuity in slope at the beginning of a profile segment,

x_{m+1} is the x -coordinate (in miles) of the discontinuity in slope at the end of a profile segment,

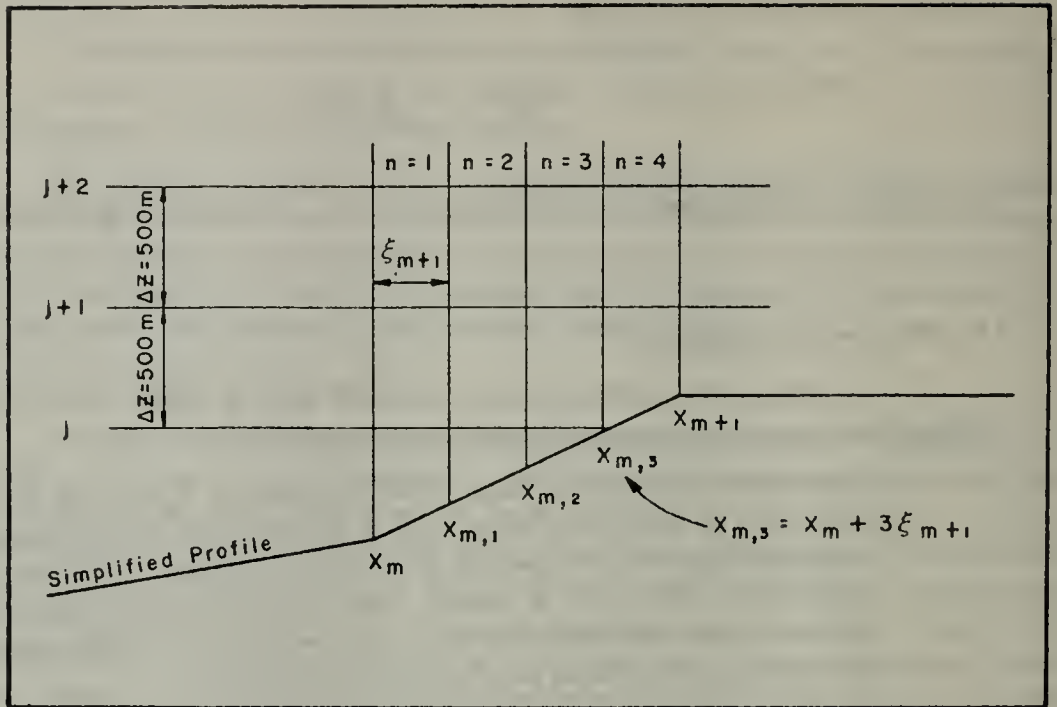
ξ_{m+1} is the mesh constant in the x -direction, such that the distance $(x_{m+1} - x_m)$ is subdivided into n equal intervals,

n is the integer nearest to $(x_{m+1} - x_m)/\xi_{m+1}$,

Δz is selected as 500 meters,

j is a positive integer.

These quantities are illustrated in the following schematic sketch:



Schematic Sketch of Grid for u, w Computation

4. To apply numerical methods to the computation of u, w in the model, we will, from Equations (1) and (2), devise a computationally stable finite difference approximation by proceeding as follows. The continuity equation is expanded into the form

$$\frac{\partial u}{\partial x} = -\frac{1}{\rho} \frac{\partial}{\partial z} (\rho w) = -\left[\frac{\partial w}{\partial z} + w \frac{1}{\rho} \frac{\partial \rho}{\partial z} \right] \quad (5)$$

From Equation (1)

$$\frac{\partial w}{\partial z} = w(x, z) \frac{\ln(1/2)}{1000} = u(x, z_s) S(x) \left(\frac{1}{2}\right)^{\left(\frac{z-z_s}{1000}\right)} \frac{\ln(1/2)}{1000}, \quad (6)$$

where $S(x)$ is the slope of the simplified terrain. The substitution of Equations (6) and (1) in (5) gives the following expression for divergence of the horizontal wind,

$$\frac{\partial u}{\partial x} = -u(x, z_s) S(x) \left[\left(\frac{1}{2}\right)^{\left(\frac{z-z_s}{1000}\right)} \frac{\ln(1/2)}{1000} + \frac{1}{\rho} \frac{\partial \rho}{\partial z} \left(\frac{1}{2}\right)^{\left(\frac{z-z_s}{1000}\right)} \right] \quad (7)$$

For purposes of calculation, we shall neglect the horizontal variation of density; the consequence of this assumption is that once the saturation potential temperature of

the model is selected, the density and its variation with height are known. In this way, Equation (7) may be written in the form

$$\frac{\partial u}{\partial x} = -u_n(x) F(x, z), \quad (8)$$

where $F(x, z)$ is readily computed.

To illustrate the use of Equation (8) in computing $u_n(x)$ on successive verticals, suppose that on the vertical $i=1$, $u_n(1)$ and $u(1, j)$ are known. To compute $u_n(2)$, we replace the differential equation, (8), by a finite difference equation,

$$\frac{u_n(2) - u[1, z_n(2)]}{\xi} = -u_n(2) F[z_n(2)]. \quad (9)$$

Solving the above equation for $u_n(2)$, we obtain

$$u_n(2) = u[1, z_n(2)] \left\{ 1 + \xi_1 F[z_n(2)] \right\}^{-1} \quad (10)$$

or a more general form of (10) is

$$u_n(n+1) = u[n, z_n(n+1)] \left\{ 1 + \xi F[z_n(n+1)] \right\}^{-1} \quad (11)$$

Once $u_n(1)$ and $u_n(2)$ are known, the distribution of vertical velocity on these verticals is computed from Equation (1). For the calculation to be successful, the difference equation, (11), must be computationally stable; the stability of Equation (11) is discussed in Appendix B.

5. At this stage of the calculation $u_n(2)$ and the vertical velocity $w(2, z)$ are known; from this information and the u, w values on vertical 1, we calculate $u(2, z)$. This is accomplished with the following difference equation,

$$\frac{u(i+1, j+1) - u(i, j+1)}{\xi} = \frac{i}{\rho_{j+1}} \frac{(\rho w)_{1, 1, j+2} - (\rho w)_{1, 1, j+1}}{2 \Delta z} \quad (12)$$

6. The calculations outlined in Paragraphs 4 and 5 (above) are continued until a vertical of discontinuous terrain slope is reached. With the horizontal wind component u_n known on this vertical and ignoring the slope discontinuity in the calculation of the vertical velocity, we obtain

$$\bar{w}_n = u_n \bar{S},$$

where \bar{S} is the average slope, $\frac{1}{2}(S_1 + S_2)$. To compute the remaining vertical velocities on this vertical, \bar{w}_n is substituted in Equation (1), and the resulting values of vertical velocity are subsequently substituted into (12) in order to calculate the horizontal wind as a function of height on the $(i+1)$ vertical. With the horizontal wind known

on the (i+1) vertical, the computing routine begins again with calculations discussed in Paragraph 4. In this manner, the horizontal wind and the vertical velocity are calculated on successive verticals until the region of interest is covered.

At the conclusion of the u, w computation, one is confronted with the question as to whether the computing program is error free. To determine this, a series of three checks is set up to examine the solution:

1. Since the orographic model is assumed to be a steady state, the u, w numerical solution must, if correct, have no net inflow of dry air into the region between the first vertical and the last (downwind) vertical. In the test problem (composed of over fifty verticals) the mass outflow of dry air exceeded the mass inflow by three per cent. Both the sign and magnitude of this error compare well with the estimated truncation error (of five per cent) discussed in Appendix B.
2. The vertical velocity decreases by a factor of two every thousand meters.
3. The behavior of the first and second differences (in the x-direction) of the horizontal wind, u, must be orderly, and changes in these differences from one vertical to another must have a physical basis.

2.3 THE TRAJECTORIES OF PRECIPITATION PRODUCTS

The next problem in calculating the hourly rate of orographic precipitation is the determination of the trajectories of raindrops of a given size where the raindrops terminate their earthward fall at the bottom of verticals in the computational grid. Given the horizontal and vertical velocities of the air in the model, and the terminal fall velocity of the selected raindrop, an approximate trajectory determination is possible with the following assumptions:

1. The terminal fall velocity of a raindrop of arbitrary shape can be approximated by the terminal fall velocity of a spherical drop of the same mass.
2. The dependence of the terminal fall velocity on atmospheric density can be neglected.
3. The effect of change of phase of the precipitation products on the trajectory can be neglected in calculations of maximum possible precipitation.
4. The condensation products are assumed to be large drops of 2100 micron diameter, reported by Byers (1944) to correspond to excessive rain.

Physically, assumptions 3 and 4 maximize the windward precipitation by bringing condensation products to the ground quickly.

The oblique raindrop trajectories, shown schematically in Figure 4, define skew-shaped volumes of air from which the rain is falling onto both the windward and leeward slopes. For example, precipitation arriving on the windward slope between X_2 and X_3 originates from the skew-shaped volume contained between trajectories T_2 and T_3 shown in Figure 4. The rate at which precipitation falls on a unit horizontal area from regions of positive vertical motion in the atmosphere is given by the following expression, derived by Smagorinsky and Collins (1955),

$$P_1 = \frac{1}{\rho_w} \int_{r_s(\psi_s)}^{r_s(\psi_t)} \rho_w \delta r_s \quad (13)$$

where r_s is the saturation mixing ratio, δr_s is the change in the saturation mixing ratio during the saturated adiabatic ascent of the air through a pressure interval δp , w is the vertical velocity, ρ is the density of air, and ρ_w the density of water. The rate of precipitation, computed from Equation (13), is subject to the following assumptions: (a) sufficient condensation nuclei are present, (b) no super-saturation, (c) no super-cooling, (d) no non-adiabatic processes other than those occurring from changes in state, and (e) both cloud storage and evaporation from falling droplets are negligible compared to P_1 . The assumptions, with the exception of (d), maximize the rate of precipitation P_1 . It is proposed that the orographic rate of precipitation be calculated by applying Equation (13) to the skew-shaped volumes terminating on the windward slope, and that the spillover (occurring, for example, at vertical X_7 in Figure 4), be computed in an analogous way.

To devise a simple numerical scheme for calculating the coordinates of a raindrop trajectory, we proceed as follows. Consider the raindrop of diameter D (where $D=2100\mu$ and the terminal fall velocity $W_D = 6$ m/s) that strikes the terrain at the i -th vertical (see Figure 5). Suppose we designate the height of the intersection of this raindrop trajectory on the $(i-1)$ vertical by

$$z_D(i-1, i).$$

In addition, two hypothetical drops, whose trajectories are shown in Figure 5, are of interest; namely, (1) the raindrop passing through the $(i-1)$ vertical at height z_0 and striking the terrain at the i -th vertical, and (2) the raindrop passing through the $(i-1)$ vertical at the height z_1 and striking the terrain at the i -th vertical. These two raindrops are of quite different size; from their fall velocities relative to the earth, designated by W'_0 and W'_1 , the corresponding terminal fall velocities W_0 and W_1 are computed from the u, w solution as follows:

$$W'_0 = 0 = \frac{1}{2} \left\{ w[i, z_s(i)] + w[i-1, z_s(i)] \right\} + W_0, \quad (14)$$

and

$$W'_1 = \frac{1}{2} \left\{ w[i, z_s(i)] + w[i-1, j+1] \right\} + W_1, \quad (15)$$

where

$$W'_1 = -[z(j+1) - z_s(i)] / \Delta t_1, \quad (16)$$

and

$$\Delta t_1 = \xi / \frac{1}{2} \left\{ u[i, z_s(i)] + u[i-1, j+1] \right\} \quad (17)$$

Once W_1 and W_0 are calculated, we determine if W_D (selected as 6 m/s) lies between W_0 and W_1 . If $|W_0| < |W_D| < |W_1|$, then $z(i-1, i)$ may be calculated from the divided difference formula,

$$z_D(i-1, i) = z_0 + \frac{6 - |W_0|}{|W_1| - |W_0|} \left[z(j+1) - z_0 \right] \quad (18)$$

In the event W_D exceeds the magnitude of both W_1 and W_0 , then the calculation on the (i-1) vertical is repeated using hypothetical raindrops passing through the levels (j+1) and (j+2); then

$$z_D(i-1, i) = z(j+1) + \frac{6 - |W_1|}{|W_2| - |W_1|} \left[z(j+2) - z(j+1) \right] \quad (19)$$

Once the height of this trajectory on the (i-1) vertical is calculated, we repeat the computation in order to determine $z_D(i-2, i-1)$. Equations similar to (18) and (19) are used for this purpose; for example,

$$\begin{aligned} z_D(i-2, i-1) &= z_D(i-1, i) + \frac{6 - |W_{z_D(i-1, i)}|}{|W_{j+2}| - |W_{z_D(i-1, i)}|} \left[z_{j+2} - z_D(i-1, i) \right] \\ &= z_D(i-1, i) + \beta(i-2) [z_{j+2} - z_D(i-1, i)], \end{aligned} \quad (20)$$

where

$$|W_{z_D(i-1, i)}| < |W_D| < |W_{j+2}|.$$

This portion of the machine program (designated as the trajectory subroutine) calculates and outputs (a) the raindrop trajectory by tracing the locus of the intersection of a given trajectory with successive verticals, and (b) the interpolated value of vertical motion at these intersection points. The calculation of a particular trajectory ceases when it intersects the isobaric tropopause in the model.

The computational stability of the trajectory routine may be examined in the following way: Equation(20) is of the form

$$z_D(i-k-1) = A(i-k) z_D(i-k) + B(i-k).$$

If the index $k=1, 2 \dots k$, we obtain the following set of equations:

$$z_D(i-2) = A(i-1) z_D(i-1) + B(i-1)$$

$$z_D(i-3) = A(i-2) z_D(i-2) + B(i-2) = A(i-2) \left\{ A(i-1) z_D(i-1) + B(i-1) \right\} + B(i-2)$$

$$\begin{aligned} z_D(i-4) &= A(i-3) z_D(i-3) + B(i-3) \\ &= A(i-3) A(i-2) \left\{ A(i-1) z_D(i-1) + B(i-1) \right\} + B(i-3) \end{aligned}$$

$$\begin{aligned} z_D(i-k) &= A(i-k+1) z_D(i-k+1) + B(i-k+1) \\ &= \left\{ A(i-k+1) \dots \dots A(i-3) A(i-2) \right\} \left\{ A(i-1) z_D(i-1) + B(i-1) \right\} + B(i-k+1). \end{aligned}$$

The functions A and B, computable from u, w, are regarded as known in the above set. For the last equation in the set, the influence of an error $\delta z_D(i-1)$, introduced on the (i-1) vertical, on the trajectory height at the (i-k) vertical is computed as

$$\delta z_D(i-k) = \left\{ A(i-1) A(i-2) A(i-3) \dots A(i-k+1) \right\} \delta z_D(i-1). \quad (21)$$

The error propagated to the (i-k) vertical is less than (or equal to) the error introduced on the (i-1) vertical if all the values of A are less than or equal to one in magnitude. From Equation (20), it can be seen that if $|\beta| \leq 1$, the magnitude of A(i-k+1) is less than or equal to one. In this case the propagated error becomes smaller (or remains the same) as the calculation proceeds from one vertical to the next. Hence, the trajectory computing routine is stable.

An illustration is shown in Figure 6 of raindrop trajectories computed for verticals No. 35 and No. 55 on Profile A in the Feather River Basin. Consider the trajectory intersecting the terrain at vertical No. 36. On the portion of the trajectory between the points A and B the orographic component of vertical motion produces (in the model) precipitation products falling earthward at a known terminal fall velocity. Similarly, on the trajectory segment CD forced orographic ascent provides additional precipitation, which (in the model) also falls along this trajectory.* However, on the trajectory segment EF the orographic component of vertical motion is zero; no new orographic precipitation products are formed in the air parcels momentarily located on this segment. But those precipitation products formed on the trajectory between A and E free fall along EF, striking the ground at the 36th vertical. The precipitation deposited on the ground at vertical No. 36 is (as we have previously defined) spillover. Precipitation deposited on the ground upwind of vertical No. 36 (for example, verticals 21 through 34) is the familiar orographic precipitation on the windward slope.

2.4 THE RATE OF OROGRAPHIC PRECIPITATION

The rate of orographic precipitation on the windward slopes and the spillover are readily computed from Equation (13) with the data from the trajectory subroutine. Figures 7a, b, and c show the hourly rate of orographic precipitation calculated for the storm of December 1955, as a function of x for terminal fall velocities of 4, 6, and 8m/s on Profile A. The precipitation rate on the windward slope is, of course, the greatest for the largest terminal fall velocity, 8m/s, while the precipitation rate on the lee slope, or the spillover, is the largest for the 4m/s terminal fall velocity. Since the field of vertical velocity is the same in all three cases, and the condensation rate in the free atmosphere is thereby the same, the change in rainfall intensity is only a matter of redistribution of precipitation products.

2.5 THE VORTICITY BUDGET CHECK ON THE u, w SOLUTION

In calculating the u, w solution for the orographic rate of precipitation, we have used only the y-component of the equation of motion. One possible check on the proposed u, w solution is to ascertain how well the proposed solution satisfies the x- and z-components of the equation of

* It should be noted that in the computation of the w-field along a vertical at a terrain-slope discontinuity an average of the slope on both sides of this vertical is used; thus, between verticals 32 and 33 and between verticals 34 and 35, the spillover computation uses positive w-values on verticals 32, 33, and 34. Orographic precipitation is, by virtue of this approximation, produced along trajectory segments UC and DE, even though these segments lie above flat terrain.

motion. These two component equations can be replaced by a vorticity theorem for the motion in the x, z plane for steady-state conditions,

$$\nabla \cdot (q\mathbf{v}) = \frac{\partial}{\partial x} (uq) + \frac{\partial}{\partial z} (wq) = 0 ,$$

where q is the vorticity of the two-dimensional motion in the x, z plane,

$$q = \frac{\partial u}{\partial z} - \frac{\partial w}{\partial x} .$$

By means of Gauss' Theorem, given in Holmboe (1944), the above steady-state requirement on the vorticity q is

$$E_q = \int_A \nabla \cdot (q\mathbf{v}) dA = \int_C q\mathbf{v} \cdot d\mathbf{n} = 0 ,$$

or the net export of vorticity, E_q , through a closed curve bounding the area A must be zero. We shall now compute the export of vorticity for a series of small areas ($\Delta z\xi$) on Profile B. By examining the E_q field afterwards, we will be able to discover the manner in which the steady-state solution differs from the proposed u, w fields.

For the storm of December 1955, the net export of vorticity, E_q , is computed for the small areas shown in Figure 8. The products uq and wq are plotted in the figure. It should be noted that (a) E_q is negative in all the areas computed, (b) both contributions to the convergence of $q\mathbf{v}$ are negative, (c) the computed E_q is small compared to the large contributions to the export, and (d) the computed E_q is of the same order as the small contributions of wq to the export. It is clear that in the 1000-meter to 1500-meter layer that we are somewhat removed from a steady-state solution. From the computed E_q field we are able to find the proper behavior of u, w in this layer. To do this, we shall first simplify the u -profile on verticals 18 and 25 as shown in Figure 8. Suppose $\frac{\partial}{\partial x} (uq)$ remains negative in the region under the u -profile kink (at 1000 meters); we could then ask what distribution of w is required in this layer to balance the vorticity budget. It is readily seen that to achieve vorticity balance (under the profile kink) the vertical velocity must increase with height up to the u -profile kink.

This latter result obtained by physical inference is supported by a theoretical study. Using the analytical results of Döös (1958) and methods similar to Holmboe (1953), the author has studied steady-state, two-dimensional flow in an adiabatic atmosphere,* containing a double Couette flow profile, and bounded (above and below) by rigid planes (see Figure 9). The result of the analysis shows that the vertical velocity increases upwards to the sinusoidal interface between the two Couette flows, and that the vertical velocity decreases with height above the interface. Estimates made from this theoretical model indicate that vertical velocities at the sinusoidal interface are of the order of 1.1 to 2.0 times the vertical velocities on a sinusoidal upwind slope, for conditions appropriate to the December 1955 storm.

Since we have demonstrated a probable departure of the proposed vertical velocity from reality, we should pause and consider the principal sources of error for the orographic rate of

* An adiabatic atmosphere is a "model atmosphere" in which the potential temperature, θ , is independent of the three space coordinates.

precipitation. The principal sources of error are: (a) the z-dependency of the vertical velocity, (b) the assumed homogeneously large raindrop size, and (c) the neglect of the effect of change of state on the trajectory of the precipitation products. The effects of these errors on the orographic rate of precipitation are as follows:

1. The assumption that w halves every one thousand meters underestimates the rate of precipitation in the layer under the u -profile kink.
2. The assumption of homogeneously large raindrop size overestimates the steepness of the trajectory, and hence overestimates the rate of precipitation.
3. With the neglect of the effect of change of state on the trajectory of precipitation products, the assumed terminal fall velocities of 4, 6, and 8 m/s exceed the snowflake terminal fall velocities of 0.5 to 3 m/s, reported by Douglas, Gunn, and Marshall (1957). Since snow traverses a trajectory more nearly horizontal than assumed, by overestimating the upper trajectory slope we in turn overestimate the orographic rate of precipitation.

It is quite possible that these contributing errors nearly compensate, or cancel, one another. The capability of the proposed model and methods to specify accumulated precipitation distributions can be determined empirically in meteorological case studies. The necessary computations can be readily performed with the electronic computing program developed. When the capability of the model to specify accumulated precipitation (or rate of precipitation) is confirmed, the parameters of the model can be maximized to obtain the estimated maximum possible precipitation.

3.1 THE MODEL FOR RAINFALL FROM LARGE-SCALE SYNOPTIC DISTURBANCES

Since the development of weather forecasting by dynamical methods, models depicting the evolution of large-scale disturbances have been proposed in which the rate of precipitation (due to large-scale vertical motion) can be computed. This evolution is physically governed by the principle of conservation of mass, the first law of thermodynamics, and the three equations of motion. Once the differential equations expressing these principles are "tailored" to describe synoptic (or large) scale disturbances, a partial differential equation in vertical velocity is obtained [see Eliassen (1955, 1957) and Smebye (1958)]. The adequate solution of the complete partial differential equation for the vertical velocity in three dimensions has not yet, to the author's knowledge, been achieved. However, Smagorinsky and Collins (1955) and Smebye (1958) have reported on the use of a two-level model for the calculation of vertical velocity and the prediction of precipitation. By maximizing the physical parameters in the two-level model used by these investigators, we may obtain an estimate of the extreme precipitation rate from large-scale processes. In one case study of precipitation prediction involving both showery and large-scale precipitation, it was shown that the predicted precipitation was in good agreement with the observed average in zones defined by the predicted isohyets.

The vertical velocity distribution, as mentioned, may be obtained from the two-level model, Charney and Phillips (1953), and Sawyer and Bushby (1953). In the two-level model it is assumed that the individual rate of change of pressure on an ascending air parcel, $\omega(p) = dp/dt$, is

$$\omega(p) = \omega(500) (1 - \alpha^2),$$

or the vertical velocity is

$$w(p) = \frac{\rho(500) w(500)}{\rho(p)} (1 - \alpha^2), \quad (22)$$

where $\rho(p)$ is the density as a function of pressure,
 $\rho(500)$ is the density at $p=500$ millibars,
 $w(500)$ is the vertical velocity at 500 millibars,
 and

$$\alpha = \frac{1000 - 2p}{1000}.$$

The vertical velocity at the 500 mb level in the two-level model may be computed from synoptic maps with the following expression given by Gates (1958),

$$w_{500} = -(0.150) I_s \Delta\zeta \quad (\text{cm/sec}), \quad (23)$$

where I_s = the change in temperature ($^{\circ}\text{C}$) measured normal to the isotherm over an interval of 3 degrees of latitude,

and $\Delta\zeta$ = the change in vorticity (in units of 10^{-5} sec^{-1}) measured over a distance of 3 degrees of latitude along the isotherms.

With the substitution of Equations (23) and (22) in Equation (13), we can compute the rate of precipitation from large-scale synoptic disturbances.

In this study, we will examine two methods of computing maximum possible precipitation. The first method uses the simultaneous maximization of the orographic and frontal precipitation, designated by P_o and P_f , respectively. The second method, however, maximizes the orographic precipitation P_o , but replaces an extreme value of P_f (which might be artificially large) with a value of P_f that could reasonably be expected during the storm type characterized by extreme orographic precipitation. Because these two methods give very different estimates of the maximum possible precipitation, they are of paramount interest.

In the first method, it is proposed that by computing the synoptic-scale vertical velocity field in disturbances of extreme intensity (such as the famous "Thanksgiving Storm", November 1950 in eastern United States), we may obtain estimates of the extreme vertical velocity fields and P_f accompanying large-scale synoptic disturbances by "transposition". The calculations have been performed from the weather maps of the November 1950 storm (these maps are available in the author's map file). These calculations of extreme large-scale vertical velocity and P_f may serve as a basis of comparison with the December 1955 storm in California. The vertical velocity at 500 mb, the date of the storm, and the hourly rate of synoptic-scale precipitation, P_f (for a saturation potential temperature of 70°F), are listed below in Table 3.1 for reference.

Table 3.1
 The Hourly Rate of Synoptic-Scale Precipitation

Storm Date	w (500 mb)	P_f (for $\theta_s = 70^{\circ}$)
December 1955, California	11.2 cm/sec	0.12 inch/hr
November 1950, Eastern United States	39.0 cm/sec	0.41 inch/hr

A more detailed discussion of the methods of estimating the maximum possible precipitation is given in Section 7.1.

4.1 A MODEL OF THE TIME DISTRIBUTION OF THE PRECIPITATION RATE

An inspection of the time distribution of the precipitation records in the Feather River Basin during the December 1955 storm shows that moving frontal disturbances produce a "periodic" rate of precipitation. This appearance of precipitation records is quite normal, as this storm type is marked by a strong southwesterly basic current in which frontal waves propagate, as discussed by Weaver (1959). The construction of a model of the time distribution of the precipitation is a separate problem from that of determining the maximum hourly rate of precipitation; however, quantitative estimates of the maximum hourly rate of precipitation on the computational verticals shall be used in constructing the time distribution of precipitation. In connection with the time distribution model it should be mentioned that the saturation potential temperature θ_s , the horizontal wind, and the frontal component of vertical motion are no longer independent of time. In the time distribution model, we shall examine the effect of storm periodicity on the amount of precipitation deposited at a given location in the time interval of t_1 . For this study the instantaneous rate of precipitation, $P(x_1, t)$, on the vertical designated by x_1 is represented by an idealized sinusoidal function bearing resemblance to recorded rates of precipitation,

$$P(x_1, t) = \bar{P}(x_1) + \Delta P(x_1) \cos\left(\frac{2\pi t}{T}\right), \quad (24)$$

which we shall designate as "Distribution I". Here,

- $\bar{P}(x_1)$ is $\frac{1}{2}(P_{\max} + P_{\min})$ at the location x_1 ,
- $\Delta P(x_1)$ is $\frac{1}{2}(P_{\max} - P_{\min})$ at the location x_1 ,
- P_{\max} is the maximum hourly rate = $P_o + P_f$,
- P_{\min} is the minimum hourly rate adopted for the storm,
- P_o is the hourly rate of orographic precipitation,
- P_f is the hourly rate of frontal precipitation,
- T is the period of the time function used to describe the rate of precipitation,
- t is time.

Upon integration of $P(x_1, t)$, the depth of precipitation falling at x_1 during t_1 is

$$P(x_1, t_1) = \bar{P}(x_1) t_1 + \Delta P(x_1) \frac{T}{2\pi} \sin\left(\frac{2\pi t_1}{T}\right). \quad (25)$$

We shall now consider the periods for which the depth of precipitation $P(x_1, t_1)$ is a relative maximum. Differentiating $P(x_1, t_1)$ with respect to T , we obtain a transcendental equation in the period T ,

$$\frac{T}{2\pi t_1} = \cot\left(\frac{2\pi t_1}{T}\right), \quad (26)$$

which can be solved for the adverse periods that deposit relative maxima of accumulated precipitation during the period t_1 . If t_1 equals 72 hours, the adverse periods are 13.7, 17.0, 22.2, 32.2, and 58.5 hours. Of these adverse periods, the longest one listed (58.5 hours) is the most adverse. Certain periods are excluded from this list; namely, those too small to be of significance for large watersheds, and the physically unrealistic infinite period.

However, in the event hydrologists are interested in a time distribution of the precipitation rate with a minimum at the time origin, consider the following rate of precipitation,

$$P(x_1, t) = \bar{P}(x_1) - \Delta P(x_1) \cos\left(\frac{2\pi t}{T}\right) \quad (27)$$

which we shall call "Distribution II". For this second distribution, the adverse periods are also determined by Equation (26) and, for $t_1 = 72$ hours, are 15.1, 19.2, 26.3, 41.5, and 100.6 hours. It has been suggested by Burns (1959) that for application to some watersheds, the time interval t_1 be made equal to the "time of concentration" [defined as the time period required for all parts of the drainage basin to contribute their quotas of stream flows, Meinzer (1942)]. If in Equation (26) t_1 is selected as the unit of time, then designating

$$\eta = \frac{T}{t_1},$$

we obtain the following form of Equation (26),

$$\frac{\eta}{2\pi} = \cot\left(\frac{2\pi}{\eta}\right) \quad (28)$$

The graphical solution of Equation (28) for values of η corresponding to the adverse periods of precipitation distributions I and II is illustrated in Figure 10, and the results of this calculation are tabulated in Table 4.1. For convenience we will repeat the definitions of distributions I and II:

$$\text{Distribution I is } P(x_1, t) = \bar{P}(x_1) + \Delta P(x_1) \cos\left(\frac{2\pi t}{T}\right),$$

$$\text{Distribution II is } P(x_1, t) = \bar{P}(x_1) - \Delta P(x_1) \cos\left(\frac{2\pi t}{T}\right).$$

Table 4.1
Values of η Corresponding to Critical Periods
for Maximum Precipitation in the Interval t_1

	η_1	η_2	η_3	η_4	η_5
Dist. I	0.1902,	0.236,	0.308,	0.447,	<u>0.813</u> , ∞
Dist. II	0.2103,	0.267,	0.365,	0.576,	<u>1.397</u>

The largest physically reasonable values of η for precipitation Distributions I and II are underlined in Table 4.1. However, it should be mentioned that in the case of Distribution I, precipitation patterns of period $2.25 t_1$ and longer have precipitation totals that exceed those for $\eta = 0.813$; in fact, as $T \rightarrow \infty$ in Equation (24), we obtain upon integrating with respect to t_1 ,

$$P(x_1, t_1) \longrightarrow \bar{P}(x_1) t_1 + \Delta P t_1, \quad (29)$$

which corresponds to the maximum hourly rate of precipitation persisting for the entire duration of t_1 . This limiting case, given by Equation (29), gives unrealistically high estimates of $P(x_1, t_1)$, since in a strong southwesterly basic flow, the frontal waves are rapidly moving. For this reason, the underlined values of η correspond to more realistic estimates of $P(x_1, t_1)$.

In nature, the time distribution of the hourly precipitation rate will never be a simple sine (or cosine) curve; rather, the representation of the hourly rate of precipitation may require a continuous spectrum, in which will be the periods corresponding to the critical ones. The total precipitation resulting from a complex time distribution of hourly precipitation is, however, less than the total precipitation resulting from the presence of the most adverse period alone, provided the maximum hourly precipitation in the two cases is the same.

Consider the simple case in which only two periods describe the time distribution—the most adverse period, T_c , and any other period, T_2 (such that $T_c > T_2$). The total precipitation, P_2 , at x_1 during the time interval t_1 is

$$P_2(x_1, t_1) = \bar{P}(x_1) t_1 + \Delta P_c(x_1) \frac{T_c}{2\pi} \sin\left(\frac{2\pi t_1}{T_c}\right) + \Delta P_2(x_1) \frac{T_2}{2\pi} \sin\left(\frac{2\pi t_1}{T_2}\right).$$

Subtracting P_2 from Equation (25) and assuming that the maximum hourly rate of precipitation is the same in the two idealized "storms" [that is, $\Delta P(x_1) = \Delta P_c(x_1) + \Delta P_2(x_1)$], we find

$$P - P_2 = \Delta P_2 \left[\frac{T_c}{2\pi} \sin\left(\frac{2\pi t_1}{T_c}\right) - \frac{T_2}{2\pi} \sin\left(\frac{2\pi t_1}{T_2}\right) \right].$$

Since, by assumption, $T_c > T_2$ and $\sin(2\pi t_1/T_c) = 1$, it is seen that P_2 equals P only if ΔP_2 is zero. Under these conditions, the practical result is that the total precipitation at x_1 during t_1 is a maximum for a simple sine distribution corresponding to the most adverse period.

5.1 THE CASE STUDY OF DECEMBER 1955 - THE FEATHER RIVER BASIN

In order to test the capability of the model to specify accumulated precipitation and its geographic distribution, we shall apply the model to the December 1955 storm.

This storm is marked by three periods of intense rainfall occurring at times nearly corresponding with upper air observations on (a) 1500 GCT, 19 December, (b) 0300 GCT, 22 December, and (c) 0300 GCT, 23 December. From these observations, it is possible to measure (or else compute) the parameters entering the models for orographic precipitation and frontal precipitation. The observed parameters are (a) the saturation potential temperature at 850 mb, (b) the observed wind for Oakland (and in particular the wind at 850 mb), (c) the height of the Central Valley inversion, (d) the slope of the valley inversion, and (e) the vertical velocity at the 500 mb level as determined by the two-level prediction model. The extreme value of each of these parameters found in the December 1955 storm is tabulated below:

Table 5.1
Maximum Values of Meteorological Parameters -
December 1955 Storm

θ_s at 850 mb	70°F
u at 850 mb	65 knots
Inversion height at beginning of profile strips	364 m
Inversion slope	0.001
w (at 500 mb)	11.2 cm/sec

No correction for adverse storm periodicity is used in the December 1955 storm since power spectrum analysis of the precipitation records at Brush Creek (a representative recording precipitation station on the windward slope) shows no evidence for significant spectral maxima at the critical periods. To eliminate the adverse periodicity correction from our study of this storm, we set $T_c=48$ hours in Equation (25); thus, the contribution of the periodic term in Equation (25) is zero.

With the substitution of the above values of the parameters (shown in Table 5.1) into the models discussed in Sections 2, 3, and 4, we obtain, by machine calculation, the 72-hour accumulated precipitation as a function of x on the three profiles of the Feather River Basin. Figures 11a, 11b, and 11c represent the calculated 72-hour isohyetal maps, corresponding to terminal fall velocities of 8 m/s, 6 m/s, and 4 m/s, respectively (where P_{min} in the time distribution is zero, and P_t is 0.12 inch per hour). The calculated 72-hour precipitation amounts are plotted at each vertical for the three profiles.

Consider the 72-hour precipitation pattern computed for a terminal fall velocity of 8 m/s. In this precipitation pattern, the orographic maxima stand out most dramatically; namely, along the western slope of the Sierra Nevada and to the rear of the basin on Profiles A and B. The largest 72-hour totals occur, of course, on the windward Sierra slope, since the assumed "large-sized" precipitation falls quickly from the moving air parcels. Spillover from the windward Sierra slope ceases on Profiles A and C near Mountain Meadows Reservoir and Last Chance Creek (located respectively at miles 92 and 95)--here the precipitation is frontal. However, on Profile B spillover and/or direct orographic precipitation exist the whole length of the profile, making the precipitation shadow less marked on Profile B than on Profiles A and C. The precipitation maxima at the northeastern ends of Profiles A and B are produced by ascent over a small, sharp rise in terrain on the basin rim.

As the terminal fall velocity of the raindrops is decreased, the spillover into the upper Feather River Basin increases at the expense of the orographic maxima on the windward slope. By extrapolating the isohyetal pattern to the portions of the leeward basin excluded from the calculation, the total basin precipitation increases slightly as the terminal fall velocity decreases. This is understandable in terms of the increased spillover and the geometry of the basin, in which the area of the "leeward" basin exceeds that of the "windward" basin significantly.

The observed 72-hour precipitation pattern for the December 1955 storm (for the period ending 0700 PST on December 22, 1955) is shown in Figure 12. A comparison of the computed precipitation patterns with the observed pattern gives the following salient points:

1. The observed precipitation pattern is not as detailed as the computed pattern; this arises from the sparse density of precipitation stations. It should be noted that only one precipitation station is located in a computed precipitation maximum. Because of

the large interval between the precipitation stations, many of the features in the computed pattern can not be directly confirmed. (The features might be confirmed, however, with the addition of a few new strategically-located precipitation stations.) The precipitation maximum to the rear of the leeward basin is unobserved by the current precipitation network.

2. The calculated pattern for the December 1955 storm with a raindrop terminal fall velocity $W_D = 6$ m/s compares quite well with the observed pattern for the portion of the basin covered by the profile strips. It should be noted that there exists reasonable agreement between the observed basin average precipitation (10.1 inches) and the calculated basin average precipitation (11.8 inches).
3. On windward slopes, the precipitation maxima in the observed pattern are smaller than in the predicted pattern. The observed precipitation may well be underestimated due to: (a) the influence of terrain slope on the precipitation catch as reported by Landsberg (1957) and Hamilton (1954), (b) the non-vertical fall of raindrops through the air above the rain gage, (c) the exposure of the gage, and (d) the intensity of the air flow past the rain gage. Using Hamilton's equation to estimate the precipitation measurement error, it is possible that the observed precipitation on upper windward slopes is underestimated by 20-30 per cent. In view of this possibility, the computed windward maxima appear to be quite acceptable.
4. Certain observed precipitation amounts may be seen to differ considerably from the computed amounts for the same location. In this regard, the following stations--Storrie, Strawberry Valley, Bullards Bar, and Greenville--should be checked for exposure of the rain gage and representativeness of the local terrain slope, in order to determine if there is any obvious reason for the discrepancy.

From the test case of December 1955, we conclude that the simple physical models proposed and the numerical methods employed are able to compute the rainfall distribution for a given intense storm. In the next two sections we shall consider the maximization of the parameters of the model in order to estimate the distribution of the 72-hour maximum possible precipitation for the Feather River Basin.

6.1 THE "NEAR-MAXIMUM" STORM

The purpose of this section is to obtain the distribution of the 72-hour precipitation in the Feather River Basin by estimating the extreme values of all parameters in the model with the exception of the horizontal wind field; this precipitation distribution is designated as the "near-maximum" storm. In the "near-maximum" storm, we will assume the horizontal wind field is that of the December 1955 storm. The parameters to be simultaneously maximized are given below with their estimated extreme values, and comments concerning their selection.

1. The critical periodicity of the synoptic-scale disturbance for the "near-maximum" storm is selected as 59 hours for the time distribution No. I. A critical period of 59 hours corresponds to the most adverse frequency short of a period of 162 hours or longer.
2. The saturation potential temperature of the moist tropical air mass (i.e., the air mass above the low-level inversion) is selected as 74°F . This extreme value of the saturation potential temperature exceeds the value of θ_s for the December 1955 storm by four degrees. To estimate the maximum value of θ_s , we will consider data concerning the

extreme range in sea surface temperature in winter for particular months and for one-degree intervals of latitude, as compiled by Bennett (1944). Although the sea surface temperature data cited is for the southern hemispheric winter, by selecting a latitude corresponding to the latitude of the northern hemispheric tropical source region (like 20° North), we can obtain an estimate of the range of θ_s for maritime tropical air in its source region, Palmer (1958). The interval between extreme sea surface temperatures in degrees Fahrenheit is shown below for the months of June, July, and August at 20°S latitude, from Bennett (1944),

June	July	August
6°F	6°F	7°F

From this data, the saturation potential temperature of maritime tropical air could be as much as three or four degrees higher than that in the December 1955 storm, or $\theta_s = 74^\circ\text{F}$. This latter value exceeds (by one degree) the highest value of θ_s at 700 and 850 mb during December (irrespective of wind direction) as reported from ten years of upper air data for Oakland, California (1946-1955), by the U. S. Weather Bureau (1958).

3. Assume P_{\min} (the minimum hourly rate of precipitation in the time distribution model) is 0.05 inch per hour.
4. The terminal fall velocity of the precipitation products is maximized at 8 m/s, since this selection places the largest precipitation amounts on the windward slope where it is available for rapid surface runoff.
5. The frontal hourly rate of precipitation is assumed to be twice that of the December 1955 storm. [The validity of this assumption could be tested by the application of Equations (22) and (23) to the extreme cases of precipitation associated with SW storm types during the decade (1946-1955).]

The 72-hour isohyetal map for the "near-maximum" storm is shown in Figure 13. The geometry of the pattern is similar to that in Figures 11a, b, c, which have been discussed in detail; however, the depths are significantly larger than in the December 1955 storm.

Once the 850 mb horizontal wind speed is maximized, the next step is to scale the "near-maximum" isohyetal map to this extreme wind condition. The question of how to scale the "near-maximum" storm to the estimated maximum possible storm is considered in the next section.

7.1 THE ESTIMATED MAXIMUM POSSIBLE STORM

Suppose we define the maximum possible storm as the largest accumulated precipitation that can reasonably be expected to occur for a given watershed during a 72-hour period. The specific problem considered in this section is that of reasonably scaling the "near-maximum" storm to the maximum possible storm. We shall proceed in three steps: (a) the estimated maximum possible storm will be calculated by simultaneously maximizing *all* the parameters in the model, (b) a critique of this procedure will then be offered, and (c) a more reasonable method of scaling to the maximum possible storm will be proposed.

The simultaneous maximization of all parameters in the model may be achieved in the following way: if the 850 mb extreme wind exceeds the 850 mb wind used in the December 1955 storm by a factor C, and if it is assumed that the wind at all levels is similarly scaled, then the orographic precipitation scales by a factor of C. In addition, if it is assumed that the perturbation

vorticity is the same as in the "near-maximum" storm, the frontal contribution to the precipitation also scales by a factor of C. Under these conditions, the isohyetal map of the estimated maximum possible storm (as well as the mean depth of water applied to the basin) can be produced by multiplying the isohyets of the "near-maximum" storm (or its mean depth of water) by the factor C. An adaptation of Gumbel's extreme value theory, reported by Gringorten (1959), enables us to compute the extreme wind at 850 mb for periods of 50, 100, and 500 years. The results of the calculation, with a 95 per cent confidence limit, are tabulated below with the corresponding scaling factor C. The simultaneous maximization of *all* parameters leads to the 72-hour accumulated precipitation (Column 4 below) for the portion of the Feather River Basin covered by the profile strips.

Period	u_{max}	Scaling Factor C	$P(72)_{max}$
50 yrs	89 knots	1.34	27.9 inches
100 yrs	93 knots	1.41	29.4 inches
500 yrs	103 knots	1.56	32.5 inches

If the u_{max} for the 500-year period is selected for the development of the maximum possible storm, the 72-hour mean accumulated precipitation with simultaneous maximization of parameters is 32.5 inches in the portion of the Feather River Basin covered by the profile strips. This accumulated precipitation exceeds the greatest observed mean basin depth by a factor of 2.75. Since the simultaneous maximization of all parameters leads to a very large mean basin depth, it might be well to consider conditions under which simultaneous maximization is physically inconsistent.

During southwest storm types, it may well be argued that when the basic flow is very strong, any frontal wave disturbance forming in this current will move very rapidly towards the northeast. The rapid northeast movement is important for two reasons. First, the travel time of the disturbance from its place of birth to the Sierra Nevada will be so short that the wave will have little chance for development. Secondly, the wave disturbance, by virtue of its rapid movement, will spend little time over the Sierra watersheds. It therefore seems physically inconsistent to maximize simultaneously the wind normal to the barrier and the precipitation from synoptic-scale disturbances.

Suppose we now consider a way to estimate maximum possible precipitation devoid of simultaneous parameter maximization. All parameters with the exception of the precipitation of synoptic-scale disturbances will be maximized, and then the precipitation from the synoptic scale is approximated by a reasonable upper limit consistent with other extreme parameter values. We shall estimate the upper limit of the precipitation from the synoptic scale by the observed synoptic-scale precipitation, 0.12 inch per hour, in the December 1955 storm. To scale the "near-maximum" storm to maximum possible precipitation for non-simultaneous parameter maximization, we proceed as follows. From Equation (25) we obtain the change in $P(x_1, 72)$, designated by $\delta P(x_1, 72)$, for a change in frontal precipitation, δP_f .

$$\delta P(x_1, 72) = 36 \delta P_f + \frac{T}{4\pi} \delta P_f.$$

The change in P_f is equal to -0.255 inch per hour,* so that the change in $P(x_1, 72)$ is -10.36 inches. So, to obtain the 72-hour isohyetal map of the maximum possible precipitation from the "near-maximum" storm, we use

$$P_{\max}(x_1, 72) = 1.56 P_{n.\max}(x_1, 72) - 10.36. \quad (30)$$

The resulting estimated 72-hour maximum possible precipitation for the Feather River Basin (e.g. those portions covered by the profile strips) is reduced from 32.5 inches to a more reasonable estimate of 22.1 inches. The corresponding 72-hour isohyetal map of the maximum possible storm for the Feather River Basin is shown in Figure 14.

The numerical results obtained in this study for the Feather River Basin are shown in Table 7.1; the upper part summarizes the 72-hour accumulated precipitation for the portion of the basin covered by the profile strips. The lower part of Table 7.1 gives the results extended to cover the entire basin. The estimated maximum possible 72-hour storm (extended to the entire Feather River Basin) has a mean basin depth of 19.3 inches. This result is ten per cent less than the preliminary (December) estimate by the Hydrometeorological Section of the U. S. Weather Bureau (unpublished paper, March 1959).

Table 7.1
Average 72-Hour Precipitation
Feather River Basin

Storm	Terminal Fall Velocity	Depth (Windward)	Depth (Leeward)	Depth (Windward & Leeward)
FOR PORTION OF BASIN INCLUDED WITHIN PROFILE STRIPS.				
Dec. 19-22, 1955 observed*	---	16.0 in	7.0 in	10.1 in
Dec. 1955 calculated	8 m/s	18.5 in	8.3 in	11.9 in
Dec. 1955 calculated	6 m/s	16.6 in	9.1 in	11.8 in
Dec. 1955 calculated	4 m/s	14.1 in	9.9 in	11.4 in
"Near-Maximum"	8 m/s	28.5 in	16.7 in	20.8 in
Estimated Maximum Possible	8 m/s	34.1 in	15.8 in	22.1 in
FOR ENTIRE BASIN.				
Dec. 19-22, 1955 observed*	---	16.0 in	6.5 in	8.9 in
"Near-Maximum"	8 m/s	28.5 in	15.8 in	19.0 in
Estimated Maximum Possible	8 m/s	34.1 in	14.3 in	19.3 in

* For the 72-hour period ending 0700 PST, December 22, 1955.

8.1 CONCLUDING REMARKS

The objectives accomplished in this hydrometeorological study may be summarized as follows:

* When the scaling factor of 1.56 is applied to $P_f = 0.24$, we get $0.24 \times 1.56 = 0.375$. Thus, if we adopt $P_f = 0.12$, the change in P_f would be $0.12 - 0.375 = -0.255$ inch per hour.

1. A physical model and numerical methods have been devised for the computation of maximum possible precipitation produced by orographic ascent and large-scale synoptic processes over large watersheds;
2. The spillover and its geographical distribution can be calculated with the assumption of uniform but extreme drop size;
3. The application of the model and the computing methods to the December 1955 storm shows the capability of the model in describing the distribution of precipitation over a large watershed like the Feather River Basin;
4. The 72-hour isohyetal map for the "near-maximum" storm has been calculated; this isohyetal map may be simply scaled to the estimated maximum possible storm by means of the "wind scaling" factor C and Equation (30);
5. A machine program now exists so that the distribution of maximum possible precipitation over a given large watershed may be computed, given the geometry of the terrain in simplified profiles, the extreme values of certain meteorological parameters (enumerated in Table 5.1), and the critical period $T_C(t_1)$.

It should be stressed, however, that the model and the machine program should not be applied to watersheds in regions where the major precipitation results from intense convective activity. In such regions, the extreme value and duration of high intensity precipitation of small spatial scale must be estimated in other ways.

Certain limitations in the methodology of this study exist and represent areas for future endeavor. First, no completely adequate method currently exists for computing the three-dimensional spatial distribution of vertical velocity of large-scale atmospheric disturbances; however, future basic research may furnish the necessary computing methods and meteorological case studies. Secondly, a statistical study of the annual extreme vorticity in southwesterly type storms (in California) is needed in order to insure that this parameter is maximized consistently in the proposed model. Thirdly, the assumption that condensation products form in a uniform, large drop size is physically unrealistic; however, this assumption maximizes the precipitation on the windward slope.

It may well be appropriate to outline, briefly, areas in which future hydrometeorological research would be advantageous:

1. The capability of the proposed model to delineate the distribution of 24- to 72-hour precipitation should be tested in other hydrometeorological case studies.
2. In computing the wind scaling factor (using Gumbel's theory of extreme values) the sample of annual extremes numbers only thirteen; because of the small sample size, the scaling factor may be overestimated. We may be able to increase the size of the sample by applying the model diagnostically to the extreme annual storms for the past 20 to 50 years.
3. A statistical study of the annual extreme value of vorticity in southwesterly type storms is needed to insure that the vorticity is maximized consistently.
4. A power spectrum analysis of the hourly precipitation in several major storms should be performed to determine the relative importance of different frequencies to total precipitation, and to aid in the extrapolation of the results from large watersheds to watersheds of small area.

5. Sea surface temperature anomalies should be studied on a monthly basis in order to determine their magnitude, spatial extent, and time duration; work of this type is being performed by Mr. J. F. T. Saur and Mr. L. E. Eber of the Bureau of Commercial Fisheries, Biological Laboratory, Stanford University. Liaison with this group may well be advantageous.
6. Since the proposed model for predicting the "maximum possible" precipitation results in an isohyetal map of greater detail than can be observed in the Feather River Basin, it would be interesting to increase the density of precipitation stations in this basin. The purpose of such a program would be to verify the features in the predicted isohyetal maps (for southwest storm types) that are currently unobservable.
7. To facilitate future applications of the code to other basins and to meteorological case studies, a manual for computers and programmers might be profitably prepared, describing the input, the operations required between computing phases, and the program structure.

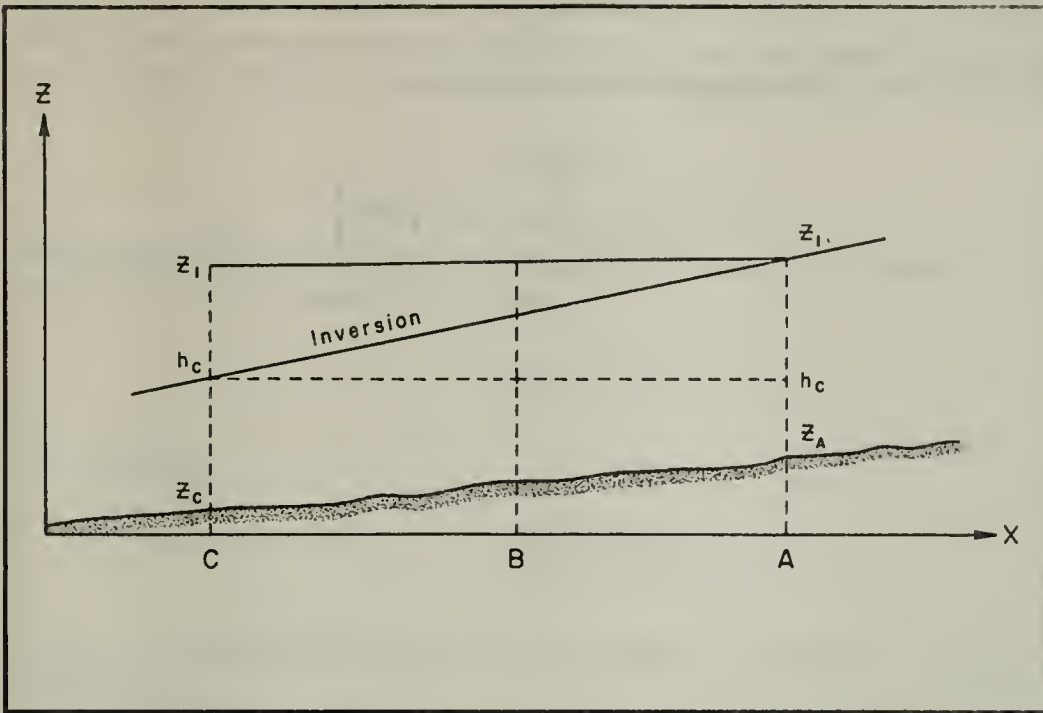
REFERENCES

1. Bennett, M. A. F. (1944), "Note on Sea Surface Temperature between New Zealand and Samoa". Misc. Met. Notes, Meteorological Office, Air Department, Wellington, New Zealand.
2. Bjerknæs, J. (1940), "A Method of Approximate Computation of Orographic Precipitation". Unpublished report for the U. S. Engineers.
3. Bjerknæs, J. (1946), "Report to the Chief of the U. S. Engineers about Methods in use at the Hydrometeorological Section of the U. S. Weather Bureau for Computation of Maximum Possible Precipitation". Unpublished.
4. Burns, Joseph I. (1959). Private communication.
5. Byers, H. (1944), "General Meteorology". McGraw-Hill Co., p. 386.
6. Charney, J. and Phillips, N. A. (1953), "Numerical Integration of the Quasi-Geostrophic Equation for Barotropic and Simple Baroclinic Flow". Journal of Meteor., Vol. 10, No. 2, p. 71.
7. Döös, Bo R. (1958), "The Effect of the Vertical Variation of Wind and Stability on Mountain Waves". Technical Report No. 13, Project NR-082-071, Contract NONR-1600(00), Office of Naval Research.
8. Douglas, R. H., et al (1957), "Pattern in the Vertical of Snow Generation". Journal of Meteor., Vol. 14, No. 2, pp. 95-114.
9. Eliassen, A. (1955), "Lectures in Physical Weather Prediction". University of California at Los Angeles.
10. Eliassen, A. (1957), "Handbuch der Physik", Vol. 48.
11. Gates, W. L. (1958). Paper presented to the American Meteorological Society Seminar, Los Angeles, California.
12. Gringorten, I. I. (1959), "Extreme Value Statistics--A Revised Application". Paper presented to the San Diego Meeting of the AMS, June 1959.
13. Hamilton, E. L. (1954), "Rainfall Sampling on Rugged Terrain". U. S. Department of Agriculture, Tech. Bulletin No. 1096, 41 pp.
14. Holmboe, J. (1944), "Dynamic Meteorology". John Wiley and Sons, Inc., New York, New York.
15. Holmboe, J. (1953), "The Upper Level Winds Project". Final Report, Contract W 28-099 ac-403, Geophysical Research Directorate, AFCRC, Cambridge, Mass.
16. Landsberg, H. E. (1957), "Review of Climatology, 1951-1957". Meteorological Monographs, Vol. 13, No. 12, pp. 1-43.
17. Levee, R. (1959). Private communication.
18. Meinzer, O. E. (1942), "Hydrology". Dover Publications, Inc., New York, New York.
19. Myers, V. (1959), "Factors in California Orographic Precipitation". Paper presented at the 177th Meeting of the AMS, San Diego, California, June 1959.

20. Palmer, C. E. (1958). Private communication.
21. Richtmyer, R. D. (1957), "*Difference Methods for Initial Value Problems*". Interscience Publishers, Inc., New York, New York.
22. Sawyer, J. S. and Bushby, F. H. (1953), "*A Baroclinic Model Atmosphere Suitable for Numerical Integration*". *Journal of Meteor.*, Vol. 10, No. 1, p. 54.
23. Smagorinsky, J. and Collins, C. O. (1955), "*On the Numerical Prediction of Precipitation*". *Monthly Weather Review*, Vol. 83, No. 3, pp. 53-68.
24. Smebye, S. J. (1958), "*Computation of Precipitation from Large-Scale Vertical Motion*". *Journal of Meteor.*, Vol. 15, No. 5, pp. 547-560.
25. Weaver, R. L. (1959), "*Types and Synoptic Characteristics of Major California Storms*". Paper presented to the 177th Meeting of the AMS, San Diego, California, June 1959.
26. U. S. Weather Bureau, Technical Paper No. 32 (1958), "*Upper Air Climatology of the United States, Part 2 - Extremes and Standard Deviations of Average Heights and Temperatures*".

APPENDIX A. THE COMPUTATION OF THE TOPOGRAPHY OF THE SACRAMENTO VALLEY INVERSION

The topography of the inversion, overlying the Sacramento Valley, may be calculated as follows. Consider the (x, z) profile, through verticals A, B, and C, shown in the following figure:



Schematic Sketch of Height Relationships used for Computing Inversion Slope

At the vertical B, a radiosonde station reports wind, temperature, pressure and mixing ratio as a function of height. From this data the inversion height on vertical B is known. Above the inversion the wind is normal to the mountains in the model; thus, the intersection of the isobaric surface with the (x, z) plane, above the inversion, is horizontal. Let $\rho(z)$ denote the density below the inversion, and $\rho'(z)$, the density above; then the station pressure at C is

$$p_C = p_C(z_1) + \int_{h_C}^{z_1} \rho' g \delta z + \int_{z_C}^{h_C} \rho g \delta z, \quad (\text{A.1})$$

and the station pressure at A is

$$p_A = p_A(z_1) + \int_{z_A}^{z_1} \rho g \delta z = p_A(z_1) + \int_{z_A}^{h_C} \rho g \delta z + \int_{h_C}^{z_1} \rho g \delta z. \quad (\text{A.2})$$

Subtracting (A.1) from (A.2) we obtain

$$p_A - p_C = \int_{h_C}^{z_1} (\rho - \rho') g \delta z - \int_{z_C}^{z_A} \rho g \delta z .$$

From the above equation the vertical distance $(z_1 - h_C)$ is

$$z_1 - h_C \approx \frac{1}{(\rho - \rho') g} \left[p_A - p_C + \int_{z_C}^{z_A} \rho g \delta z \right] .$$

APPENDIX B. THE COMPUTATIONAL STABILITY OF THE FINITE DIFFERENCE APPROXIMATION IN SECTION 2.2

In this appendix we shall explore (a) the stability of the finite difference approximation, Equation (11), and (b) the error introduced into the solution by the replacement of the partial differential equation, (8), by the finite difference equation, (11). The finite difference equation, approximating the first order differential equation, is said to be stable if the error introduced on i -th vertical is not percentually increased when propagated along the constant level z to the $(i+1)$ vertical. To test the stability we proceed as follows: consider Equation (8)

$$\frac{\partial u}{\partial x} = -u \cdot (x) F(x, z). \quad (8)$$

For a segment of the simplified profile the slope of the terrain is known, between the i and the $(i+1)$ vertical, and the above equation is of the form

$$\frac{\partial u}{\partial x} = -Au,$$

whose solution is

$$u = u_0 e^{-Ax}, \quad (B.1)$$

where u_0 is a constant determined by boundary conditions. The solution to the finite difference equation, (11),

$$u_{i+1} - u_i = -\xi A u_{i+1}, \quad (B.2)$$

is found by substituting

$$u_i = u_0 r^i \quad (B.3)$$

in Equation (B.2), solving for r in terms of ξA , and then substituting r in the general solution (B.3). In this way

$$r = \frac{1}{1 + \xi A},$$

and the solution to the finite difference equation is

$$u_{i+1} = u_0 \left(\frac{1}{1 + \xi A} \right)^{i+1}. \quad (B.4)$$

Consider the error δu_i ; the finite difference equation governing the way this error is propagated to the $(i+1)$ vertical is

$$\delta u_{i+1} - \delta u_i = -\xi A \delta u_{i+1}$$

The solution to this difference equation, with the boundary condition

$$i = 0, \quad \delta u = \delta u_0$$

is

$$\delta u_{i+1} = \delta u_0 \left(\frac{1}{1 + \xi A} \right)^{i+1} \quad (\text{B.5})$$

With Equations (B.4) and (B.5), the percentual error in the solution on the $i=0$, i and $i+1$ verticals is calculated as

$$\frac{\delta u_{i+1}}{u_{i+1}} = \frac{\delta u_i}{u_i} = \frac{\delta u_0}{u_0}$$

It is seen that an error introduced into the solution on the first vertical propagates through the solution without becoming percentually larger; thus, the proposed finite difference approximation satisfies a definition of stability, given by Levee (1959).

When a partial differential equation is replaced by a finite difference equation, an error, known as truncation error, is incurred. The truncation error, as defined by Richtmeyer (1957), is

$$\epsilon = \frac{u_{i+1} - u_i}{\xi} - \left(\frac{\partial u}{\partial x} \right)_{i+\frac{1}{2}} \quad (\text{B.6})$$

and this error ϵ may be calculated from the above equations in the following way. The substitution of (B.1) and (B.2) in Equation (B.6) gives

$$\epsilon = -A u_{i+1} - \left[-A u_0 e^{-A(i+\frac{1}{2})\xi} \right] \quad (\text{B.7})$$

From Equation (B.4), we can calculate a series expansion for

$$\ln \left(\frac{u_{i+1}}{u_0} \right) = -(i+1) \ln \left(\frac{1}{1 + \xi A} \right) = -(i+1) \left(\xi A - \frac{(\xi A)^2}{2} + \frac{(\xi A)^3}{3} \dots \dots \right)$$

or

$$u_{i+1} = u_0 e^{-(i+1) \left[\xi A - \frac{(\xi A)^2}{2} \dots \dots \right]}$$

The substitution of the above expression for u_{i+1} in Equation (B.7) gives

$$\epsilon = -Au_0 \left\{ e^{-(i+1) \left[\xi A - \frac{(\xi A)^2}{2} \dots \dots \right] - \frac{-A(i+1/2) \xi}{e}} \right\},$$

or

$$\epsilon = -Au_0 e^{-(i+1/2) \Lambda \xi} \left\{ e^{-\left[\frac{\xi A}{2} - \frac{(\xi A)^2}{2} \dots \dots \right] - 1} \right\}.$$

Retaining only first order terms in ϵA , the truncation error is

$$\epsilon = -Au_{i+1/2} \left\{ e^{-\frac{A\xi}{2} - 1} \right\}.$$

If for forced orographic ascent, $A < 0$, then the truncation error ϵ is positive; this means that the proposed finite difference approximation overestimates the intensity of the u and w fields. The percentual error is

$$\frac{\epsilon}{\partial u / \partial x} = \left\{ e^{-\frac{A\xi}{2} - 1} \right\}, \tag{B.8}$$

which for a slope of five per cent, corresponds to

$$A \approx - .03 \times 10^{-3}, \quad \text{and} \quad \frac{\epsilon}{\partial u / \partial x} \approx 0.05$$

This percentual error, although not negligible, is of a reasonable order so that the proposed finite difference approximation, Equation (B.2) will yield useful results.

It should, however, be mentioned that an alternative finite difference approximation is available; namely, if the first order partial differential equation is approximated by

$$u_{i+1} - u_i = -\frac{\xi A}{2} (u_{i+1} + u_i), \tag{B.9}$$

the solution of this difference equation can be shown to be

$$u_{i+1} = \left[\frac{1 - (\xi A/2)}{1 + (\xi A/2)} \right]^{i+1} u_0. \tag{B.10}$$

This alternative finite difference equation is stable, in that an error introduced on the i -th vertical is not percentually increased when propagated to the $(i+1)$ vertical; in addition, the finite difference approximation is more accurate than Equation (B.2) in that the truncation error introduced by (B.9) is second order in ξA , Levee (1959).

PAUSE

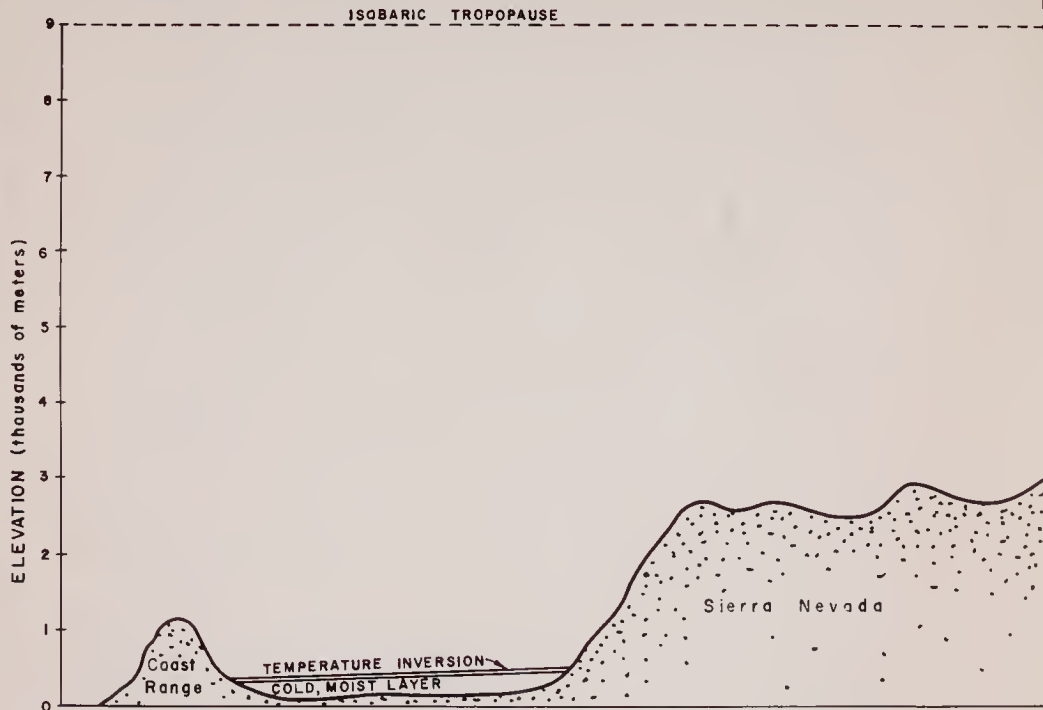


CALIFORNIA
WATER RESOURCES
AND CONSTRUCTION
NS BRANCH

OR ESTIMATING
LE PRECIPITATION

SECTION OF TERRAIN,
LEY INVERSION

Fig. 1



STATE OF CALIFORNIA
 DEPARTMENT OF WATER RESOURCES
 DIVISION OF DESIGN AND CONSTRUCTION

OPERATIONS BRANCH

PROCEDURES FOR ESTIMATING
MAXIMUM POSSIBLE PRECIPITATION

SCHEMATIC CROSS-SECTION OF TERRAIN,
 SHOWING VALLEY INVERSION

STATE OF CALIFORNIA
DEPARTMENT OF WATER RESOURCES
DIVISION OF DESIGN AND CONSTRUCTION

PROCEDURES FOR ESTIMATING
MAXIMUM POSSIBLE PRECIPITATION



LOCATION MAP
FEATHER RIVER BASIN

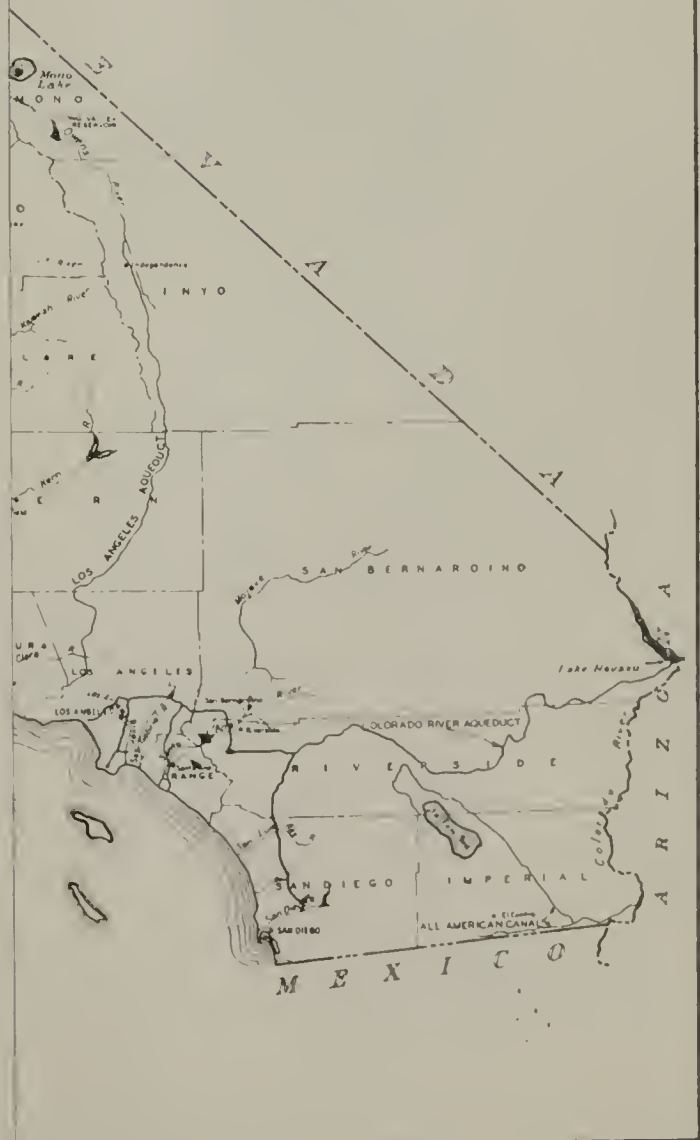


Fig. 20

STATE OF CALIFORNIA
DEPARTMENT OF WATER RESOURCES
DIVISION OF DESIGN AND CONSTRUCTION

PROCEDURES FOR ESTIMATING
MAXIMUM POSSIBLE PRECIPITATION

—+—
LOCATION MAP
FEATHER RIVER BASIN

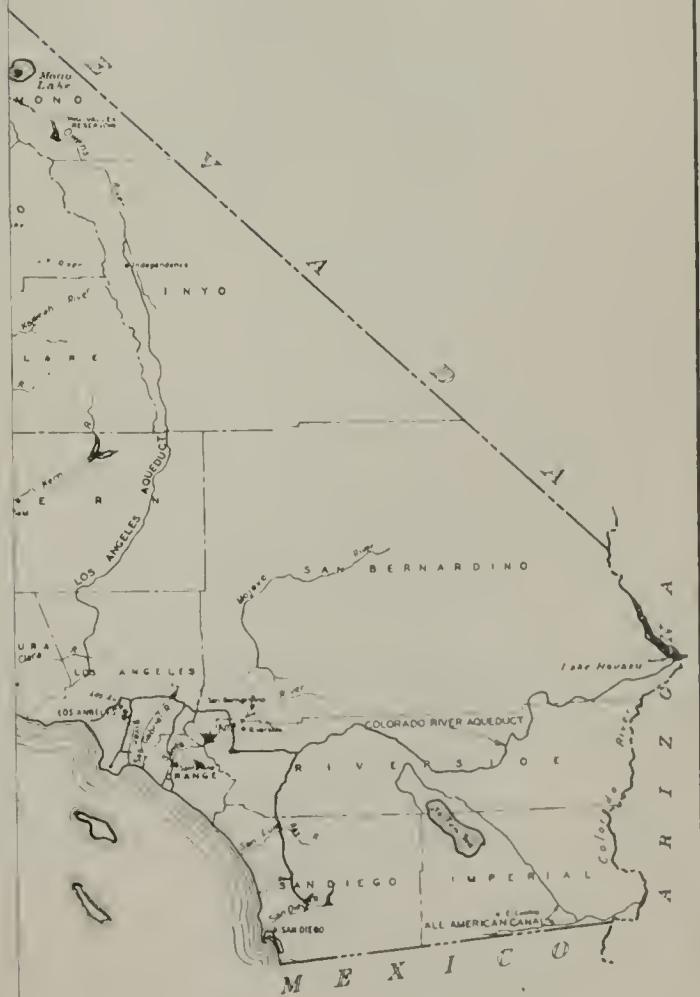
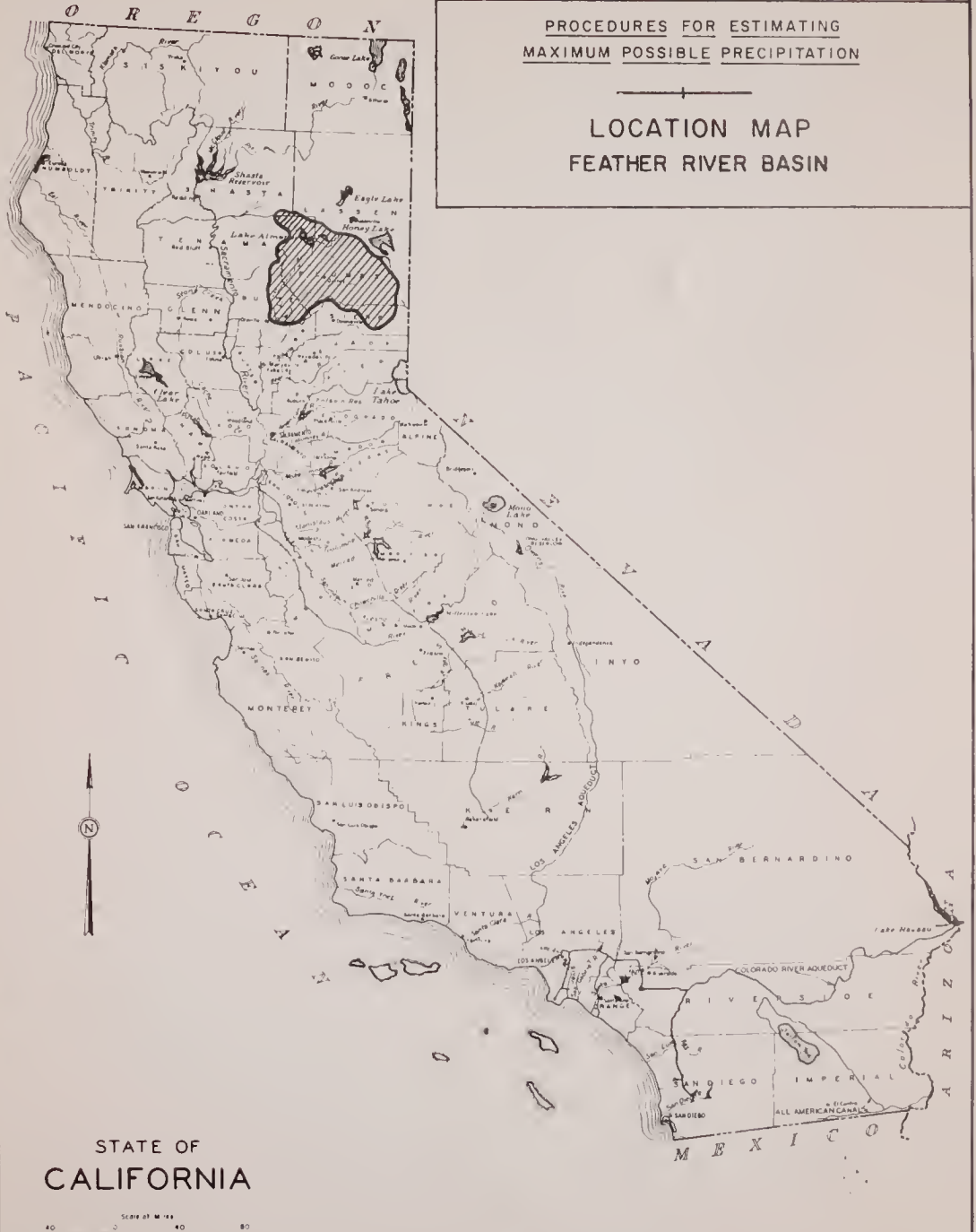


Fig. 20

PROCEDURES FOR ESTIMATING
MAXIMUM POSSIBLE PRECIPITATION

LOCATION MAP
FEATHER RIVER BASIN



STATE OF
CALIFORNIA

Scale of Miles
0 40 80

Fig. 2a

PROCEDURES FOR ESTIMATING
MAXIMUM POSSIBLE PRECIPITATION



LOCATION MAP
PROFILE STRIPS A, B. and C.

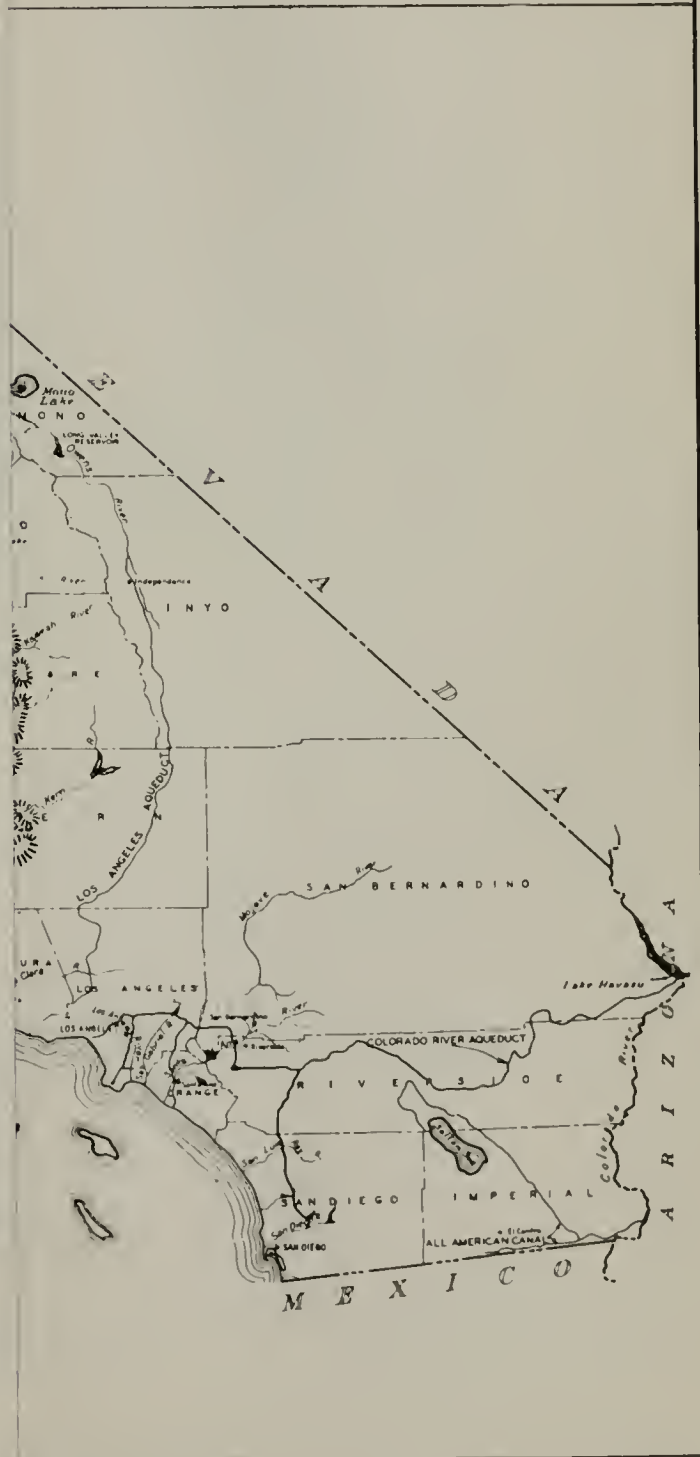


Fig. 2b

PROCEDURES FOR ESTIMATING
MAXIMUM POSSIBLE PRECIPITATION



LOCATION MAP
PROFILE STRIPS A, B. and C.

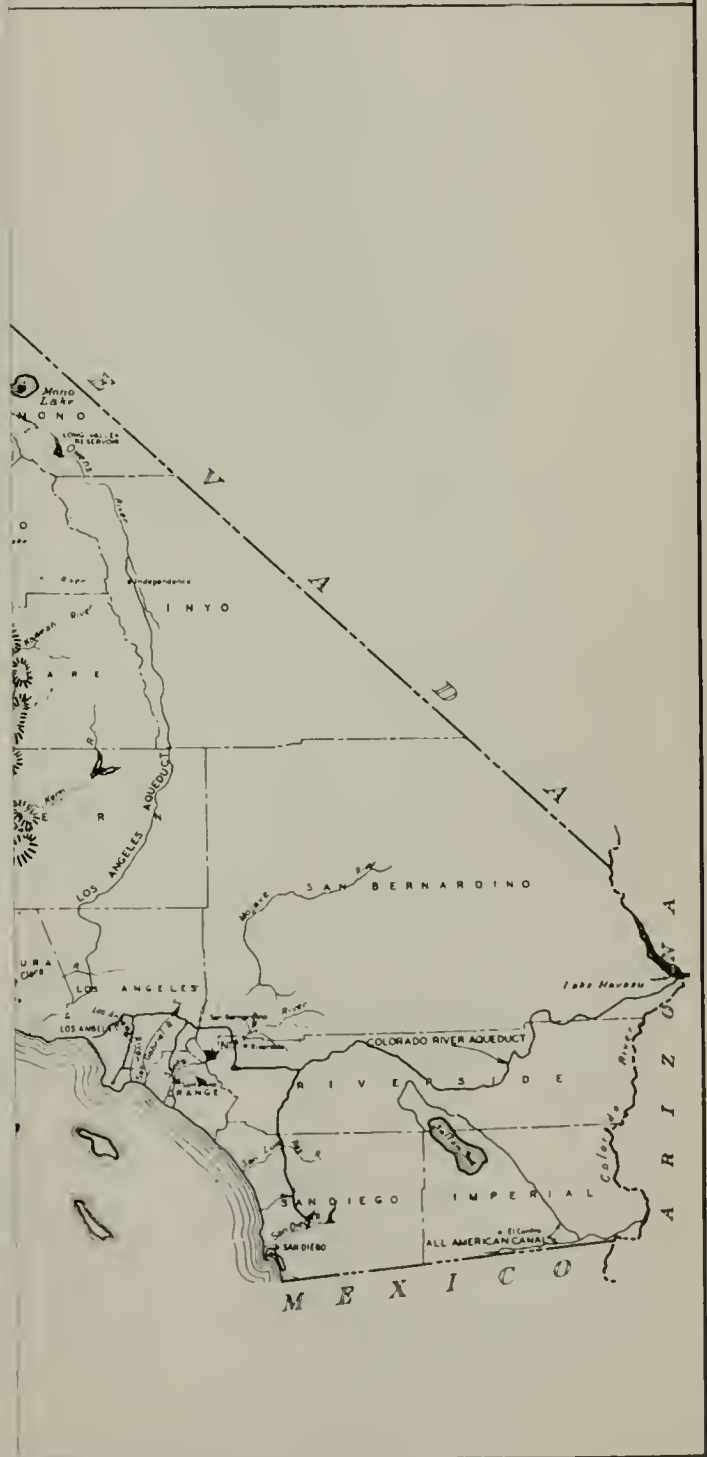


Fig. 2b

PROCEDURES FOR ESTIMATING
MAXIMUM POSSIBLE PRECIPITATION

LOCATION MAP
PROFILE STRIPS A, B, and C.

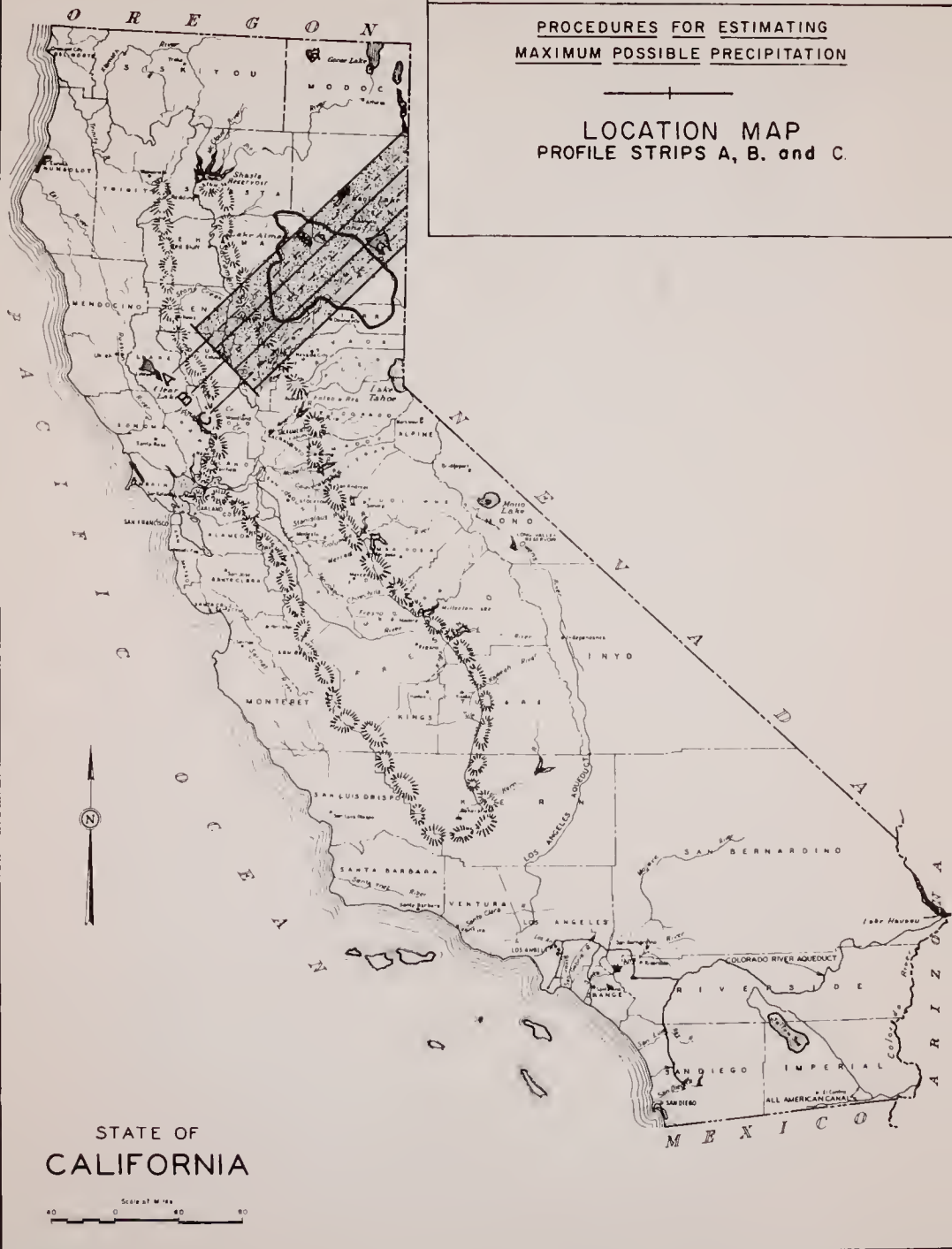
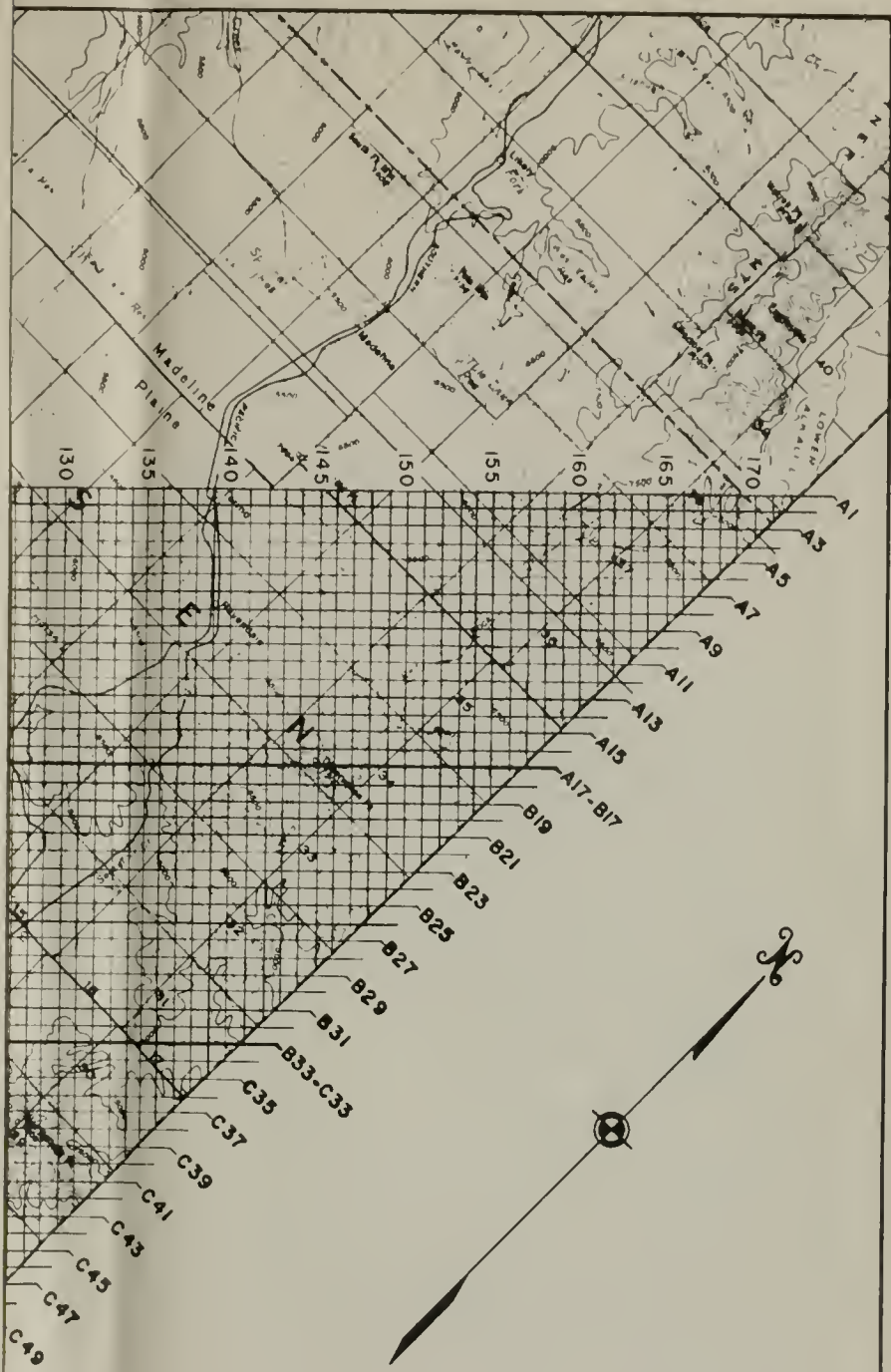


Fig. 2b



STATE OF CALIFORNIA
 DEPARTMENT OF WATER RESOURCES
 DIVISION OF DESIGN AND CONSTRUCTION
PROCEDURES FOR ESTIMATING
MAXIMUM POSSIBLE PRECIPITATION

DETAILED LOCATION OF PROFILES USED
 IN COMPUTER CALCULATIONS

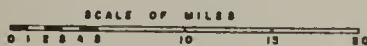
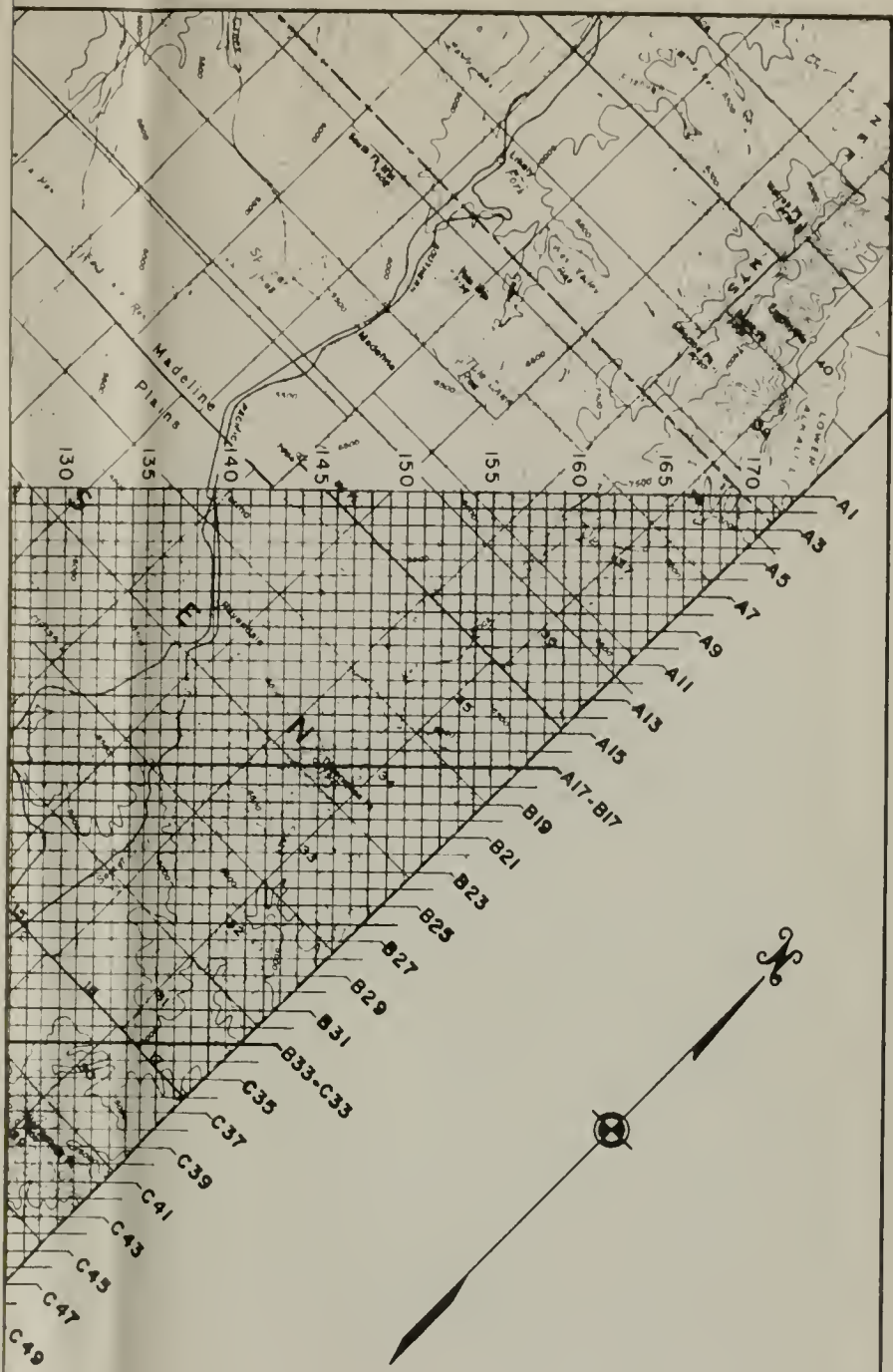


Fig 2c



STATE OF CALIFORNIA
 DEPARTMENT OF WATER RESOURCES
 DIVISION OF DESIGN AND CONSTRUCTION
PROCEDURES FOR ESTIMATING
MAXIMUM POSSIBLE PRECIPITATION

DETAILED LOCATION OF PROFILES USED
 IN COMPUTER CALCULATIONS

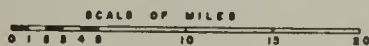


Fig 2c

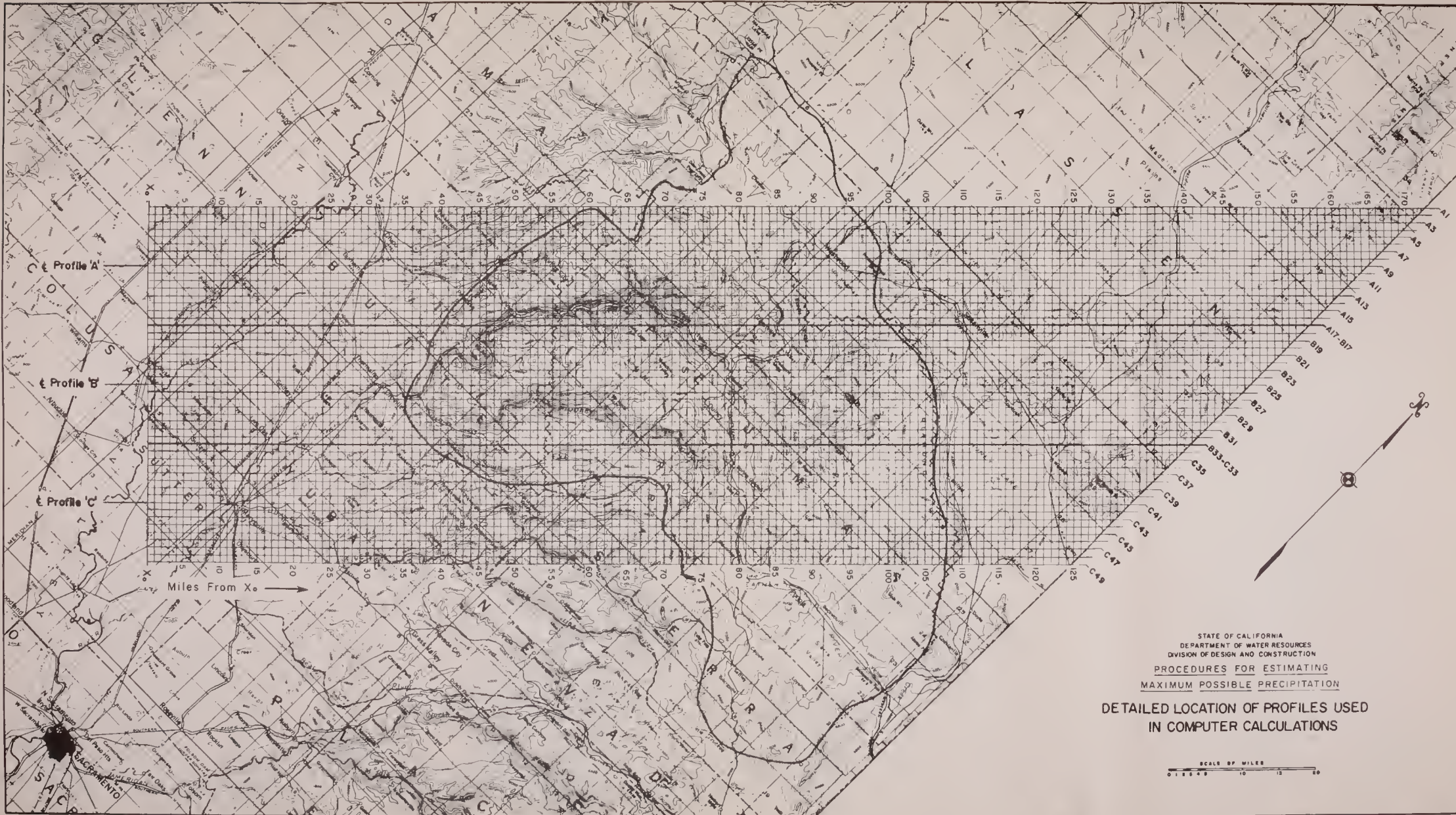
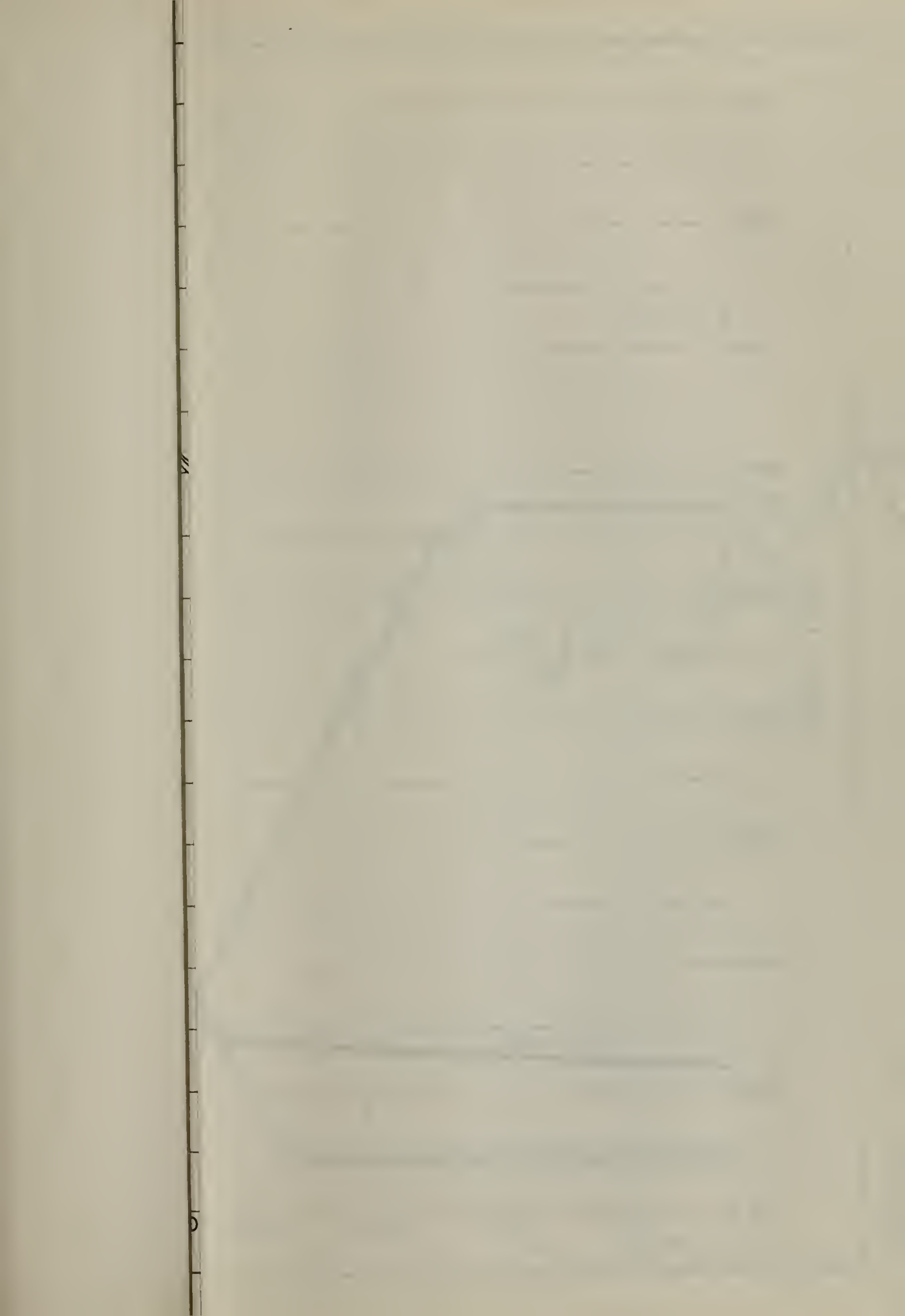
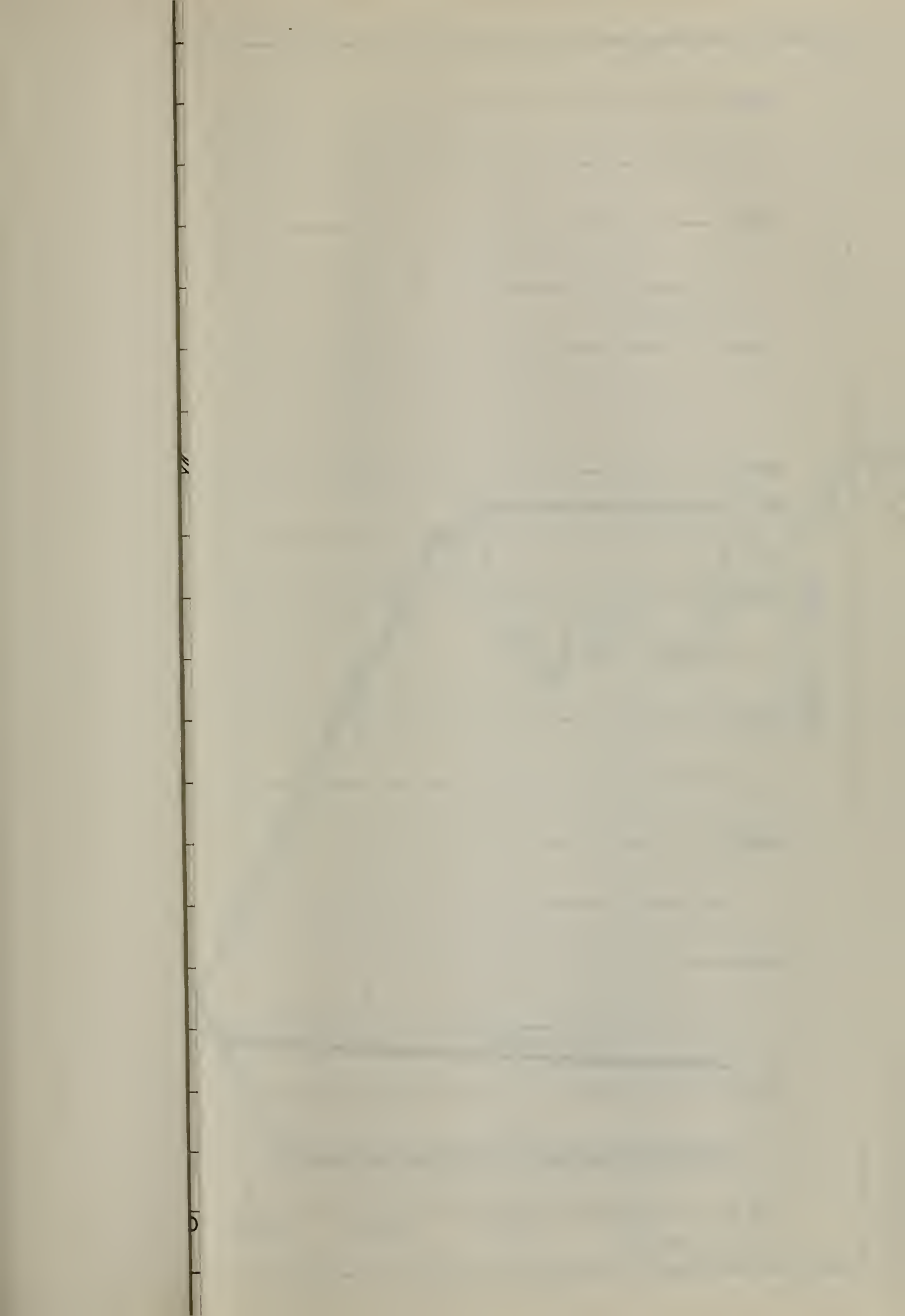
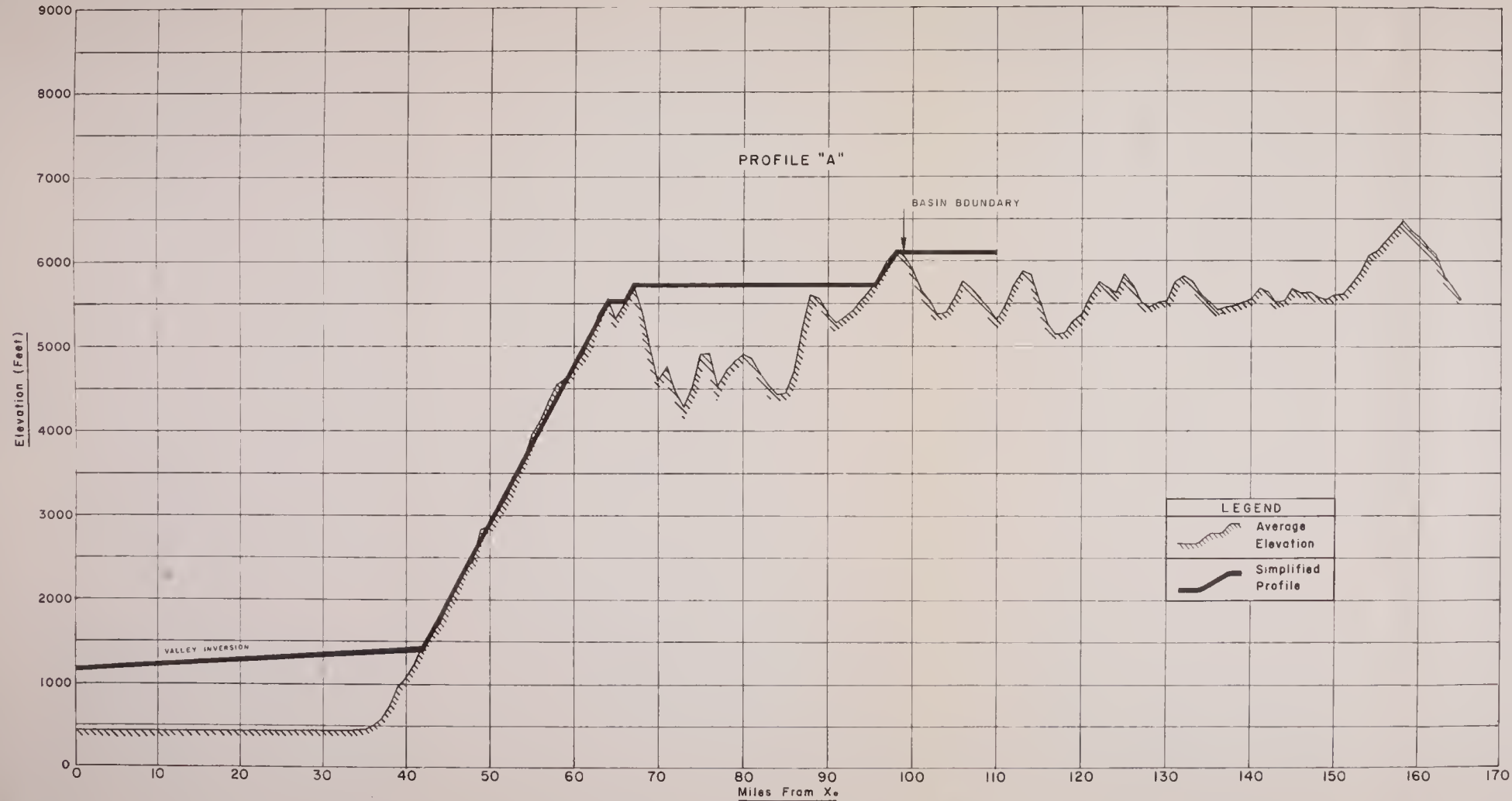


Fig 2c





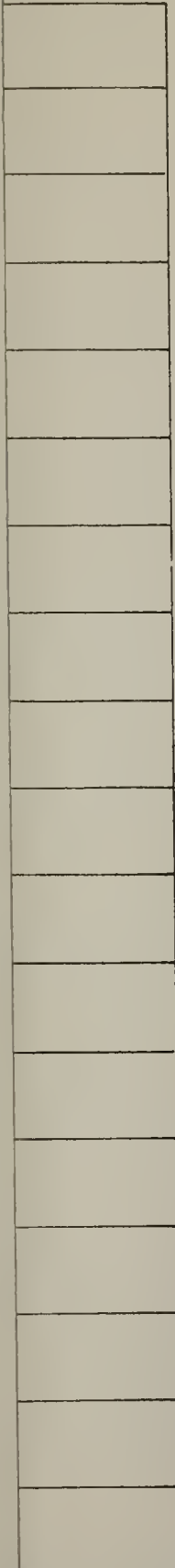


LEGEND
 Average Elevation
 Simplified Profile

STATE OF CALIFORNIA
 DEPARTMENT OF WATER RESOURCES
 DIVISION OF DESIGN AND CONSTRUCTION

PROCEDURES FOR ESTIMATING
 MAXIMUM POSSIBLE PRECIPITATION

AVERAGE ELEVATION OF PROFILE "A",
 Showing Simplified Profile Used
 In Computer Calculations.



0 170

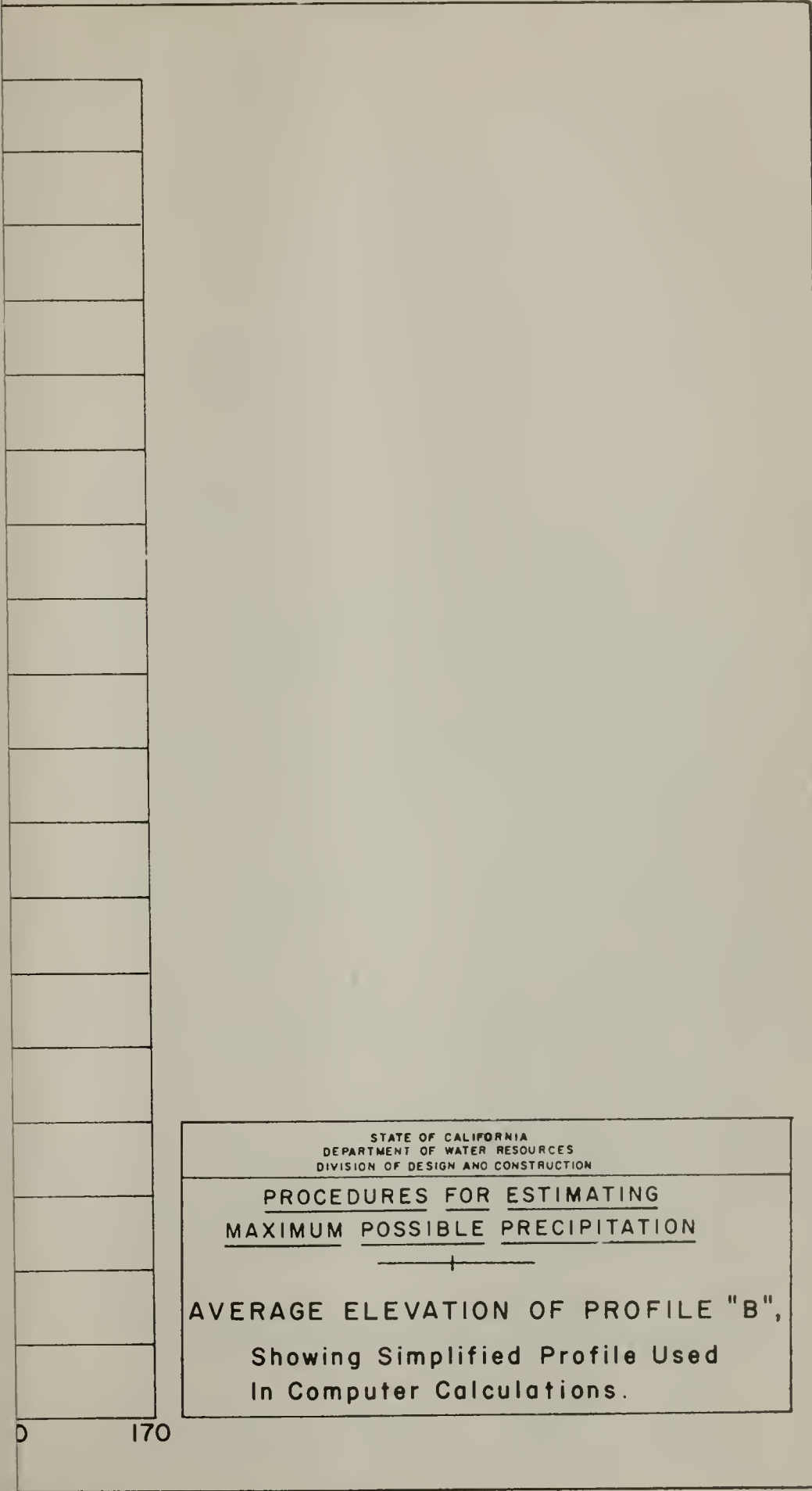
STATE OF CALIFORNIA
DEPARTMENT OF WATER RESOURCES
DIVISION OF DESIGN AND CONSTRUCTION

PROCEDURES FOR ESTIMATING
MAXIMUM POSSIBLE PRECIPITATION

—+—

AVERAGE ELEVATION OF PROFILE "B",
Showing Simplified Profile Used
In Computer Calculations.

Fig. 3b



STATE OF CALIFORNIA
DEPARTMENT OF WATER RESOURCES
DIVISION OF DESIGN AND CONSTRUCTION

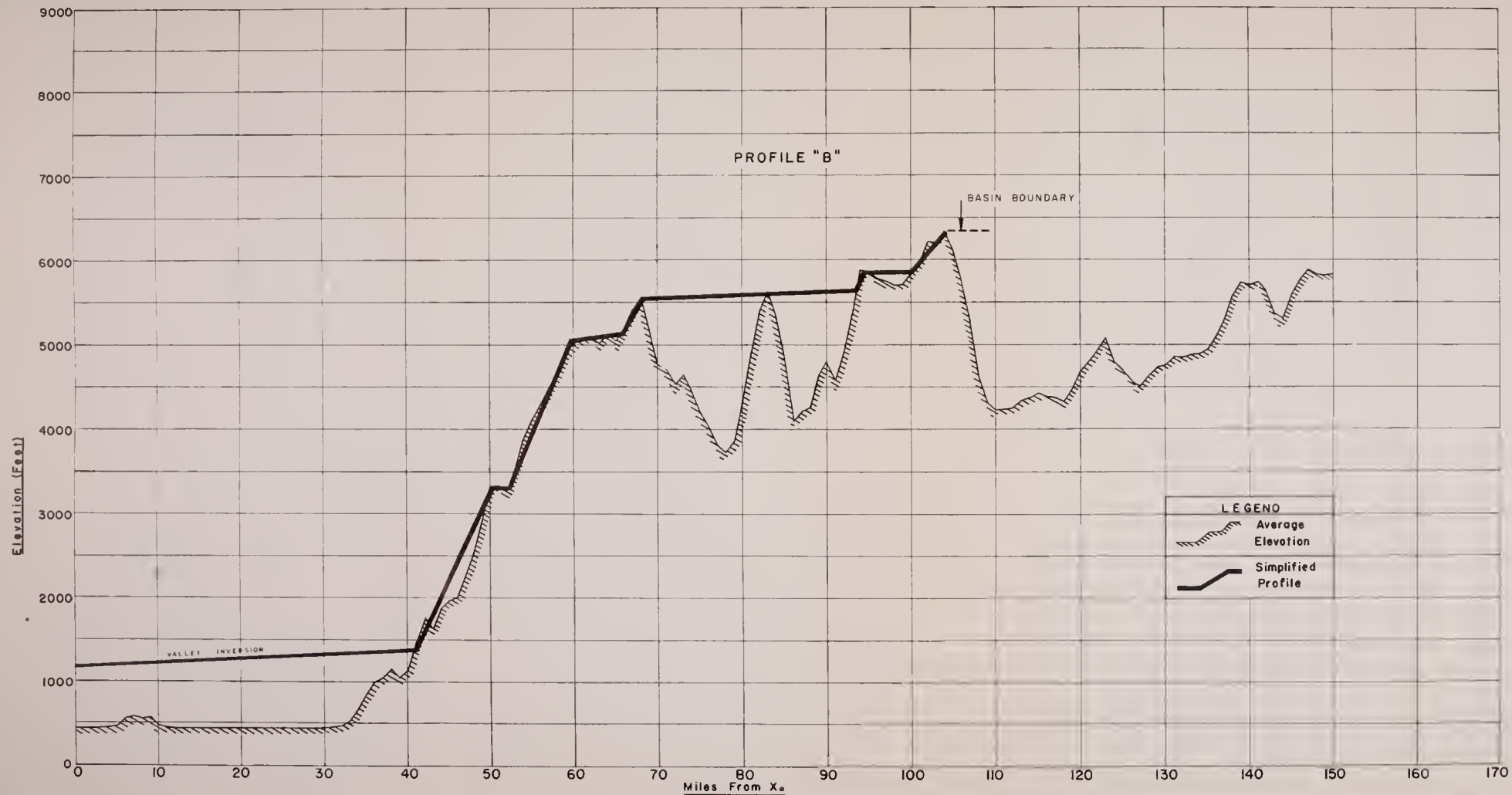
PROCEDURES FOR ESTIMATING
MAXIMUM POSSIBLE PRECIPITATION



AVERAGE ELEVATION OF PROFILE "B",
Showing Simplified Profile Used
In Computer Calculations.

0 170

Fig. 3b

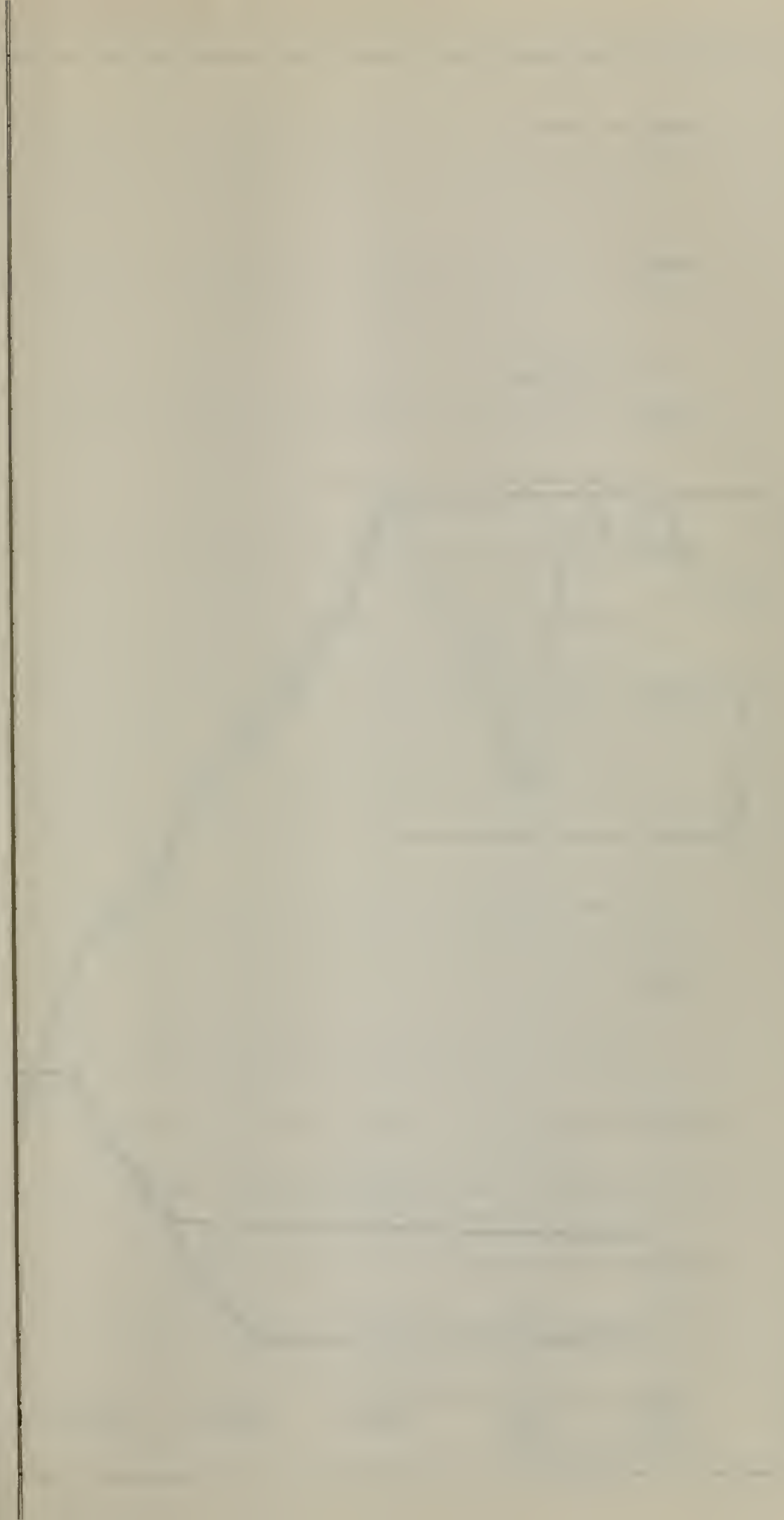


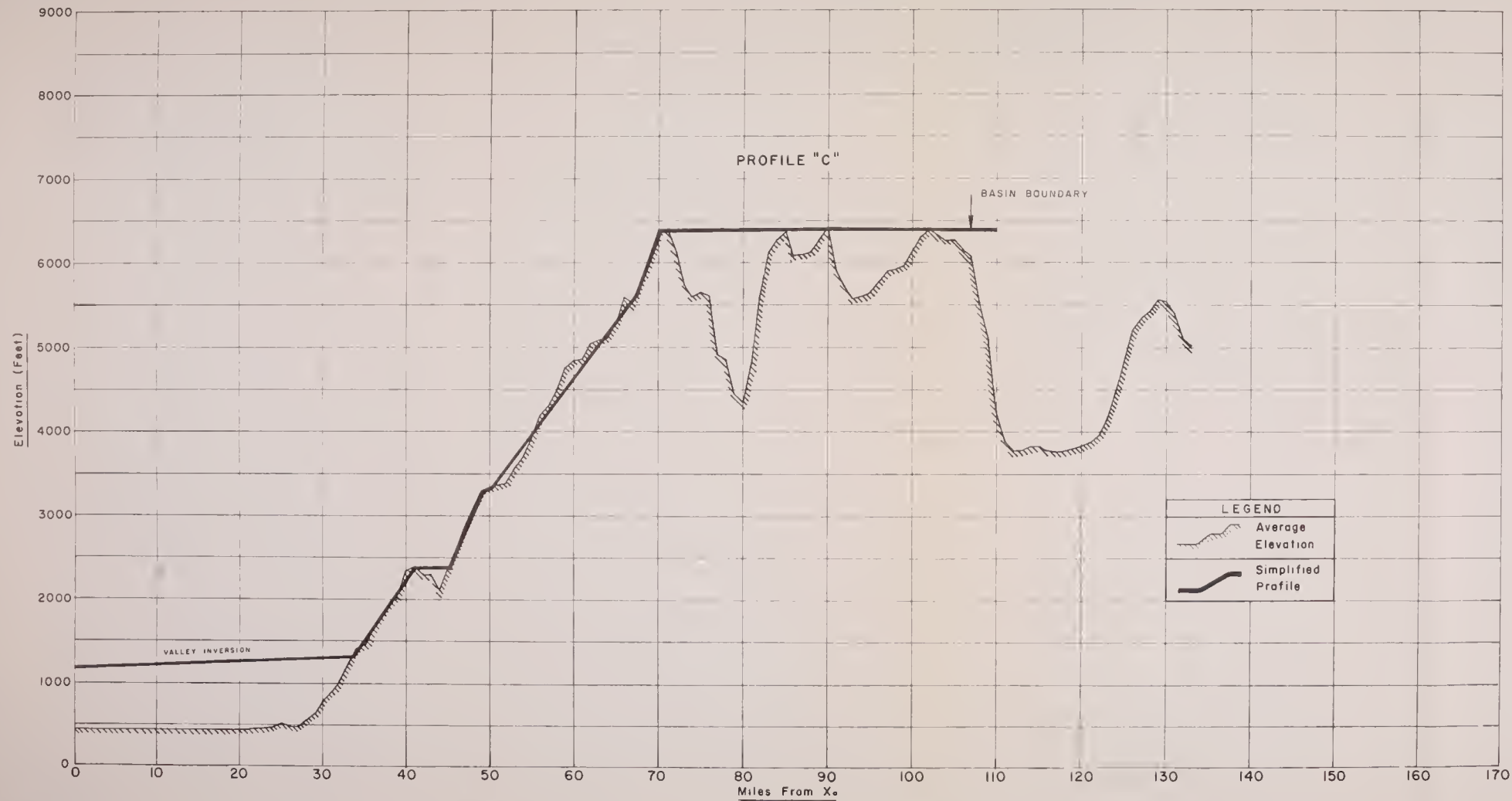
STATE OF CALIFORNIA
 DEPARTMENT OF WATER RESOURCES
 DIVISION OF DESIGN AND CONSTRUCTION

PROCEDURES FOR ESTIMATING
 MAXIMUM POSSIBLE PRECIPITATION

AVERAGE ELEVATION OF PROFILE "B",
 Showing Simplified Profile Used
 In Computer Calculations.





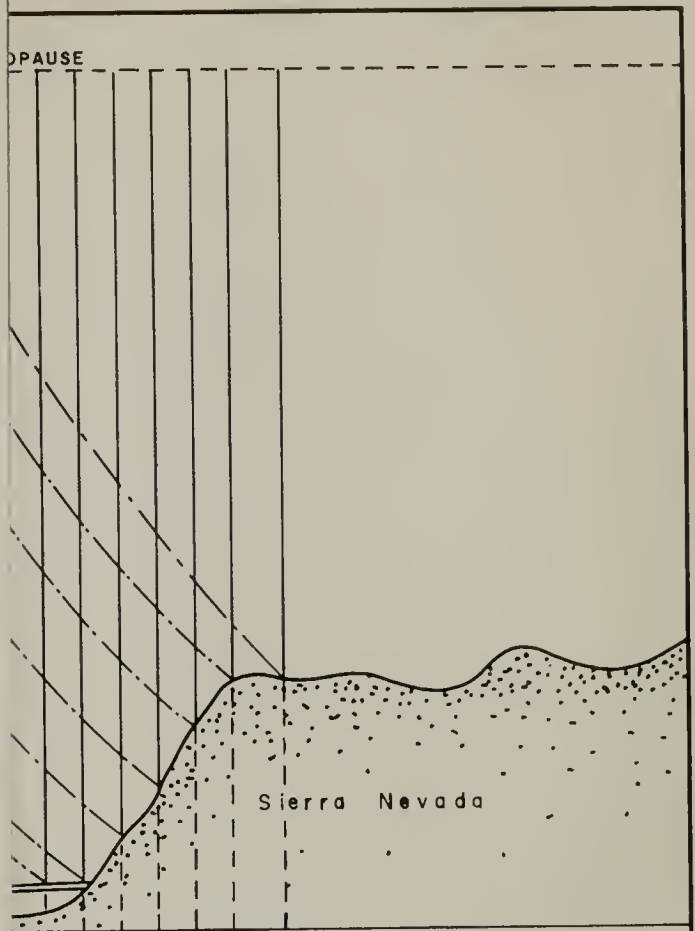


LEGEND	
	Average Elevation
	Simplified Profile

STATE OF CALIFORNIA
 DEPARTMENT OF WATER RESOURCES
 DIVISION OF DESIGN AND CONSTRUCTION

PROCEDURES FOR ESTIMATING
 MAXIMUM POSSIBLE PRECIPITATION

AVERAGE ELEVATION OF PROFILE "C",
 Showing Simplified Profile Used
 In Computer Calculations.



X1 X2 X3 X4 X5 X6 X7

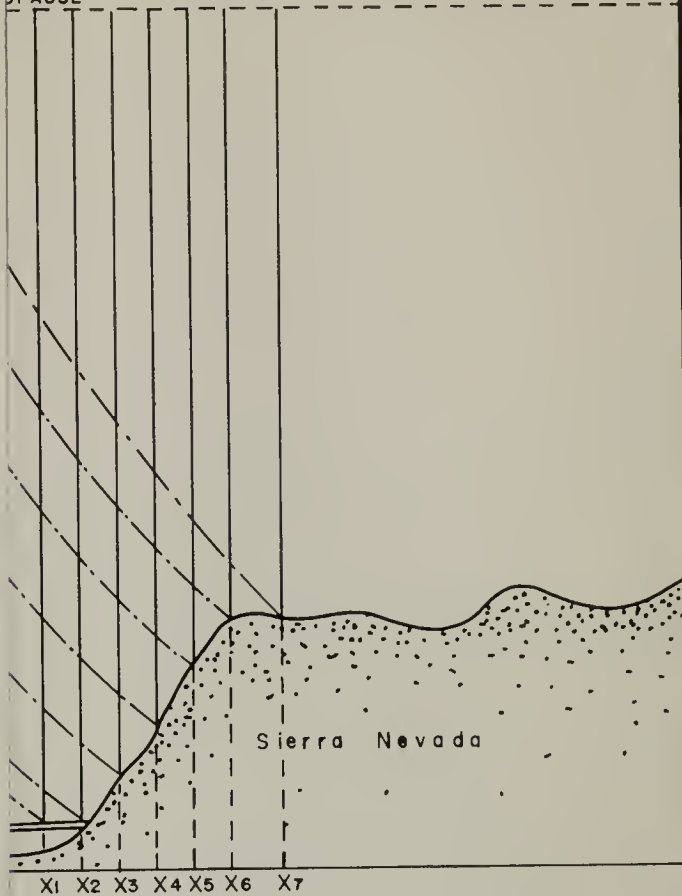
CALIFORNIA
 WATER RESOURCES
 AND CONSTRUCTION
 DIVISION
 TECHNICAL BRANCH

FOR ESTIMATING
PRECIPITATION

OF TRAJECTORIES
 OF PRECIPITATION PRODUCTS

Fig. 4

PAUSE

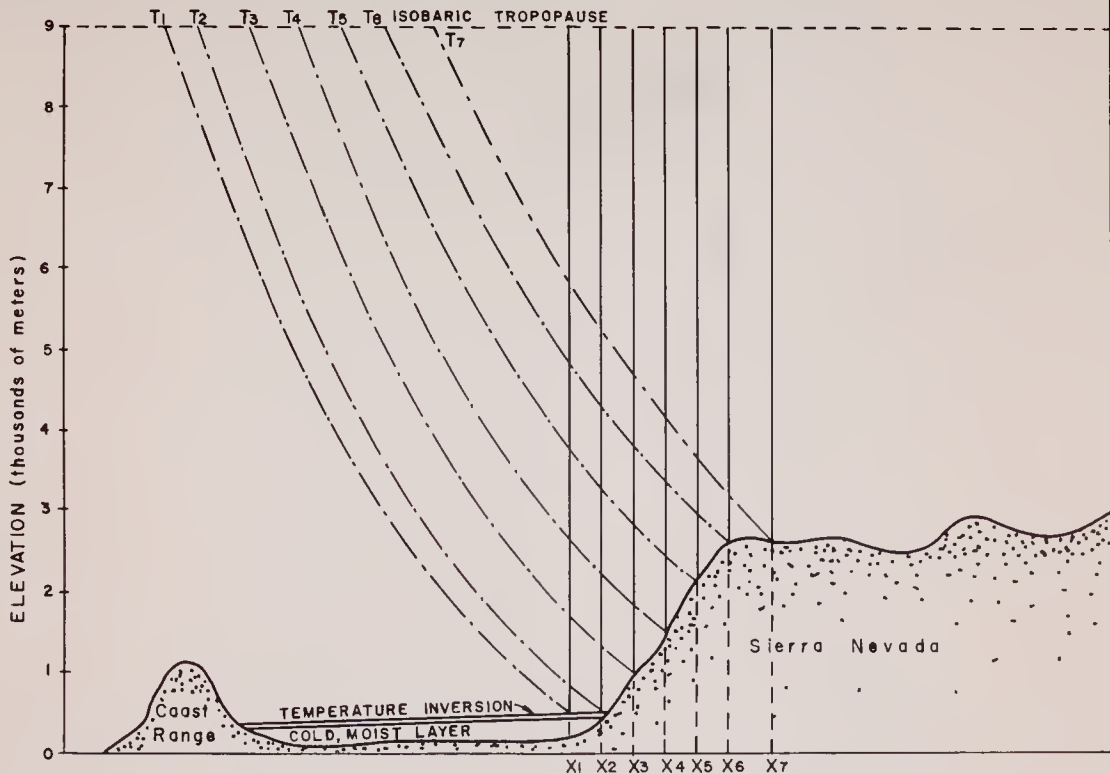


CALIFORNIA
WATER RESOURCES
AND CONSTRUCTION
DIVISION
SACRAMENTO BRANCH

FOR ESTIMATING
PRECIPITATION

OF TRAJECTORIES
OF PRECIPITATION PRODUCTS

Fig. 4

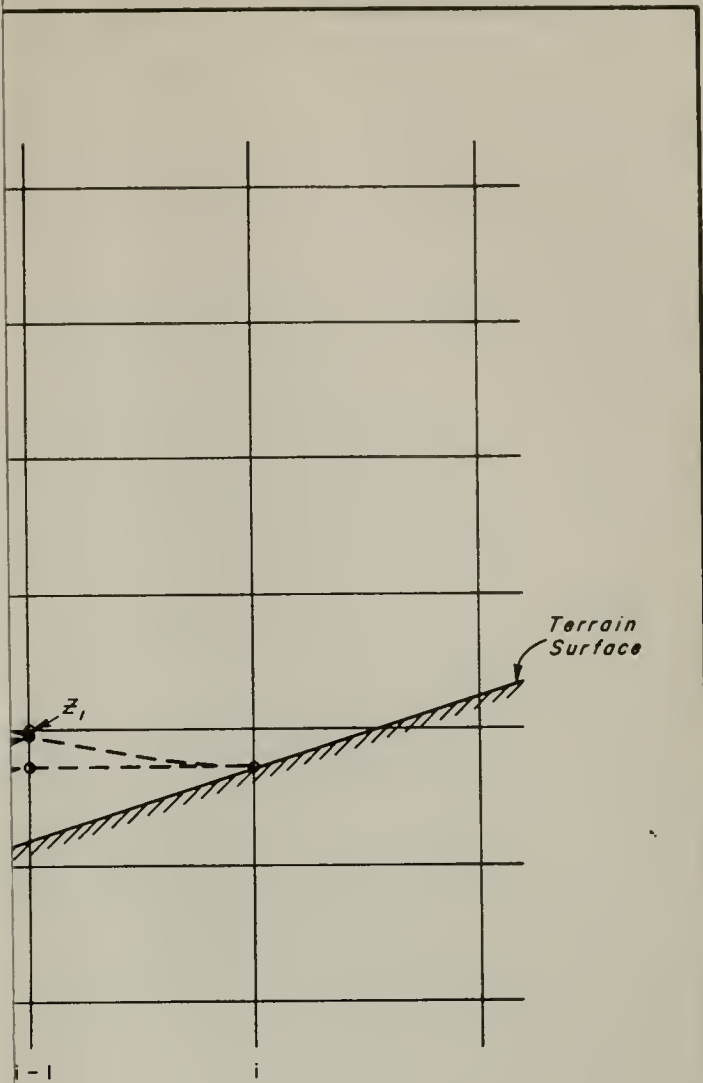


STATE OF CALIFORNIA
 DEPARTMENT OF WATER RESOURCES
 DIVISION OF DESIGN AND CONSTRUCTION
 OPERATIONS BRANCH

PROCEDURES FOR ESTIMATING
MAXIMUM POSSIBLE PRECIPITATION

—○○—
 SCHEMATIC DIAGRAM OF TRAJECTORIES
 OF PRECIPITATION PRODUCTS

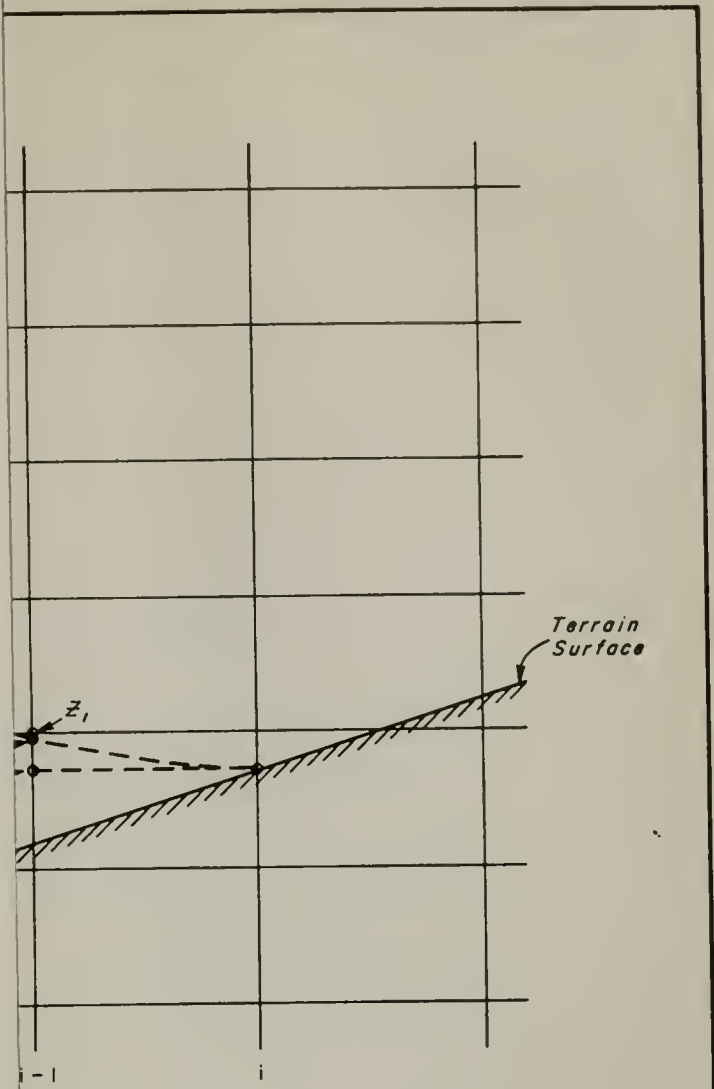
Fig. 4



OF CALIFORNIA
 OF WATER RESOURCES
 IGN AND CONSTRUCTION
 IONS BRANCH

FOR ESTIMATING
IBLE PRECIPITATION

—∞—
 A RAINDROP TRAJECTORY-
 COMPUTING SCHEME

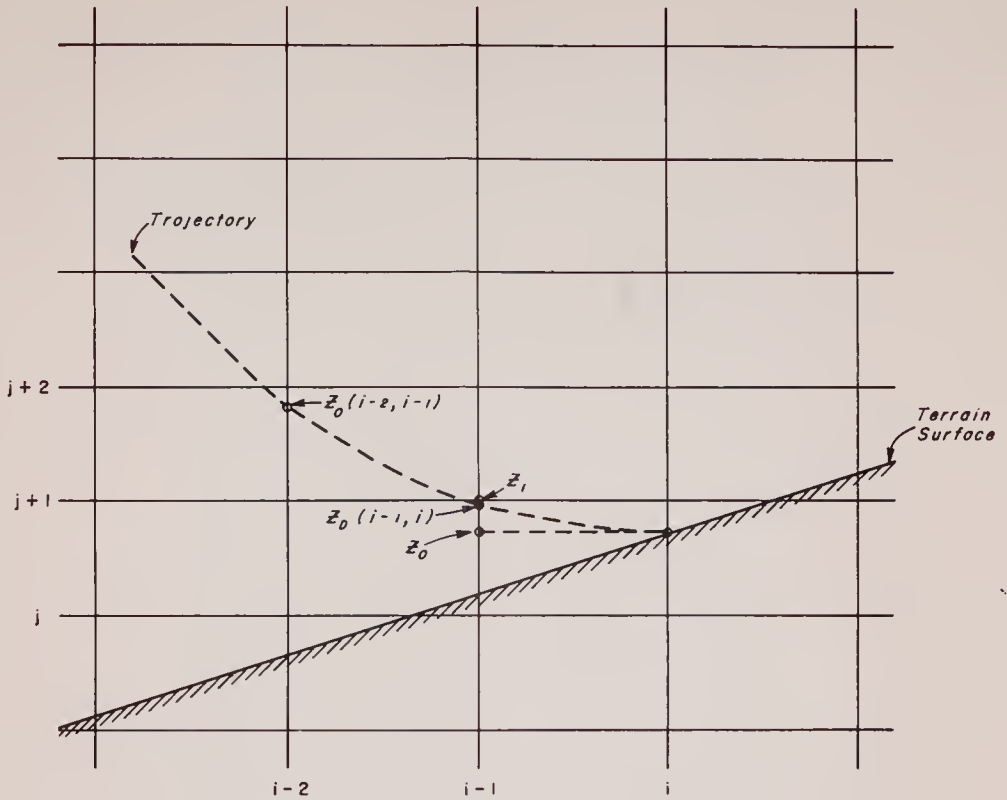


OF CALIFORNIA
 OF WATER RESOURCES
 IGN AND CONSTRUCTION
 IONS BRANCH

FOR ESTIMATING
IBLE PRECIPITATION

—∞—
 A RAINDROP TRAJECTORY-
 COMPUTING SCHEME

Fig. 5



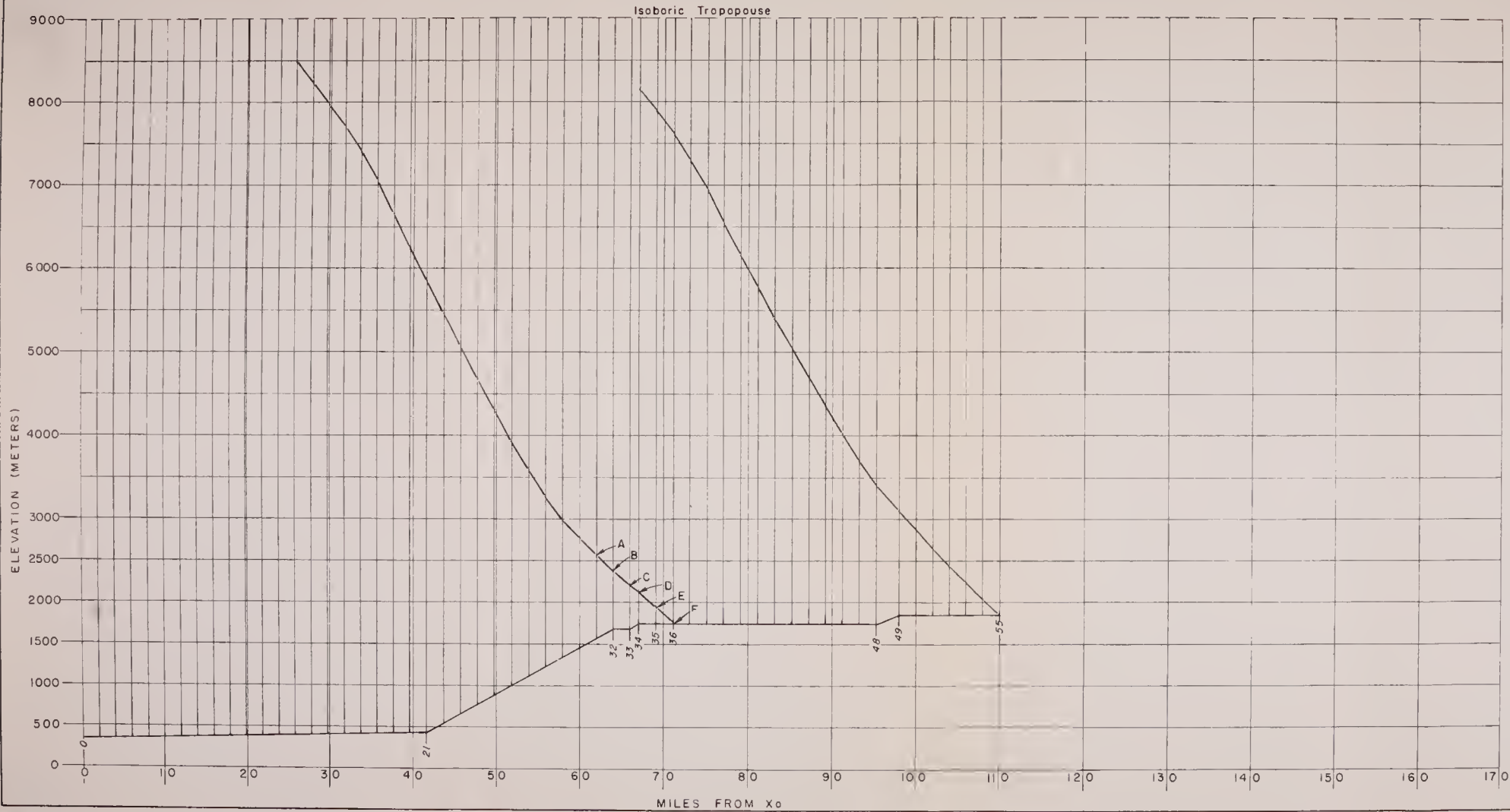
STATE OF CALIFORNIA
 DEPARTMENT OF WATER RESOURCES
 DIVISION OF DESIGN AND CONSTRUCTION

OPERATIONS BRANCH

PROCEDURES FOR ESTIMATING
MAXIMUM POSSIBLE PRECIPITATION

—oo—

SCHEMATIC DIAGRAM OF A RAINDROP TRAJECTORY—
 ILLUSTRATING THE COMPUTING SCHEME

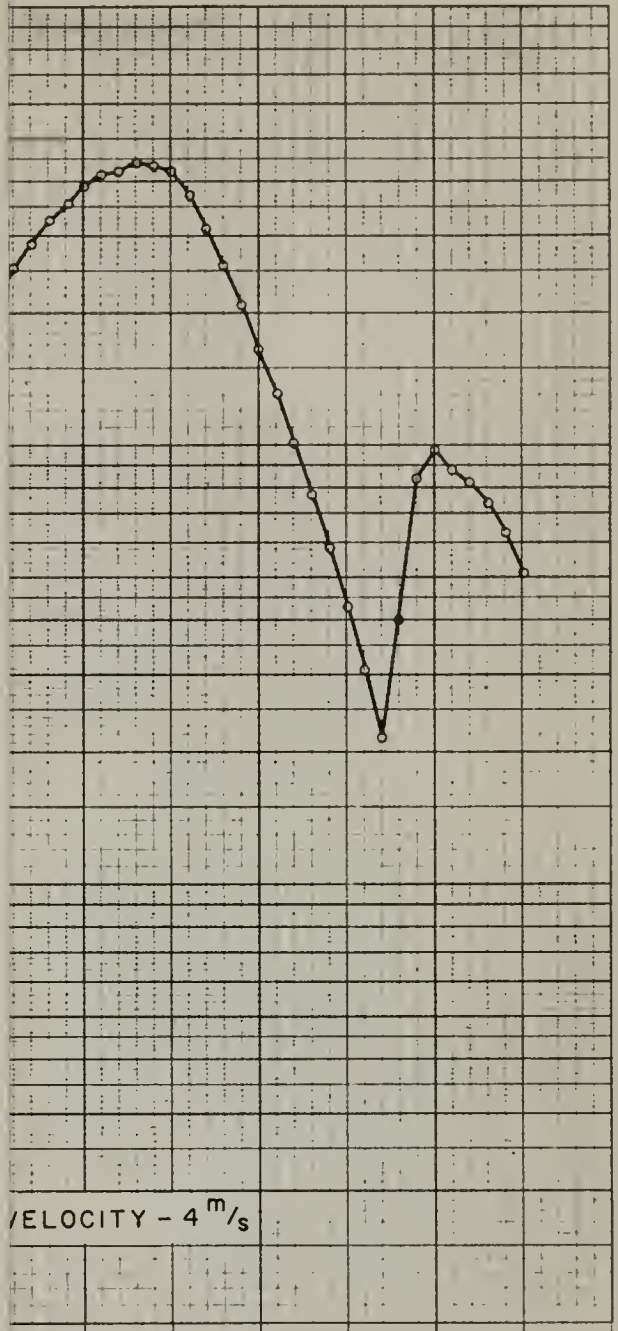


PROFILE "A"

NUMBER OF VERTICAL	MILES FROM X ₀	ELEVATION ON PROFILE (Meters)
0	0.0	364.00
21	41.72	431.14
32	64.0	1692.25
33	66.0	1692.25
34	67.0	1750.77
48	95.28	1750.77
49	98.0	1866.29
55	110.0	1866.29

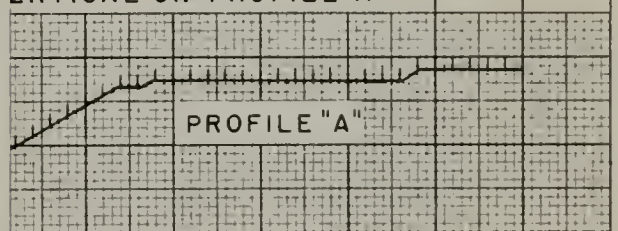
STATE OF CALIFORNIA
DEPARTMENT OF WATER RESOURCES
DIVISION OF DESIGN AND CONSTRUCTION
OPERATIONS BRANCH

**PROCEDURES FOR ESTIMATING
MAXIMUM POSSIBLE PRECIPITATION**
PLOT OF RAINDROP TRAJECTORIES
No 36 AND No 55 ON PROFILE "A"



VELOCITY - 4^m/s

VERTICAL ON PROFILE "A"



PROFILE "A"

UNIVERSITY OF CALIFORNIA
 DEPARTMENT OF WATER RESOURCES
 DESIGN AND CONSTRUCTION
 METHODS FOR ESTIMATING
 POSSIBLE PRECIPITATION

Fig. 7a

DAILY RATE OF OROGRAPHIC
 PROFILE "A", DEC. 1955 STORM

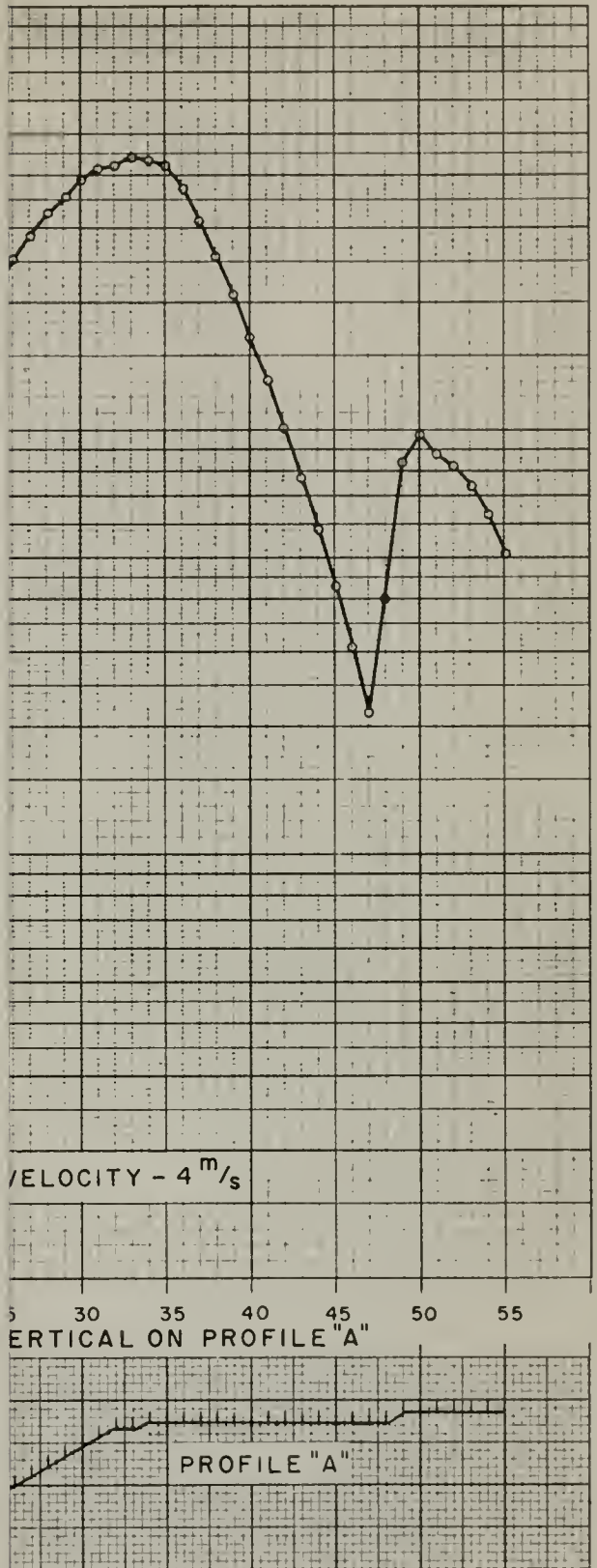


Fig. 7a

STATE OF CALIFORNIA
 DEPARTMENT OF WATER RESOURCES
 DESIGN AND CONSTRUCTION
 METHODS FOR ESTIMATING
 POSSIBLE PRECIPITATION

DAILY RATE OF OROGRAPHIC
 PRECIPITATION ON PROFILE "A", DEC. 1955 STORM

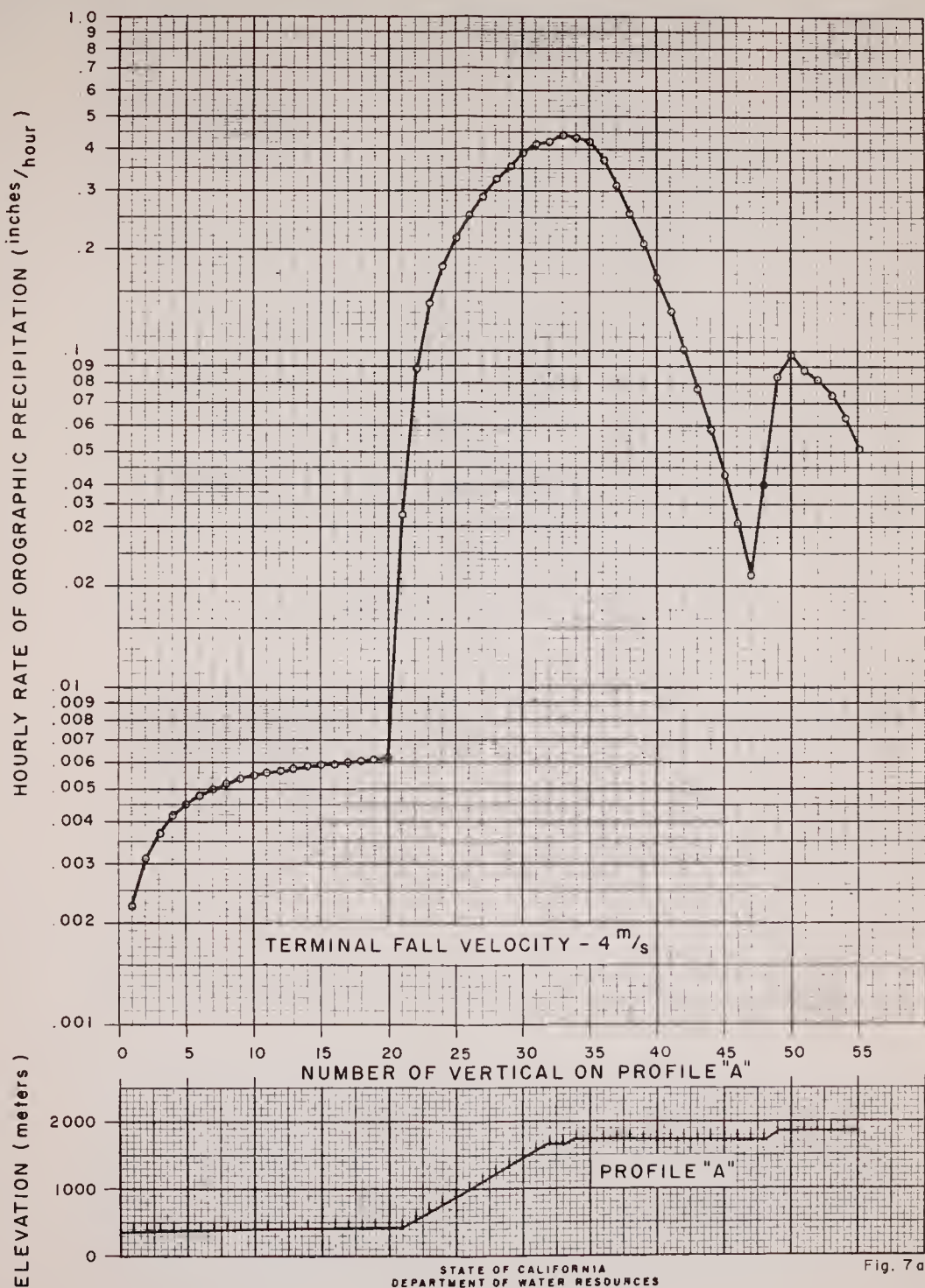
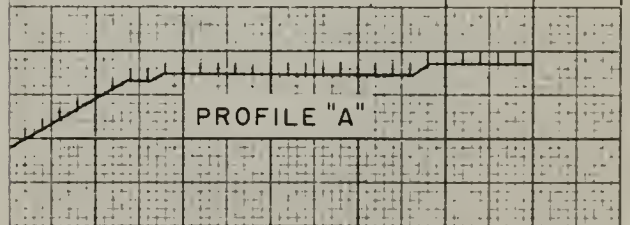
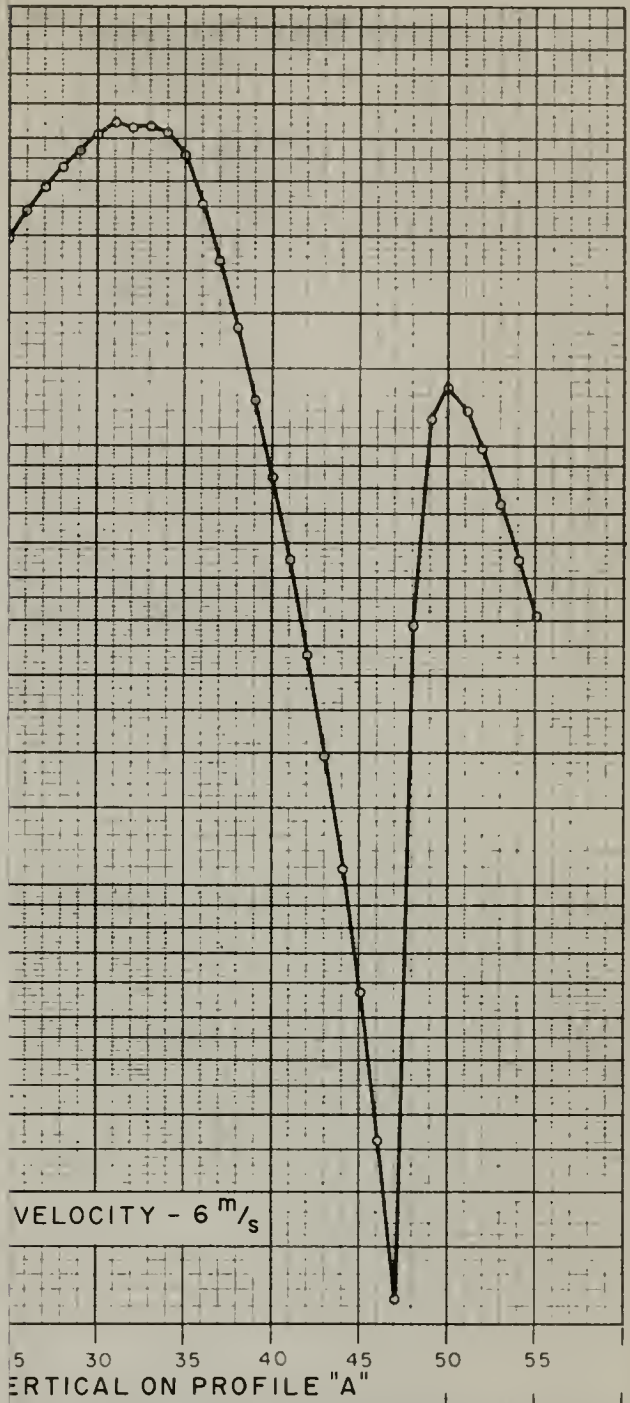


Fig. 7a

STATE OF CALIFORNIA
 DEPARTMENT OF WATER RESOURCES
 DIVISION OF DESIGN AND CONSTRUCTION
 PROCEDURES FOR ESTIMATING
 MAXIMUM POSSIBLE PRECIPITATION

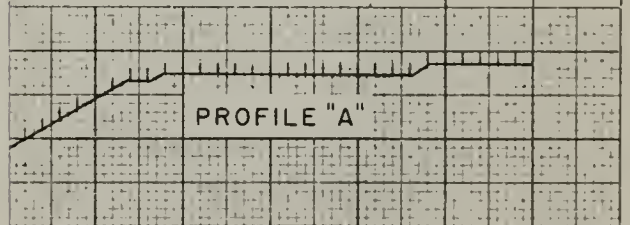
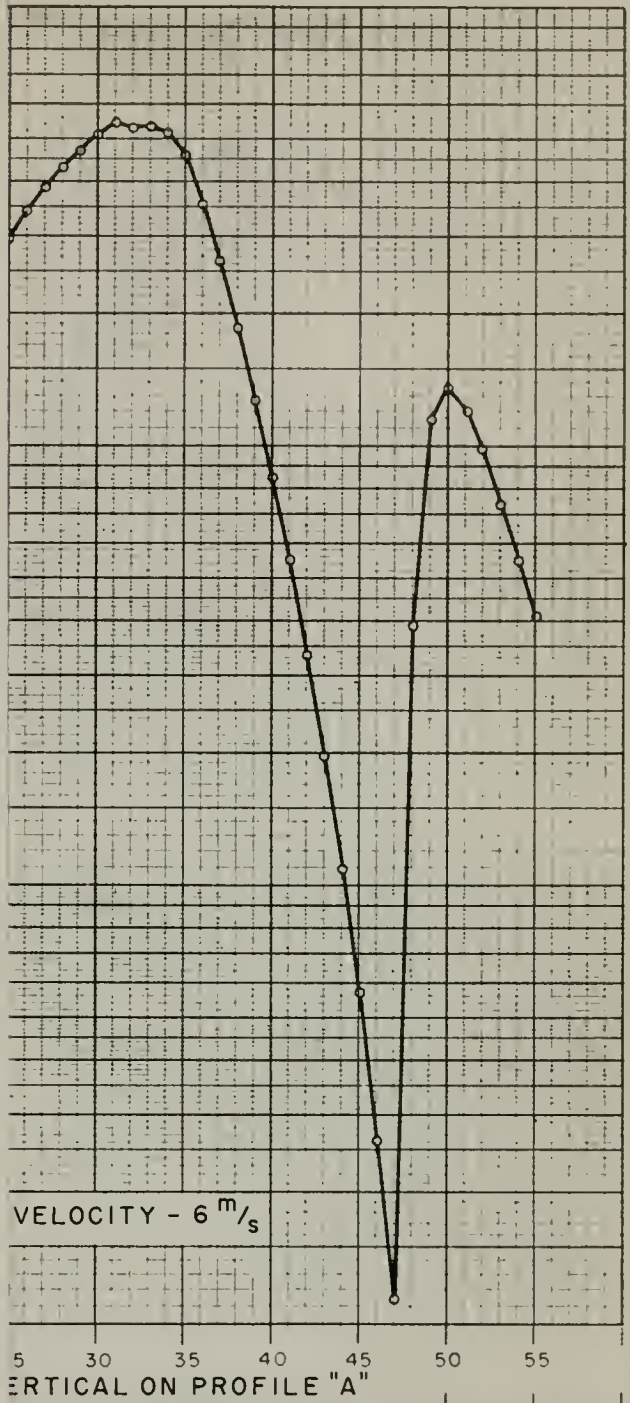
DISTRIBUTION OF HOURLY RATE OF OROGRAPHIC
 PRECIPITATION ON PROFILE "A", DEC. 1955 STORM



STATE OF CALIFORNIA
 DEPARTMENT OF WATER RESOURCES
 DIVISION OF DESIGN AND CONSTRUCTION
 PROCEDURES FOR ESTIMATING
 HOURLY POSSIBLE PRECIPITATION

Fig. 7b

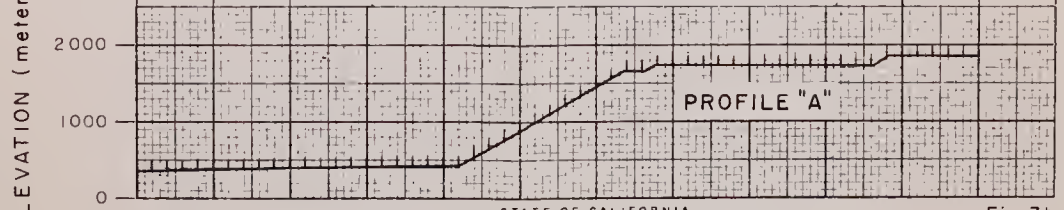
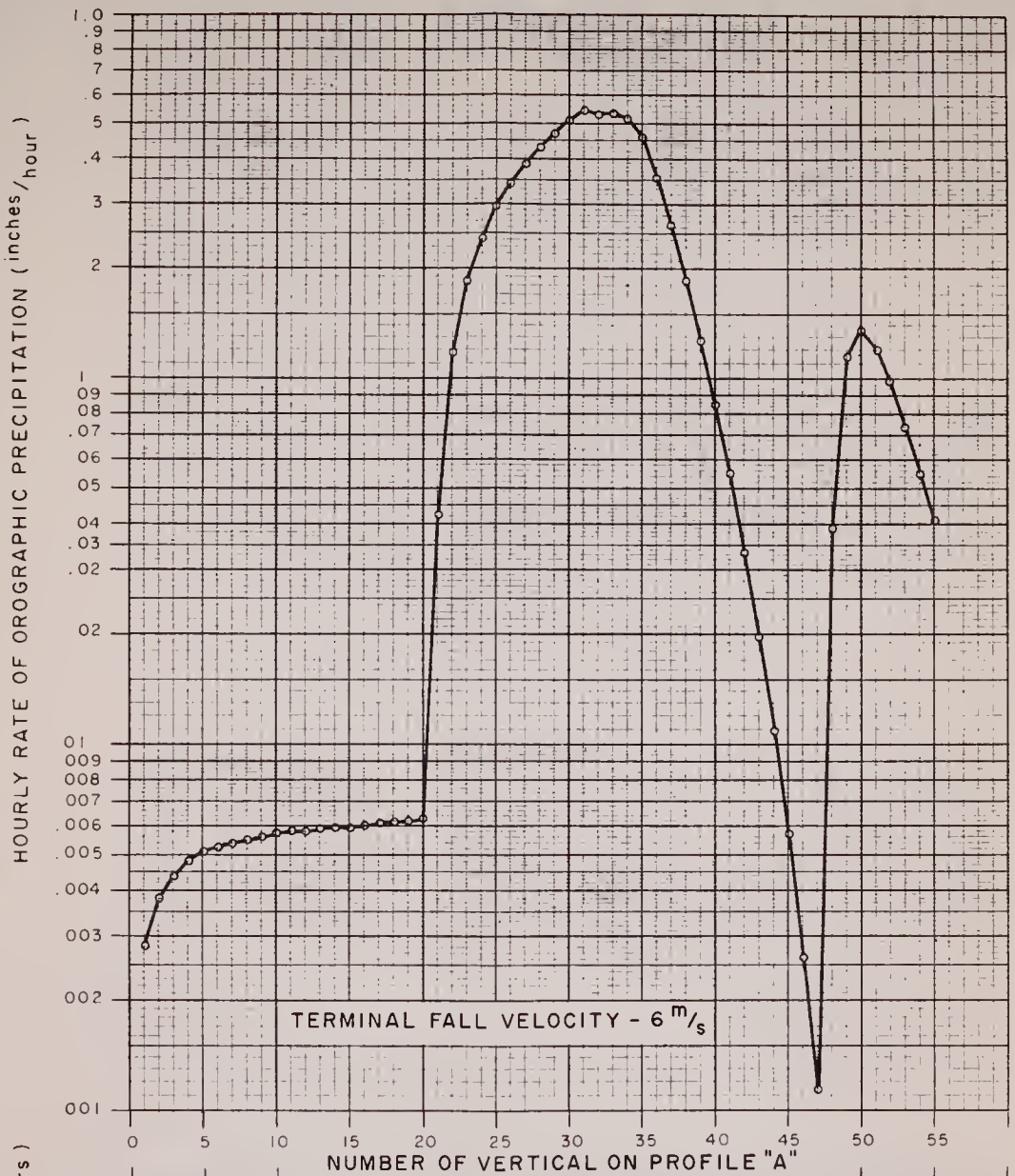
HOURLY RATE OF OROGRAPHIC
 PROFILE "A", DEC. 1955 STORM



STATE OF CALIFORNIA
 DEPARTMENT OF WATER RESOURCES
 DIVISION OF DESIGN AND CONSTRUCTION
 REQUIREMENTS FOR ESTIMATING
 POSSIBLE PRECIPITATION

Fig 7b

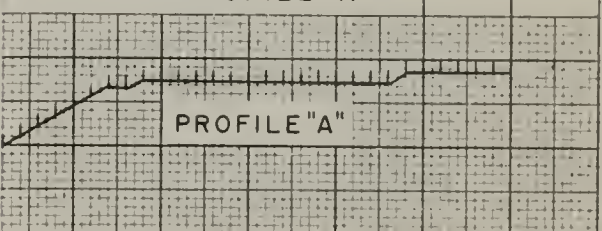
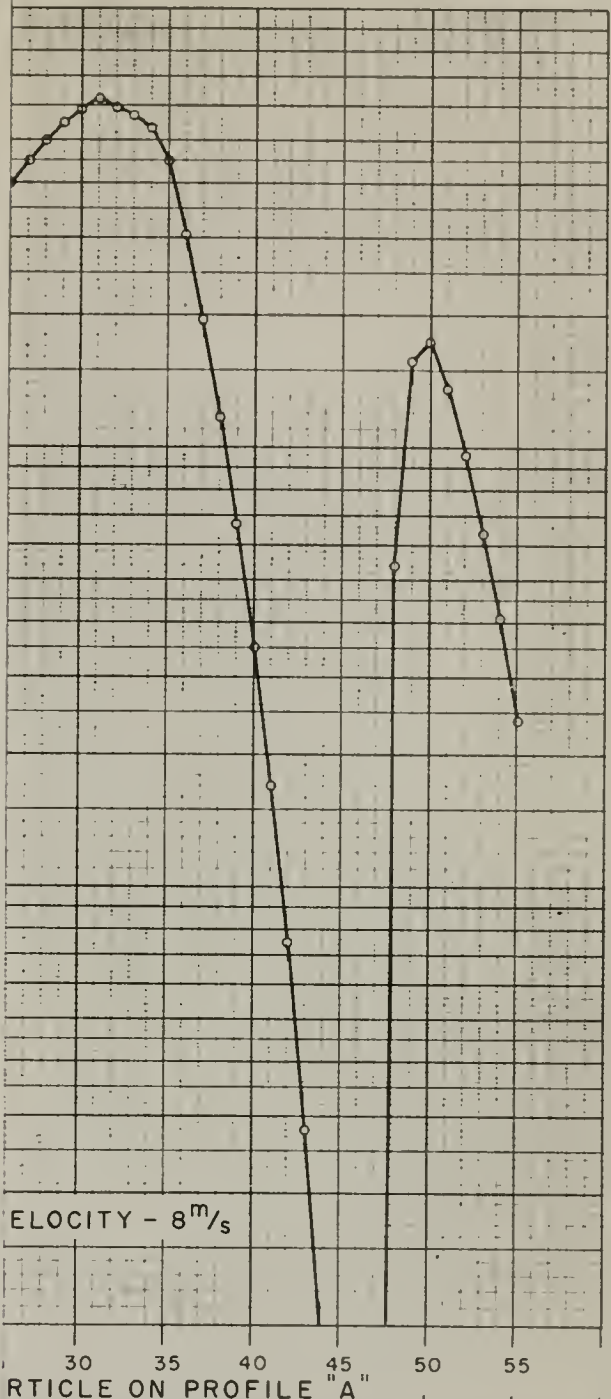
HOURLY RATE OF OROGRAPHIC
 PRECIPITATION ON PROFILE "A", DEC. 1955 STORM



STATE OF CALIFORNIA
 DEPARTMENT OF WATER RESOURCES
 DIVISION OF DESIGN AND CONSTRUCTION
 PROCEDURES FOR ESTIMATING
MAXIMUM POSSIBLE PRECIPITATION

Fig. 7b

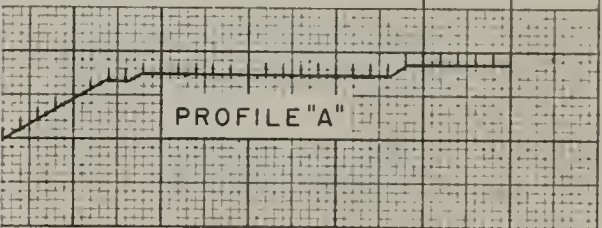
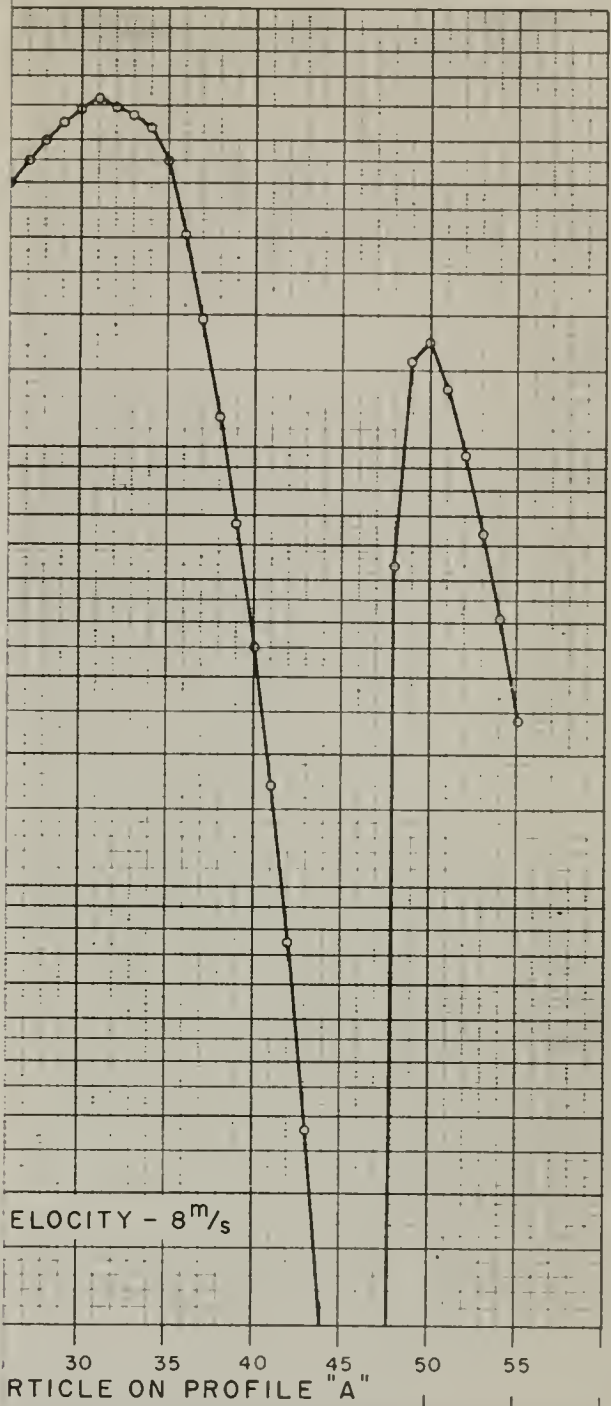
DISTRIBUTION OF HOURLY RATE OF OROGRAPHIC PRECIPITATION ON PROFILE "A", DEC. 1955 STORM



STATE OF CALIFORNIA
 DEPARTMENT OF WATER RESOURCES
 DESIGN AND CONSTRUCTION
 DIVISION OF PRECIPITATION
 POSSIBLE PRECIPITATION

Fig. 7c

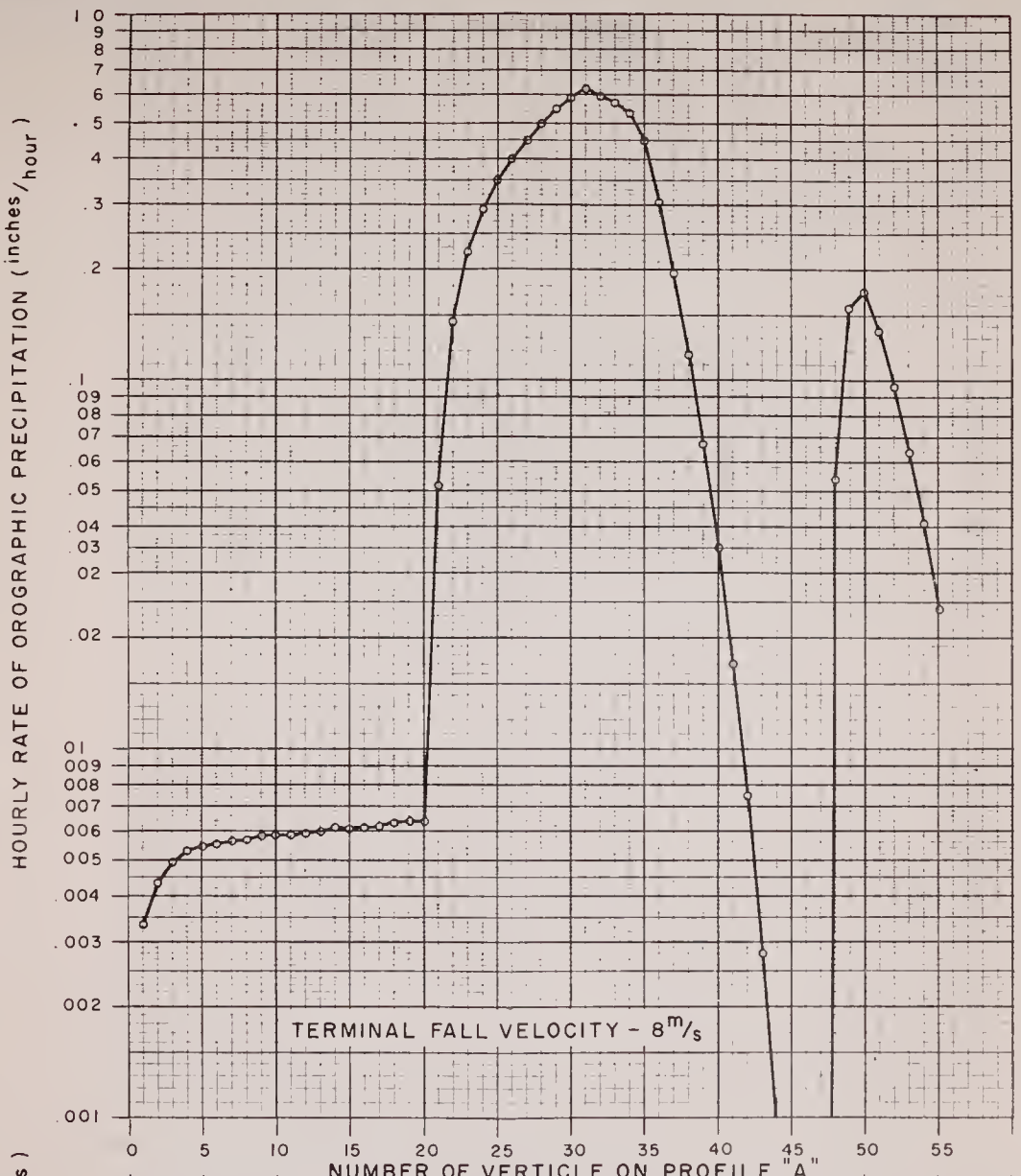
HOURLY RATE OF OROGRAPHIC
 PRECIPITATION ALONG
 PROFILE "A", DEC. 1955 STORM



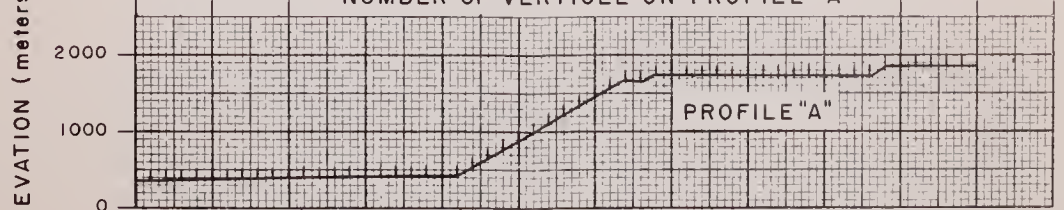
STATE OF CALIFORNIA
 DEPARTMENT OF WATER RESOURCES
 DESIGN AND CONSTRUCTION
 DIVISION
 STUDIES FOR ESTIMATING
 POSSIBLE PRECIPITATION

Fig. 7c

ANNUAL AVERAGE RATE OF OROGRAPHIC
 PRECIPITATION ALONG PROFILE "A", DEC. 1955 STORM



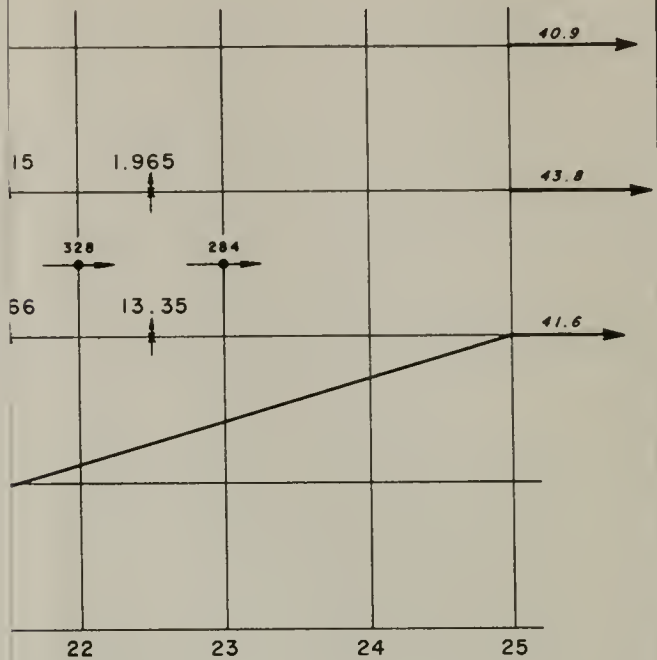
TERMINAL FALL VELOCITY - 8^m/s



STATE OF CALIFORNIA
 DEPARTMENT OF WATER RESOURCES
 DIVISION OF DESIGN AND CONSTRUCTION
 PROCEDURES FOR ESTIMATING
 MAXIMUM POSSIBLE PRECIPITATION

Fig. 7c

DISTRIBUTION OF HOURLY RATE OF OROGRAPHIC PRECIPITATION ON PROFILE "A", DEC. 1955 STORM



VERTICAL

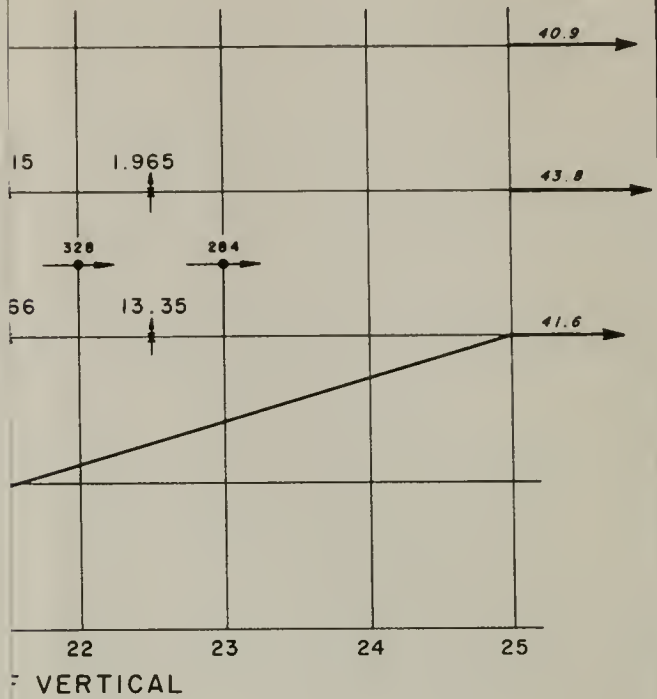
CALIFORNIA
 WATER RESOURCES
 AND CONSTRUCTION
 S BRANCH

FOR ESTIMATING
THE PRECIPITATION

x _____

ET OF THE LAYER -
 S (DEC. 1955 STORM)

Fig 8

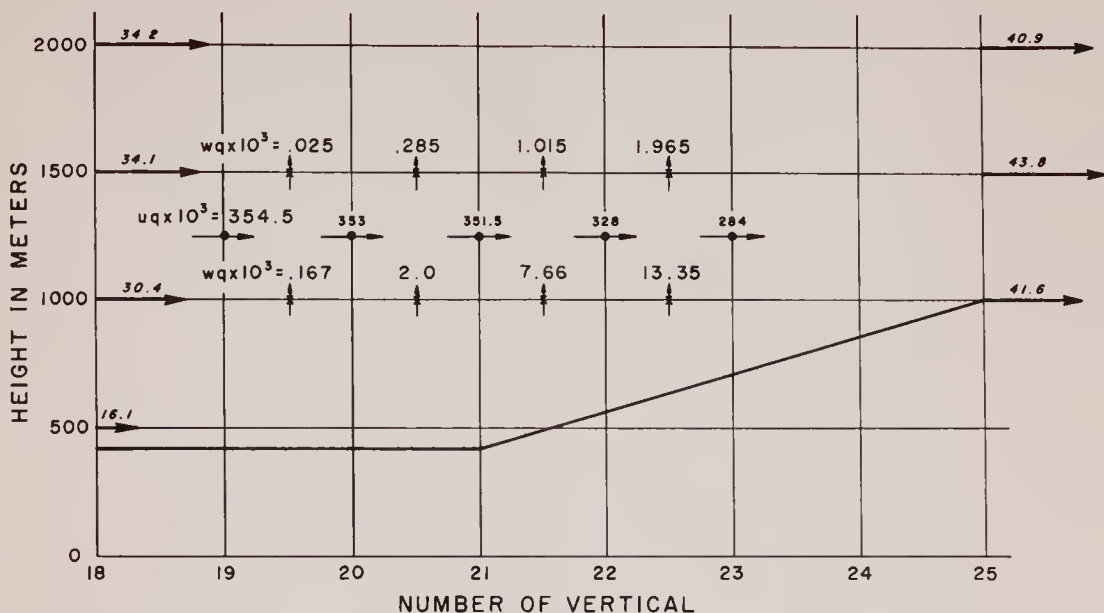


CALIFORNIA
 WATER RESOURCES
 AND CONSTRUCTION
 S BRANCH

FOR ESTIMATING
THE PRECIPITATION

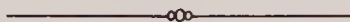
x _____

ET OF THE LAYER -
 S (DEC. 1955 STORM)

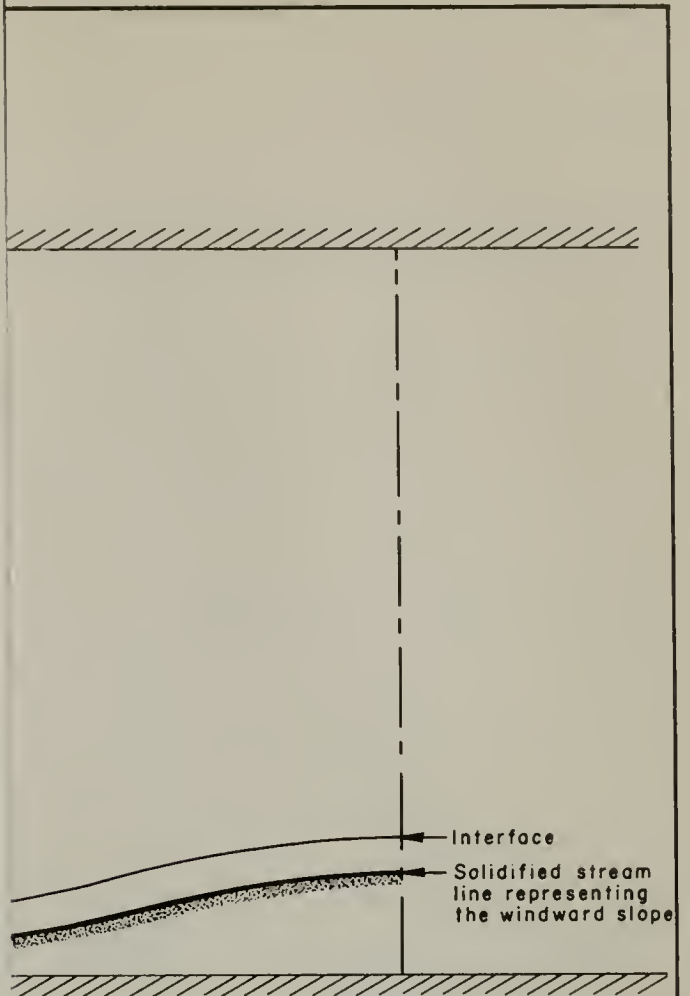


STATE OF CALIFORNIA
 DEPARTMENT OF WATER RESOURCES
 DIVISION OF DESIGN AND CONSTRUCTION
 OPERATIONS BRANCH

PROCEDURES FOR ESTIMATING
MAXIMUM POSSIBLE PRECIPITATION



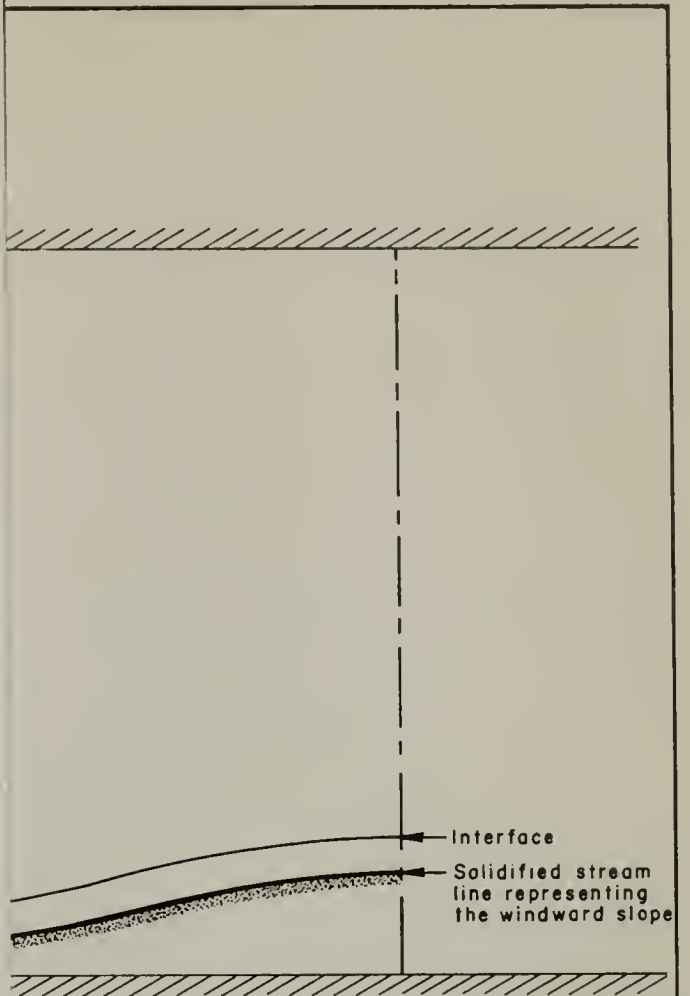
A VORTICITY BUDGET OF THE LAYER -
 1000 TO 1500 METERS (DEC. 1955 STORM)



CALIFORNIA
 WATER RESOURCES
 DIVISION AND CONSTRUCTION
 DIVISIONS BRANCH

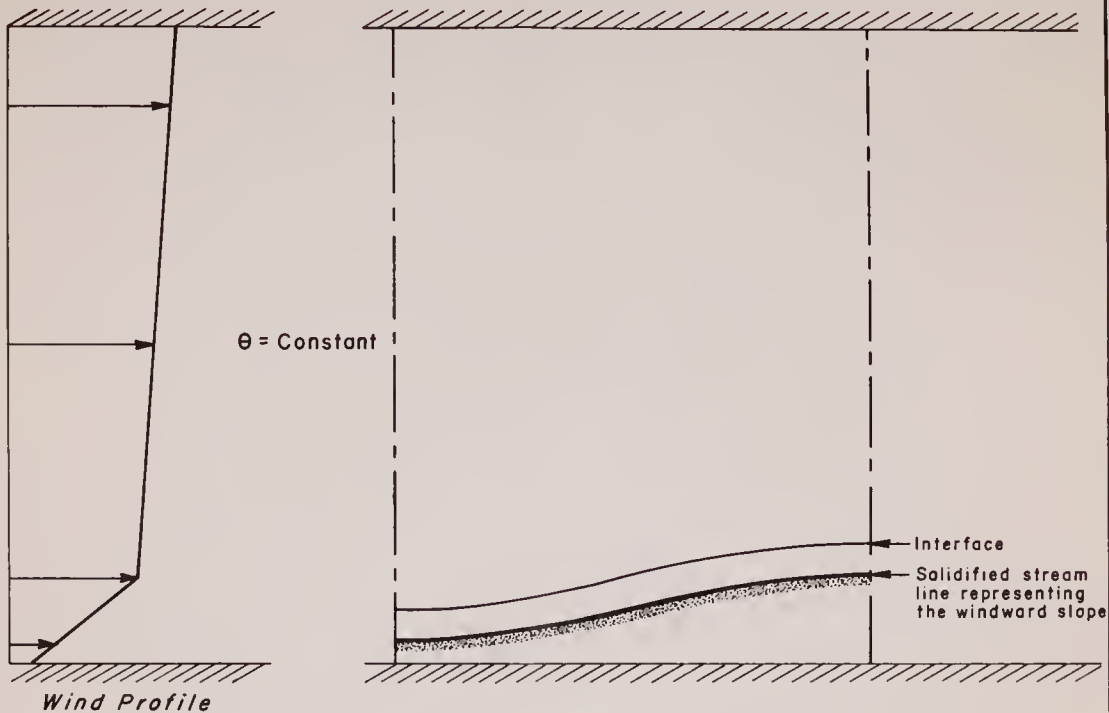
FOR ESTIMATING
PRECIPITATION
 USING AN
 ADIABATIC
 AIR FLOW MODEL

Fig. 9



CALIFORNIA
 WATER RESOURCES
 DIVISION AND CONSTRUCTION
 DIVISIONS BRANCH

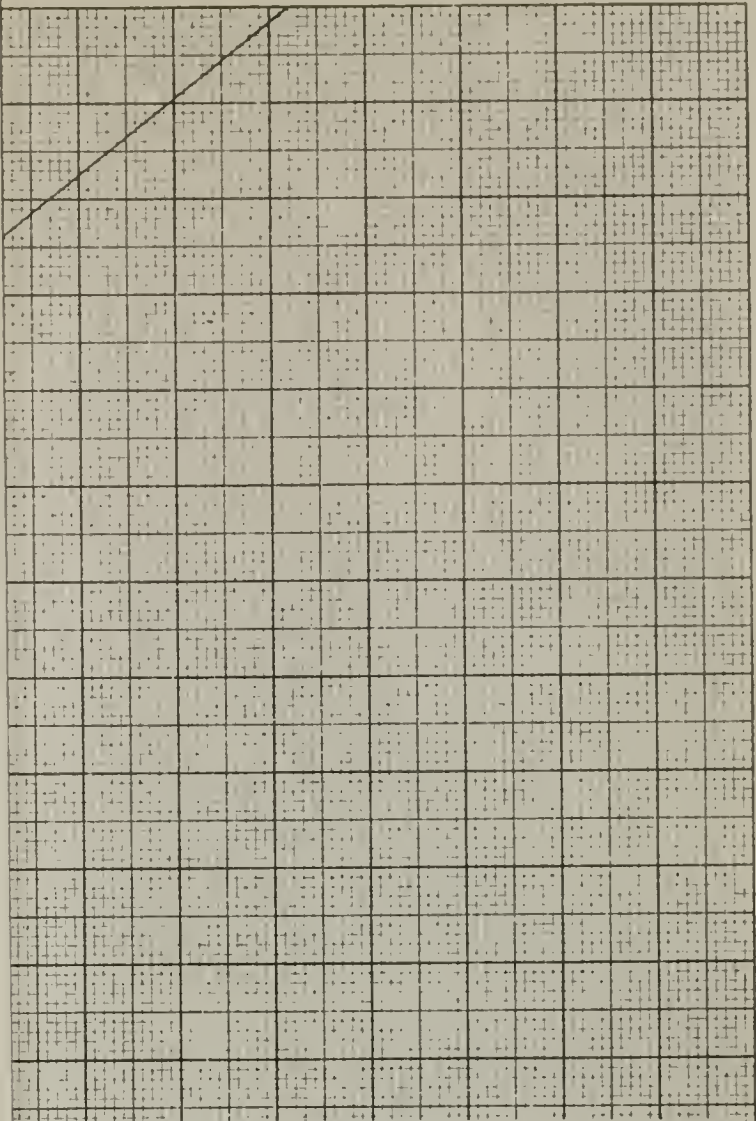
FOR ESTIMATING
POTENTIAL PRECIPITATION
 USING AN
 ADIABATIC
 AIR FLOW MODEL



STATE OF CALIFORNIA
 DEPARTMENT OF WATER RESOURCES
 DIVISION OF DESIGN AND CONSTRUCTION
 OPERATIONS BRANCH

PROCEDURES FOR ESTIMATING
MAXIMUM POSSIBLE PRECIPITATION

— ∞ —
 THE ADIABATIC
 DOUBLE COUETTE FLOW MODEL



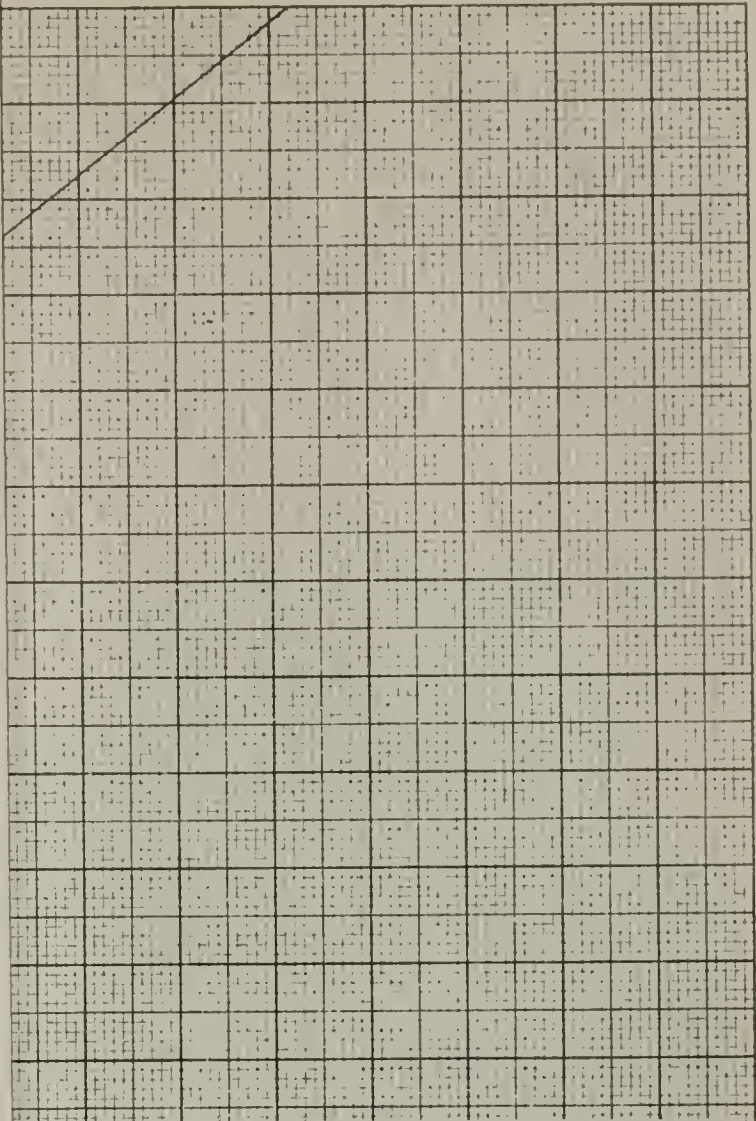
LEGEND

- ASYMPTOTE OF $\cot(\frac{2\pi}{n})$
- n ROOTS FOR MAXIMA IN DISTRIBUTION I
- x n ROOTS FOR MAXIMA IN DISTRIBUTION II

STATE OF CALIFORNIA
 DEPARTMENT OF WATER RESOURCES
 DIVISION OF DESIGN AND CONSTRUCTION
 OPERATIONS BRANCH

PROCEDURES FOR ESTIMATING
 MAXIMUM POSSIBLE PRECIPITATION

∞∞
 —————
 GRAPHICAL SOLUTION
 FOR
 ADVERSE PERIODICITY



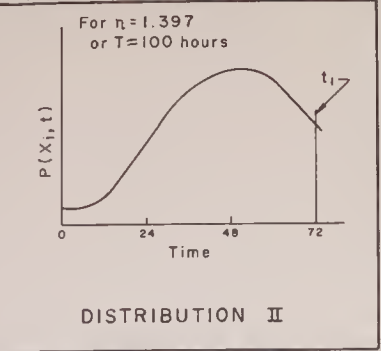
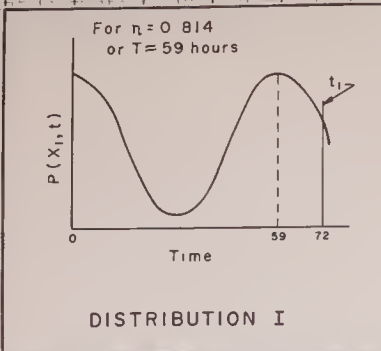
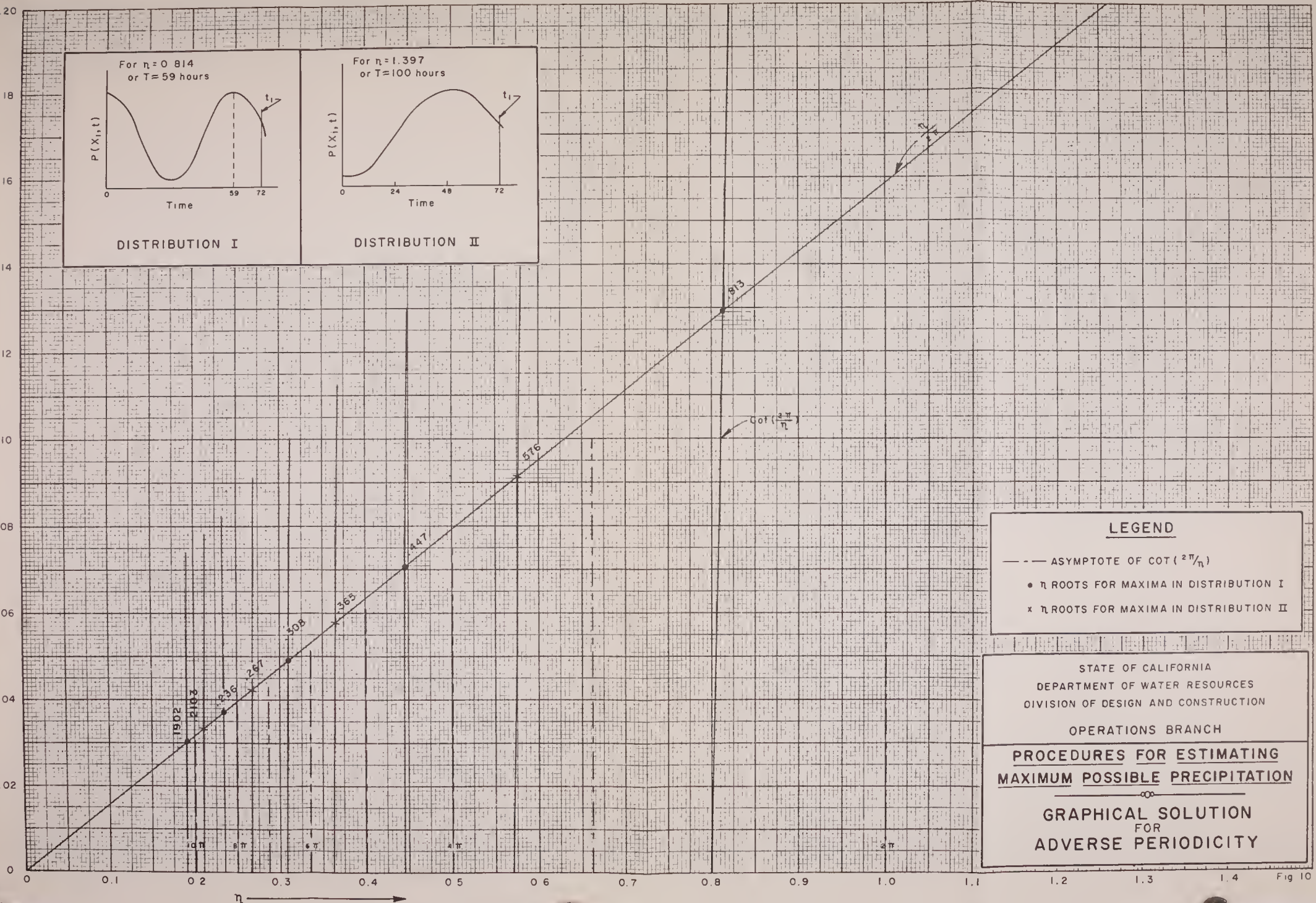
LEGEND

- — — ASYMPTOTE OF $\cot(\frac{2\pi}{n})$
- n ROOTS FOR MAXIMA IN DISTRIBUTION I
- x n ROOTS FOR MAXIMA IN DISTRIBUTION II

STATE OF CALIFORNIA
 DEPARTMENT OF WATER RESOURCES
 DIVISION OF DESIGN AND CONSTRUCTION
 OPERATIONS BRANCH

PROCEDURES FOR ESTIMATING
 MAXIMUM POSSIBLE PRECIPITATION

∞∞
 —————
 GRAPHICAL SOLUTION
 FOR
 ADVERSE PERIODICITY



LEGEND

--- ASYMPTOTE OF $\cot(\frac{\pi}{\eta})$

• η ROOTS FOR MAXIMA IN DISTRIBUTION I

x η ROOTS FOR MAXIMA IN DISTRIBUTION II

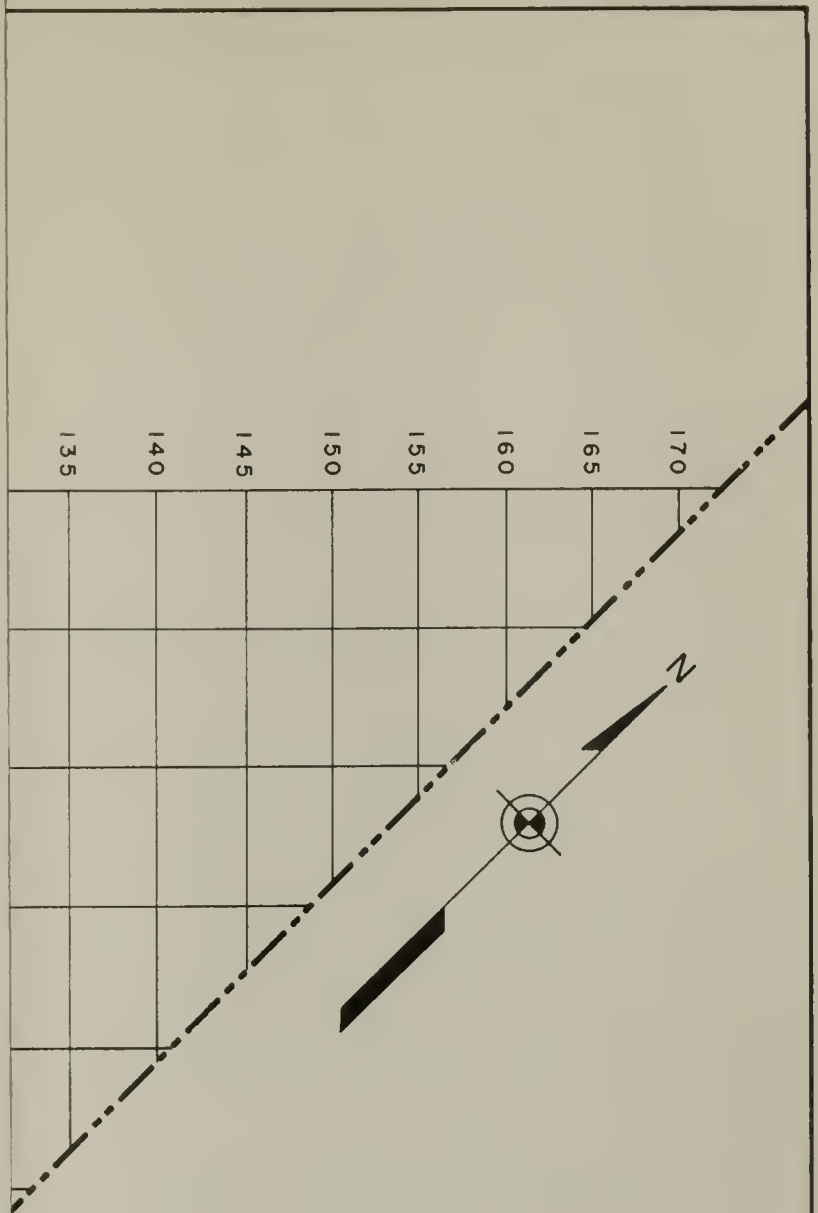
STATE OF CALIFORNIA
DEPARTMENT OF WATER RESOURCES
DIVISION OF DESIGN AND CONSTRUCTION

OPERATIONS BRANCH

**PROCEDURES FOR ESTIMATING
MAXIMUM POSSIBLE PRECIPITATION**

○

**GRAPHICAL SOLUTION
FOR
ADVERSE PERIODICITY**



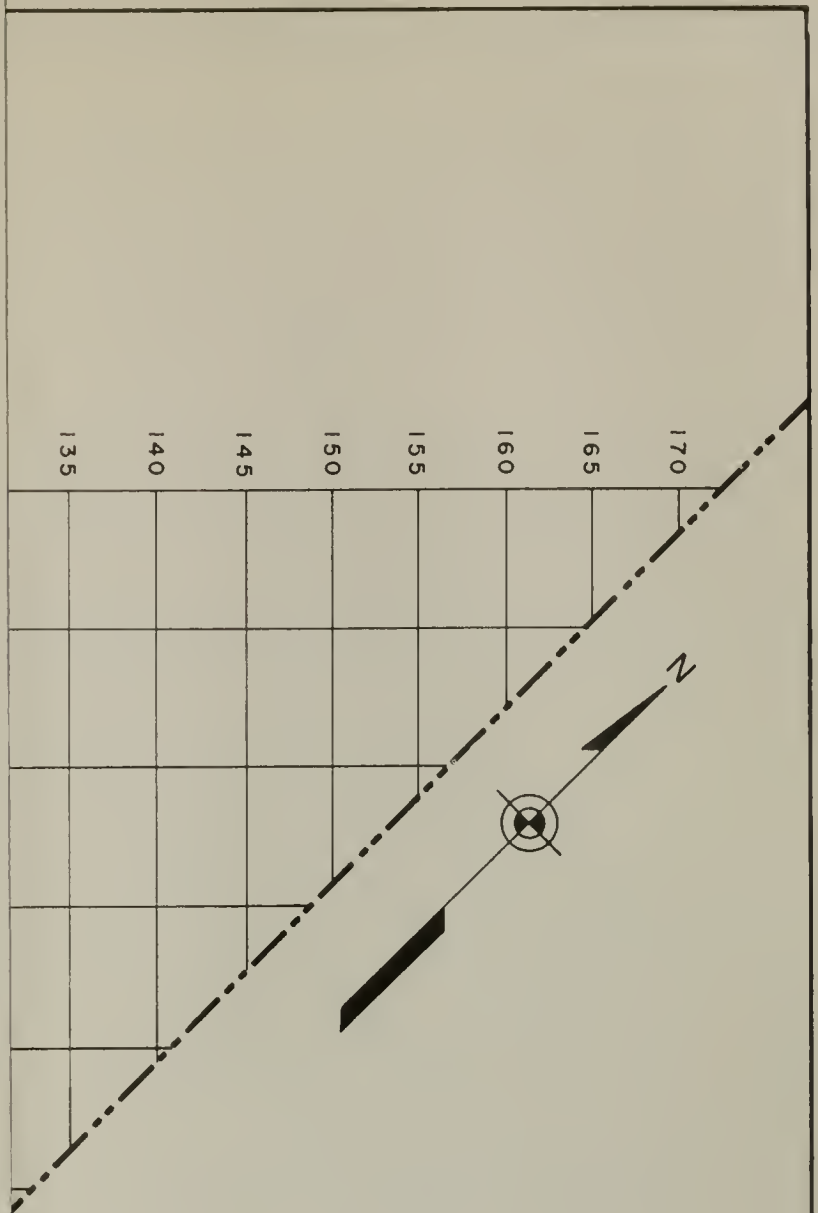
STATE OF CALIFORNIA
 DEPARTMENT OF WATER RESOURCES
 DIVISION OF DESIGN AND CONSTRUCTION

OPERATIONS BRANCH

PROCEDURES FOR ESTIMATING
MAXIMUM POSSIBLE PRECIPITATION

— 00 —
 CALCULATED 72-HOUR ISOHYETAL MAP,
 DECEMBER 1955 STORM (8 m/s),
 FEATHER RIVER BASIN

Fig. 11a



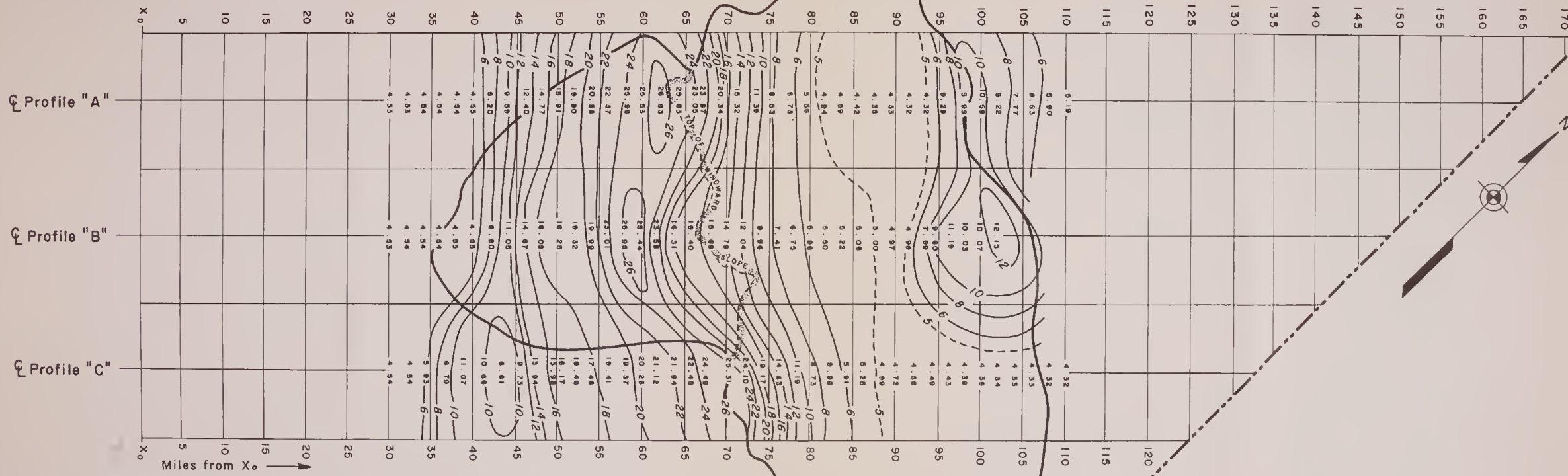
STATE OF CALIFORNIA
 DEPARTMENT OF WATER RESOURCES
 DIVISION OF DESIGN AND CONSTRUCTION

OPERATIONS BRANCH

PROCEDURES FOR ESTIMATING
MAXIMUM POSSIBLE PRECIPITATION

— 00 —
 CALCULATED 72-HOUR ISOHYETAL MAP,
 DECEMBER 1955 STORM (8 m/s),
 FEATHER RIVER BASIN

Fig. 11a



NOTE

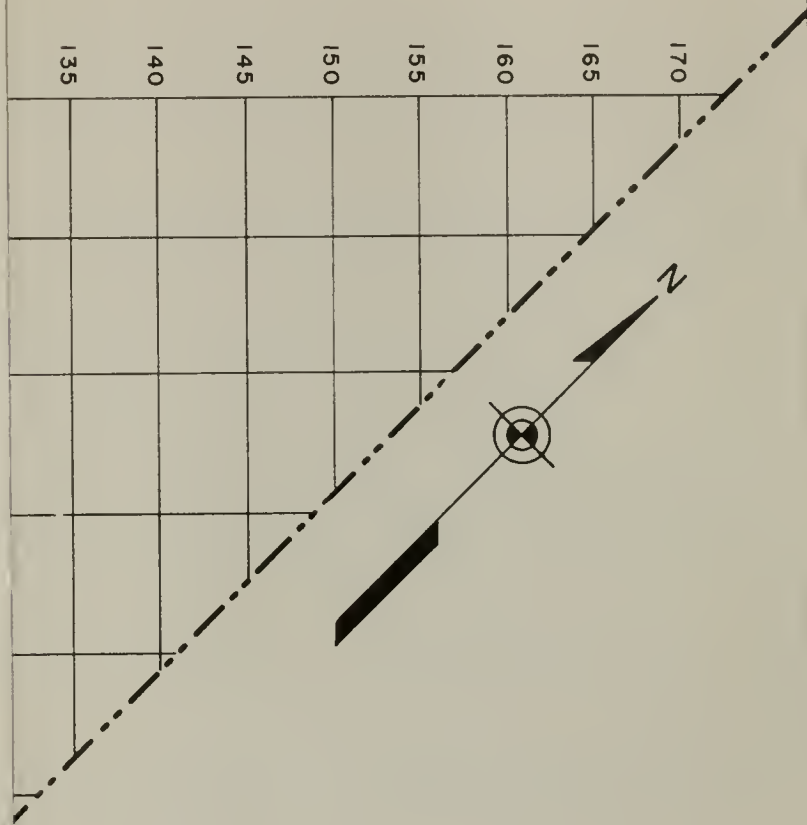
Area of windward basin = 940 square miles
 Area of leeward basin within profile strips = 1737 sq. mi.
 Area of entire leeward basin = 2675 square miles
 Total basin area = 3615 square miles

Average basin depth within profile strips on
 Leeward side = 8.3 inches
 Average basin depth within profile strips on
 Windward side = 18.5 inches
 Average depth over entire basin within profile
 strips = 11.9 inches

STATE OF CALIFORNIA
 DEPARTMENT OF WATER RESOURCES
 DIVISION OF DESIGN AND CONSTRUCTION

OPERATIONS BRANCH
PROCEDURES FOR ESTIMATING
MAXIMUM POSSIBLE PRECIPITATION

THE CALCULATED 72-HOUR ISOHYETAL MAP,
 DECEMBER 1955 STORM (8 m/s),
 FEATHER RIVER BASIN



STATE OF CALIFORNIA
 DEPARTMENT OF WATER RESOURCES
 DIVISION OF DESIGN AND CONSTRUCTION

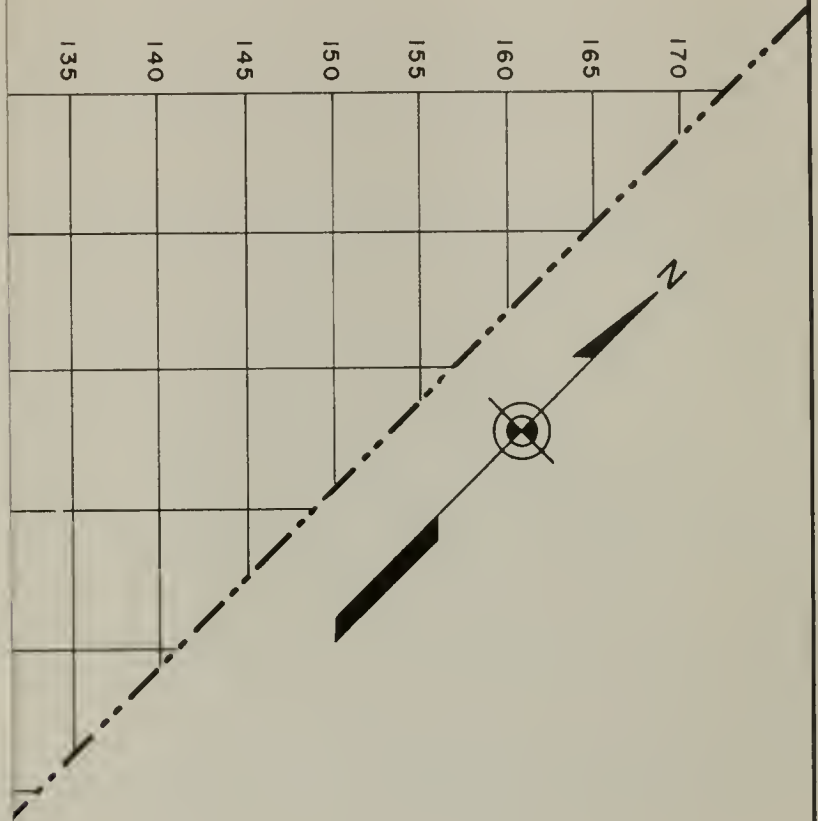
OPERATIONS BRANCH

PROCEDURES FOR ESTIMATING
MAXIMUM POSSIBLE PRECIPITATION



...CULATED 72 - HOUR ISOHYETAL MAP,
 ...EMBER 1955 STORM (6 m/s),
 FEATHER RIVER BASIN

Fig 11b



STATE OF CALIFORNIA
 DEPARTMENT OF WATER RESOURCES
 DIVISION OF DESIGN AND CONSTRUCTION

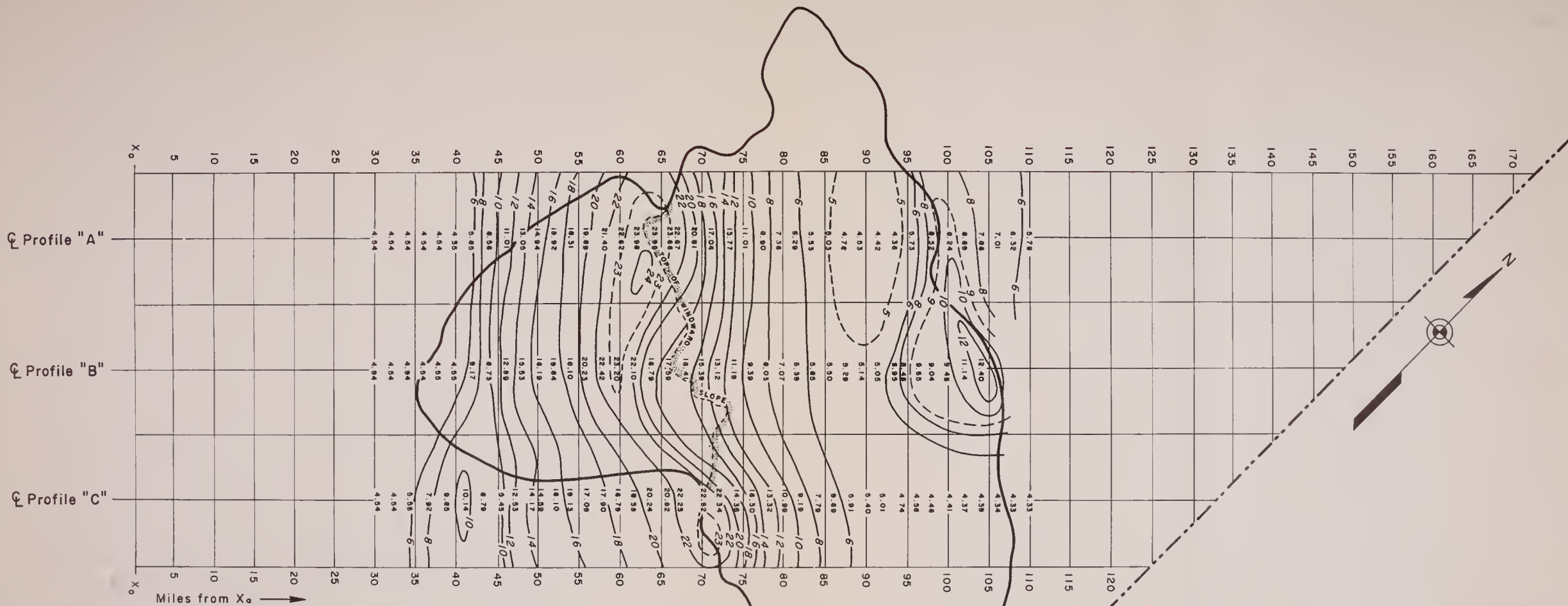
OPERATIONS BRANCH

PROCEDURES FOR ESTIMATING
MAXIMUM POSSIBLE PRECIPITATION

— 000 —

CULATED 72 - HOUR ISOHYETAL MAP,
 CEMBER 1955 STORM (6 ^m/s),
 FEATHER RIVER BASIN

Fig 11b



NOTE

Area of windward basin = 940 square miles
 Area of leeward basin within profile strips = 1737 sq mi
 Area of entire leeward basin = 2675 square miles
 Total basin area = 3615 square miles

Average basin depth within profile strips on
 Leeward side = 9.1 inches

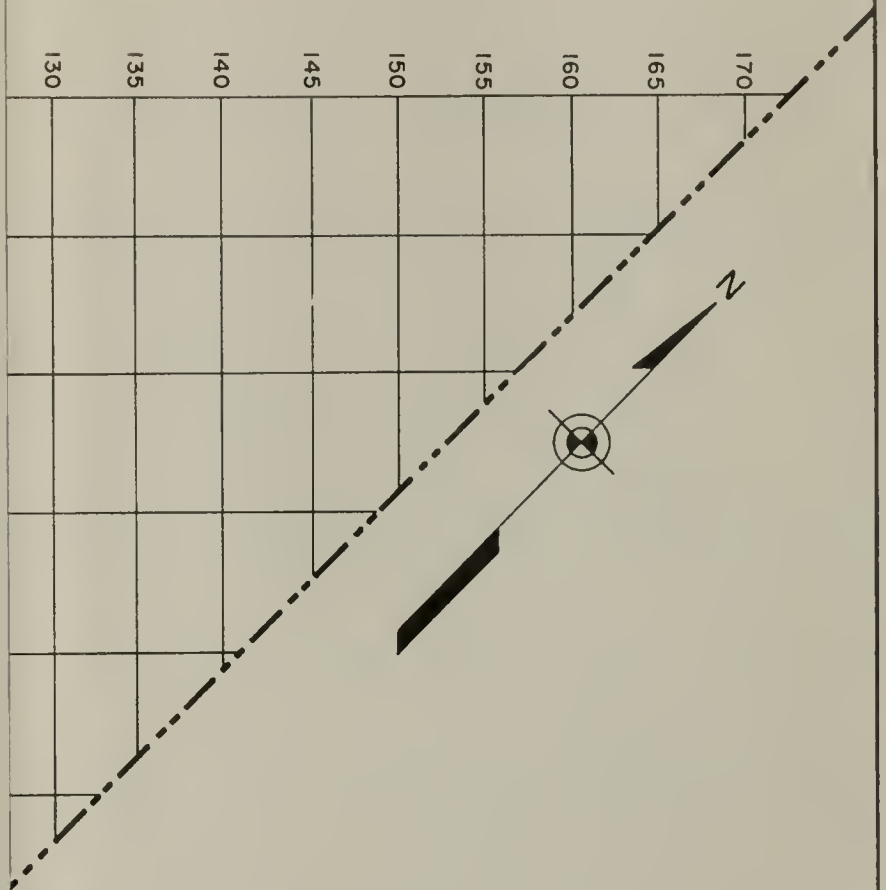
Average basin depth within profile strips on
 Windward side = 16.6 inches

Average depth over entire basin within profile
 strips = 11.8 inches

STATE OF CALIFORNIA
 DEPARTMENT OF WATER RESOURCES
 DIVISION OF DESIGN AND CONSTRUCTION

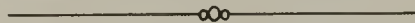
OPERATIONS BRANCH
**PROCEDURES FOR ESTIMATING
 MAXIMUM POSSIBLE PRECIPITATION**

THE CALCULATED 72-HOUR ISOHYETAL MAP,
 DECEMBER 1955 STORM (6 m/s),
 FEATHER RIVER BASIN

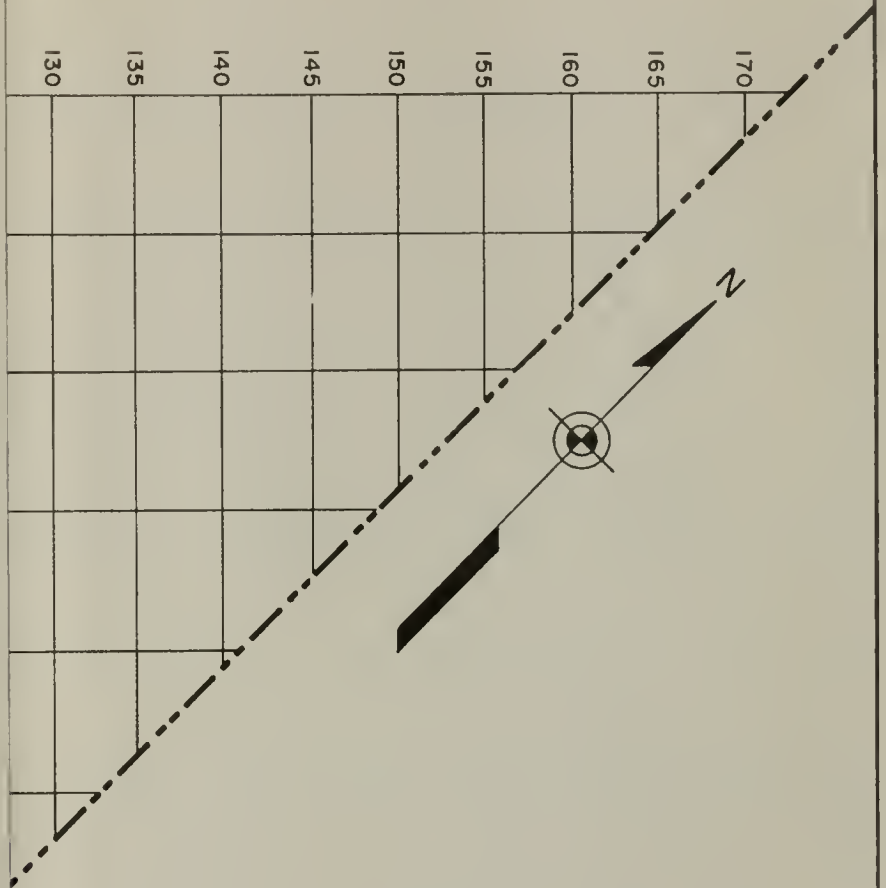


STATE OF CALIFORNIA
 DEPARTMENT OF WATER RESOURCES
 DIVISION OF DESIGN AND CONSTRUCTION

OPERATIONS BRANCH
PROCEDURES FOR ESTIMATING
MAXIMUM POSSIBLE PRECIPITATION



CALCULATED 72-HOUR ISOHYETAL MAP,
 DECEMBER 1955 STORM (4 m/s),
 FEATHER RIVER BASIN



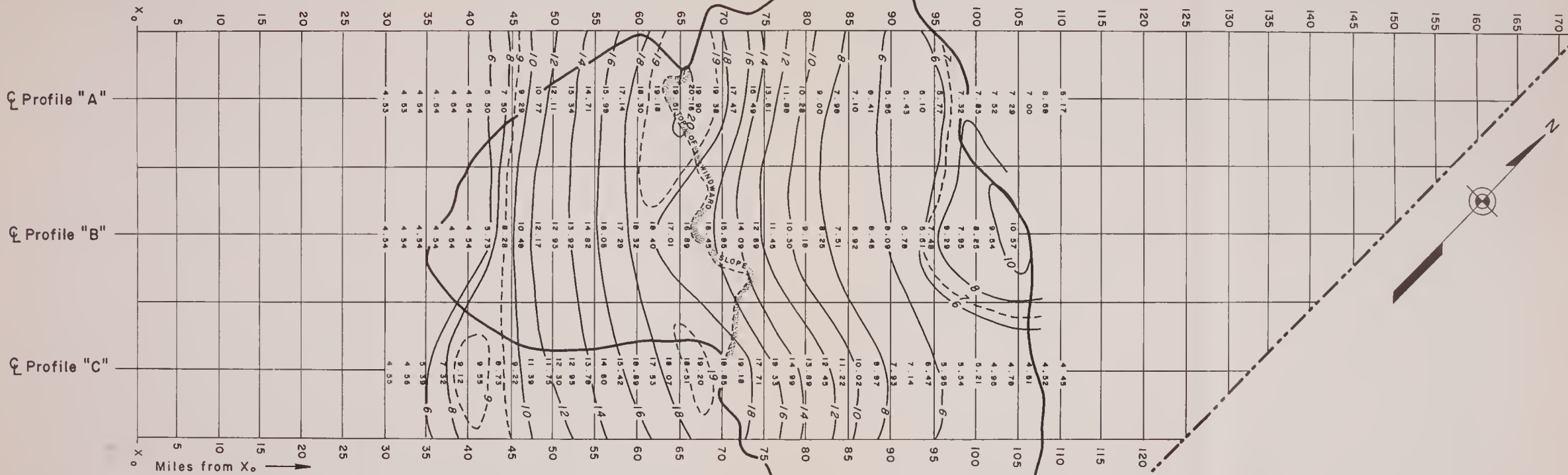
STATE OF CALIFORNIA
 DEPARTMENT OF WATER RESOURCES
 DIVISION OF DESIGN AND CONSTRUCTION

OPERATIONS BRANCH

PROCEDURES FOR ESTIMATING
MAXIMUM POSSIBLE PRECIPITATION



CALCULATED 72-HOUR ISOHYETAL MAP,
 DECEMBER 1955 STORM (4 m/s),
 FEATHER RIVER BASIN



STATE OF CALIFORNIA
 DEPARTMENT OF WATER RESOURCES
 DIVISION OF DESIGN AND CONSTRUCTION

OPERATIONS BRANCH
**PROCEDURES FOR ESTIMATING
 MAXIMUM POSSIBLE PRECIPITATION**

THE CALCULATED 72-HOUR ISOHYETAL MAP,
 DECEMBER 1955 STORM (4 m/s),
 FEATHER RIVER BASIN

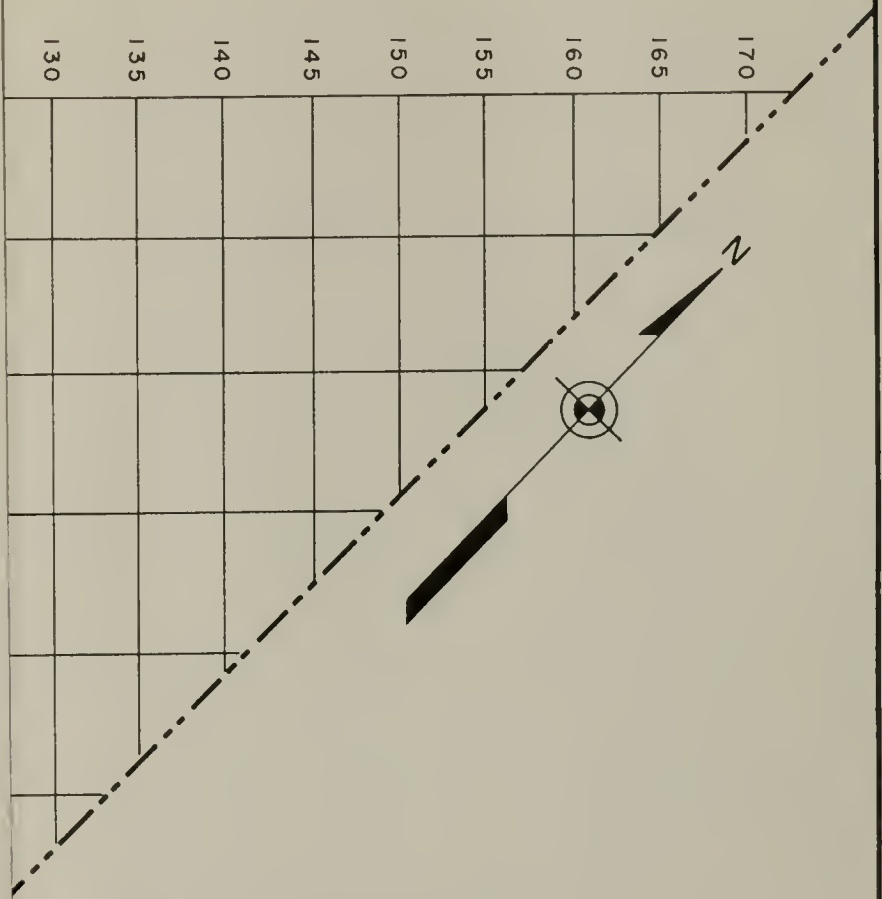
NOTE

Area of windward basin = 940 square miles
 Area of leeward basin within profile strips = 1737 sq. mi
 Area of entire leeward basin = 2675 square miles
 Total basin area = 3615 square miles

Average basin depth within profile strips on
 Leeward side = 9.9 inches.

Average basin depth within profile strips on
 Windward side = 14.1 inches.

Average depth over entire basin within profile
 strips = 11.4 inches.

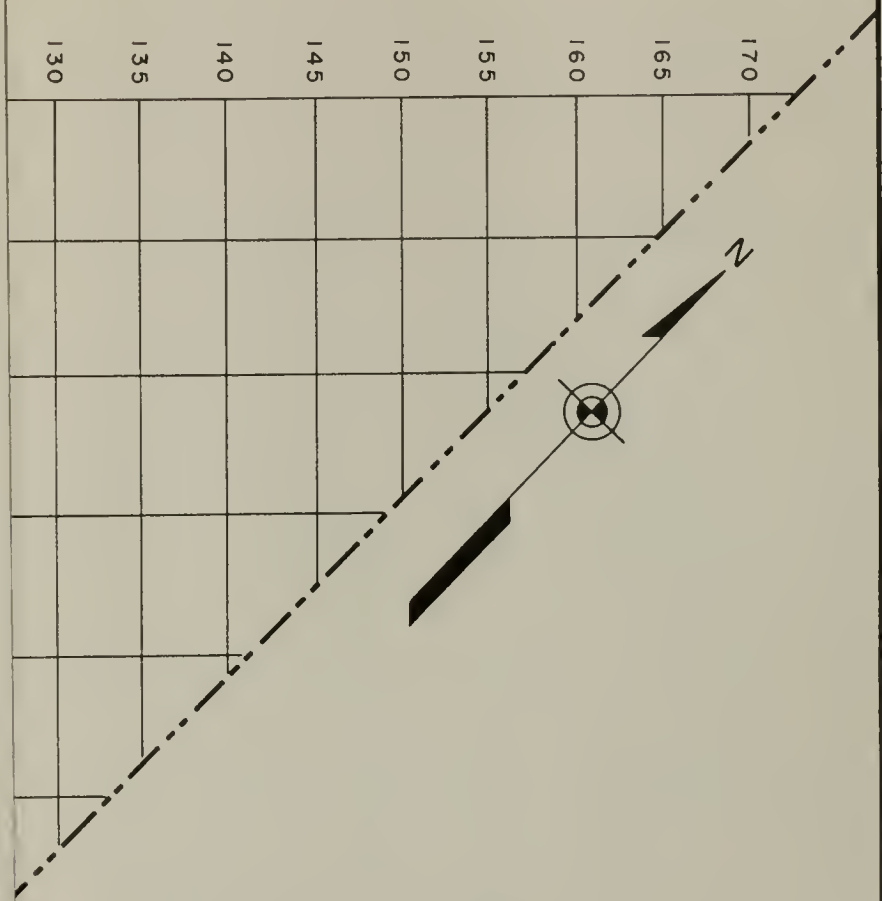


STATE OF CALIFORNIA
 DEPARTMENT OF WATER RESOURCES
 DIVISION OF DESIGN AND CONSTRUCTION

OPERATIONS BRANCH

PROCEDURES FOR ESTIMATING
MAXIMUM POSSIBLE PRECIPITATION

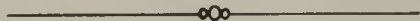
—∞—
 THE 72-HOUR ISOHYETAL MAP OF
 OBSERVED PRECIPITATION,
 DECEMBER 1955 STORM,
 FEATHER RIVER BASIN



STATE OF CALIFORNIA
 DEPARTMENT OF WATER RESOURCES
 DIVISION OF DESIGN AND CONSTRUCTION

OPERATIONS BRANCH

PROCEDURES FOR ESTIMATING
MAXIMUM POSSIBLE PRECIPITATION



THE 72 - HOUR ISOHYETAL MAP OF
 OBSERVED PRECIPITATION,
 DECEMBER 1955 STORM,
 FEATHER RIVER BASIN

Fig. 12

NOTE:
 STORM PERIOD: 72 hours ending 0700 December 22, 1955

- Recording Precipitation Station
- Non-Recording Precipitation Station

(Storm totals for non-recording stations which report at times other than 0700 PST were obtained by proration according to the nearest available recording station)



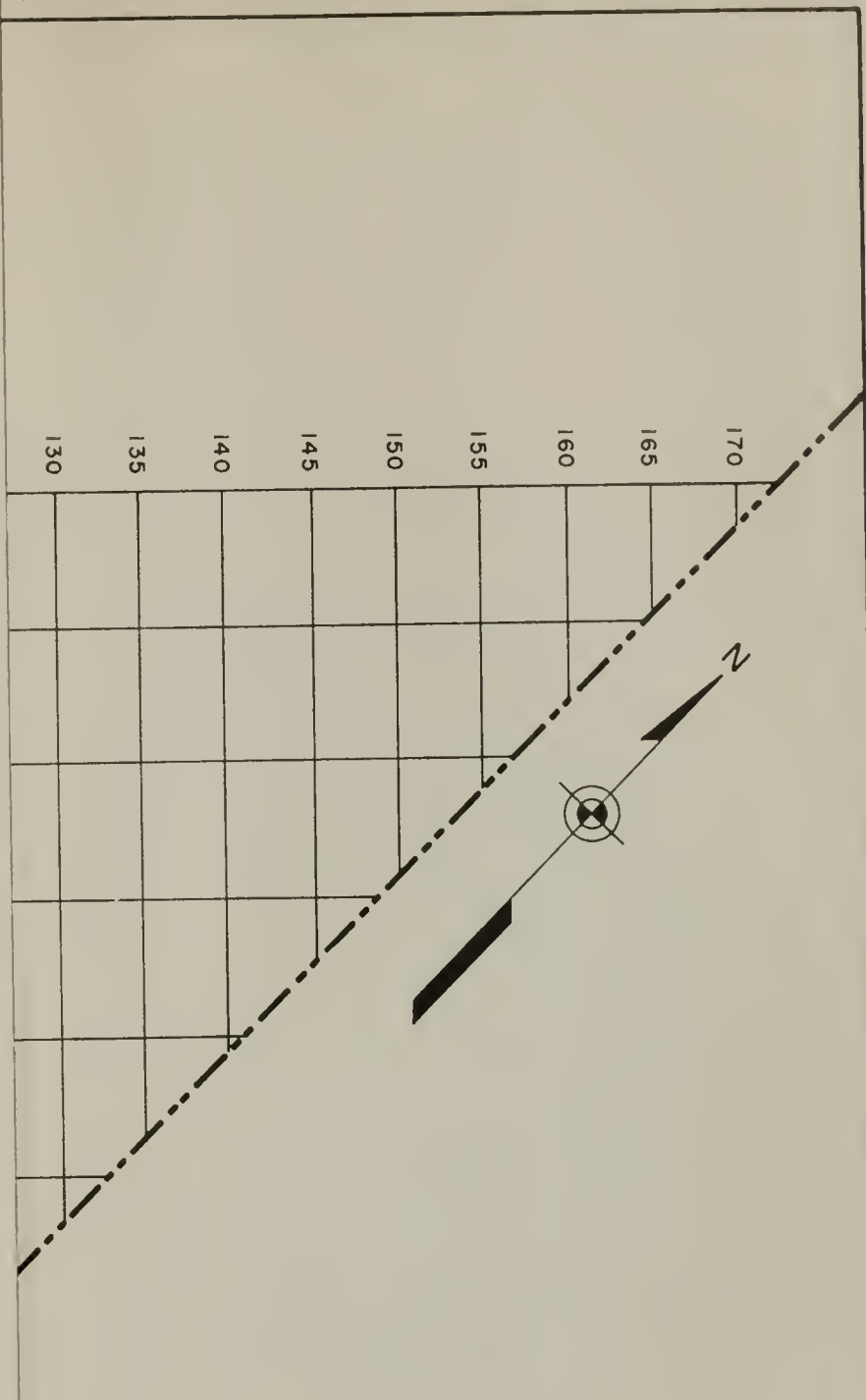
NOTE

- Area of windward basin = 940 square miles
- Area of leeward basin within profile strips = 1737 sq. mi.
- Area of entire leeward basin = 2675 square miles
- Total basin area = 3615 square miles.
- Average basin depth within profile strips on Leeward side = 7.0 inches
- Average basin depth within profile strips on Windward side = 16.0 inches
- Average depth over entire basin within profile strips = 10.1 inches.
- Average depth over entire Leeward side = 6.5 inches
- Average depth over entire basin = 8.9 inches

STATE OF CALIFORNIA
 DEPARTMENT OF WATER RESOURCES
 DIVISION OF DESIGN AND CONSTRUCTION

OPERATIONS BRANCH
PROCEDURES FOR ESTIMATING
MAXIMUM POSSIBLE PRECIPITATION

THE 72-HOUR ISOHYETAL MAP OF
 OBSERVED PRECIPITATION,
 DECEMBER 1955 STORM,
 FEATHER RIVER BASIN



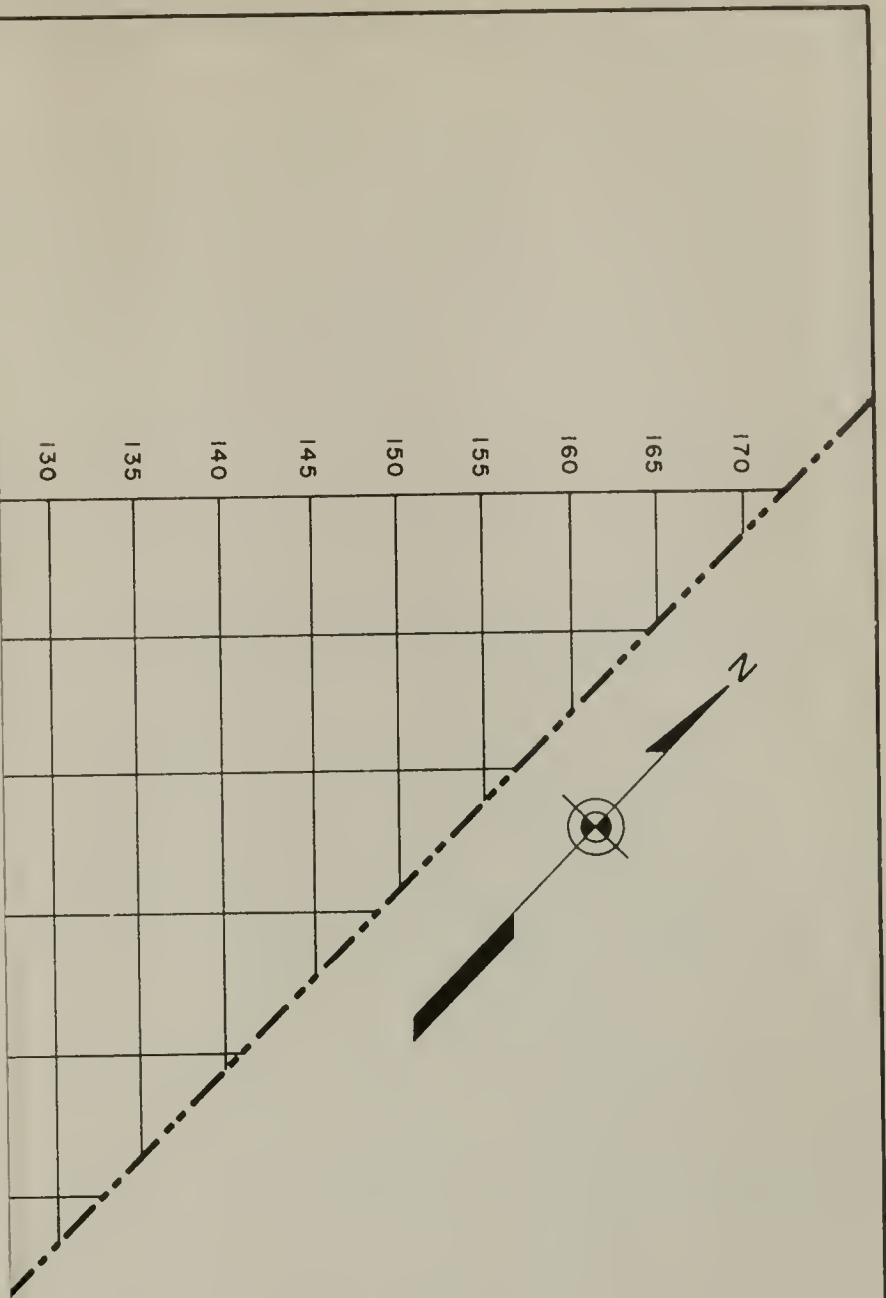
STATE OF CALIFORNIA
 DEPARTMENT OF WATER RESOURCES
 DIVISION OF DESIGN AND CONSTRUCTION

OPERATIONS BRANCH
PROCEDURES FOR ESTIMATING
MAXIMUM POSSIBLE PRECIPITATION



THE 72-HOUR ISOHYETAL MAP,
 "NEAR MAXIMUM" STORM,
 FEATHER RIVER BASIN

Fig 13

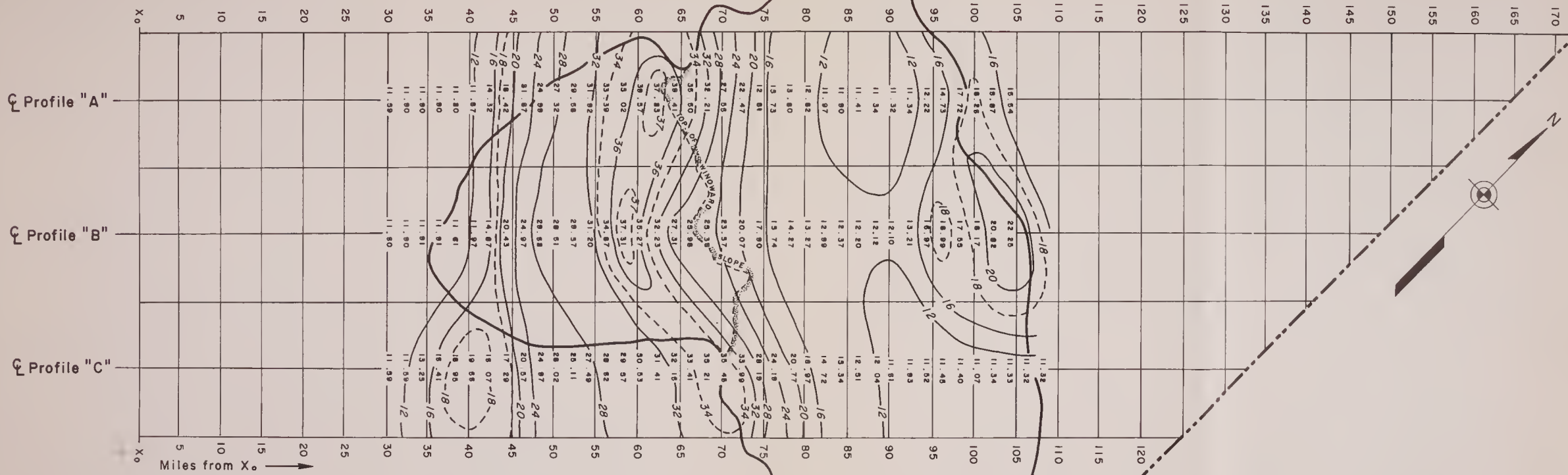


STATE OF CALIFORNIA
 DEPARTMENT OF WATER RESOURCES
 DIVISION OF DESIGN AND CONSTRUCTION

OPERATIONS BRANCH
PROCEDURES FOR ESTIMATING
MAXIMUM POSSIBLE PRECIPITATION



THE 72-HOUR ISOHYETAL MAP,
 "NEAR MAXIMUM" STORM,
 FEATHER RIVER BASIN



Profile "A"

Profile "B"

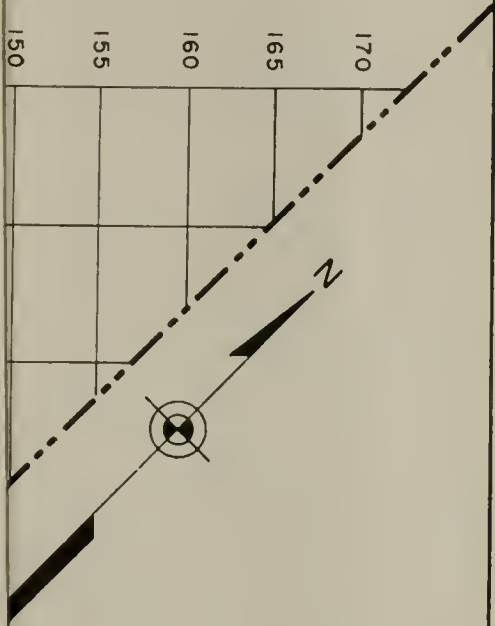
Profile "C"

Miles from X₀ →

NOTE
 Area of windward basin = 940 square miles
 Area of leeward basin within profile strips = 1737 sq. mi.
 Area of entire leeward basin = 2675 square miles
 Total basin area = 3615 square miles

Average basin depth within profile strips on Leeward side = 16.7 inches.
 Average basin depth within profile strips on Windward side = 28.5 inches.
 Average depth over entire basin within profile strips = 20.8 inches

STATE OF CALIFORNIA
 DEPARTMENT OF WATER RESOURCES
 DIVISION OF DESIGN AND CONSTRUCTION
 OPERATIONS BRANCH
**PROCEDURES FOR ESTIMATING
 MAXIMUM POSSIBLE PRECIPITATION**
 THE 72-HOUR ISOHYETAL MAP,
 "NEAR MAXIMUM" STORM,
 FEATHER RIVER BASIN



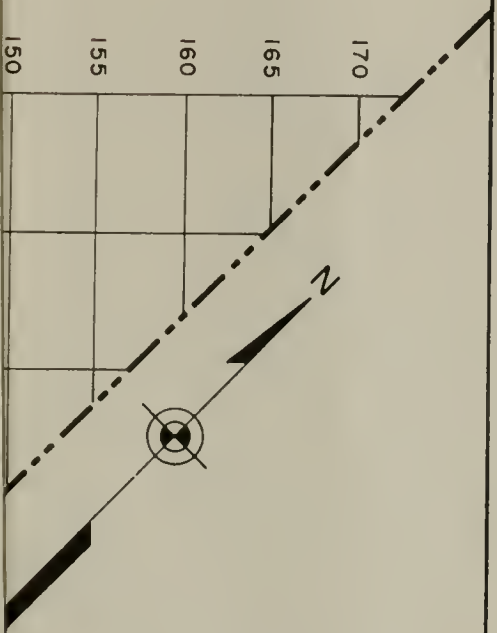
OF CALIFORNIA
 WATER RESOURCES
 AND CONSTRUCTION
 DIVISIONS BRANCH

FOR ESTIMATING
POSSIBLE PRECIPITATION



ISOHYETAL MAP,
 FOR A POSSIBLE STORM,
 IN A RIVER BASIN

Fig. 14

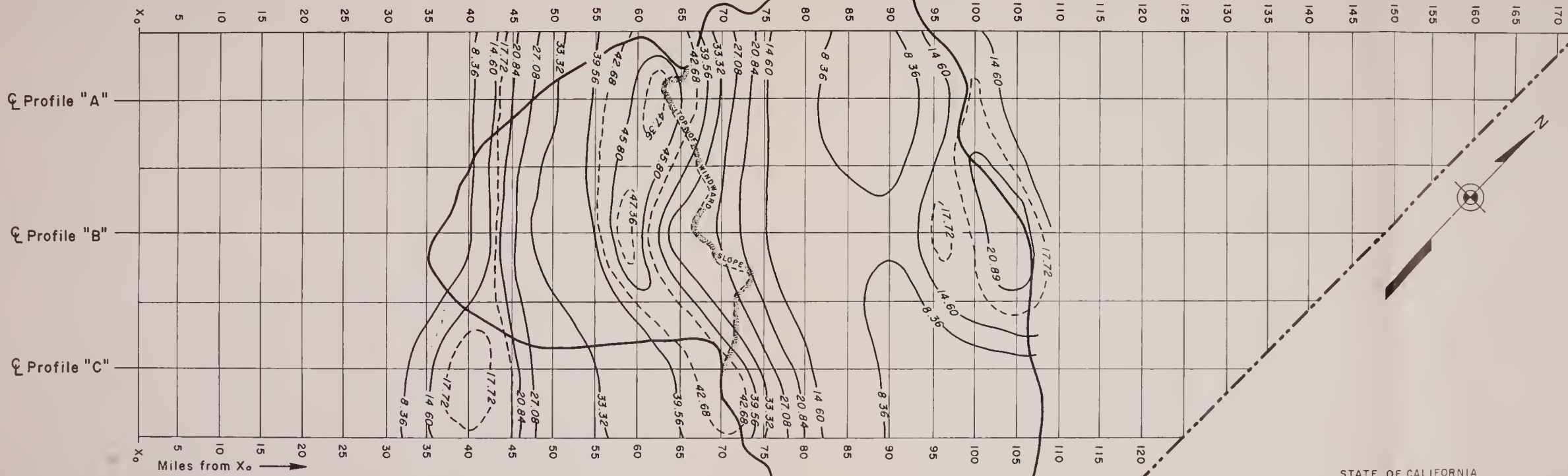


OF CALIFORNIA
 WATER RESOURCES
 AND CONSTRUCTION
 DIVISIONS BRANCH

FOR ESTIMATING
POSSIBLE PRECIPITATION

ISOHYETAL MAP,
 FOR A POSSIBLE STORM,
 IN A RIVER BASIN

Fig. 14



STATE OF CALIFORNIA
 DEPARTMENT OF WATER RESOURCES
 DIVISION OF DESIGN AND CONSTRUCTION
 OPERATIONS BRANCH

**PROCEDURES FOR ESTIMATING
 MAXIMUM POSSIBLE PRECIPITATION**

**THE 72-HOUR ISOHYETAL MAP,
 ESTIMATED MAXIMUM POSSIBLE STORM,
 FEATHER RIVER BASIN**

NOTE

Area of windward basin = 940 square miles	Average basin depth within profile strips on Leeward side = 15.8 inches
Area of leeward basin within profile strips = 1737 sq. mi.	Average basin depth within profile strips on Windward side = 34.1 inches
Area of entire leeward basin = 2675 square miles	Average depth over entire basin within profile strips = 22.1 inches
Total basin area = 3615 square miles	

THIS BOOK IS DUE ON THE LAST DATE
STAMPED BELOW

RENEWED BOOKS ARE SUBJECT TO IMMEDIATE
RECALL

JUN 5 REC'D

APR 2 1973

JUN 11 1973

JUN 13 REC'D

LIBRARY, UNIVERSITY OF CALIFORNIA, DAVIS

Book Slip-20m-8,'61 (C1623s4)458

UNIVERSITY OF CALIFORNIA DAVIS
3 1175 01911 3524

Call Science

72.874
32
A-
11 98

PHYSICAL
SCIENCES
LIBRARY

LIBRARY
UNIVERSITY OF CALIFORNIA
DAVIS
240512

